CONVERSION OF GLYCEROL TO ACRYLIC ACID OVER ZEOLITE AND $VMoO_x$/SILICIC ACID CATALYSTS IN A DOUBLE BED SYSTEM

AYUT WITSUTHAMMAKUL

A THESIS SUBMITTED IN PARTIAL FULFILLMENT

OF THE REQUIREMENT FOR THE DEGREE OF

MASTER OF SCIENCE IN PETROCHEMICALS AND HYDROCARBON CHEMISTRY

FACULTY OF SCIENCE

KING MONGKUT'S INSTITUTE OF TECHNOLOGY LADKRABANG

2010

KMITL-2010-SC-M-015-040

หัวข้อวิทยานิพนธ์	การเปลี่ยนกลีเซอรอลเป็นกรดอะครีลิคโดยใช้ตัวเร่งปฏิกิริยาซีโอไลต์และตัวเร่งปฏิกิริยาวานาเดียมโมลิบดีนัมออกไซด์บนตัวรองรับกรดซิลิซิคในระบบเบดคู่
นักศึกษา	นาย อยุทธ์ วิทย์สุธรรมกุล
รหัสประจำตัว	50068001
ปริญญา	วิทยาศาสตรมหาบัณฑิต
สาขาวิชา	ปิโตรเคมีและเคมีของไฮโดรคาร์บอน
พ.ศ.	2553
อาจารย์ที่ปรึกษาวิทยานิพนธ์	รศ. ดร. ตะวัน สุขน้อย

บทคัดย่อ

งานวิจัยนี้นำเสนอการผลิตกรดอะคริลิคโดยการออกซิเดชั่นผลิตภัณฑ์ที่ได้จากการขจัดน้ำออกจากกลีเซอรอลในเครื่องปฏิกรณ์แบบเบดนิ่ง แล้ววิเคราะห์ผลิตภัณฑ์ที่ได้ด้วยเทคนิคแก๊สโครมาโตกราฟีและตัวตรวจวัดชนิดเฟลมไอออไนเซชั่น ขั้นตอนแรกทำการศึกษาการขจัดน้ำออกจากกลีเซอรอลด้วยซีโอไลต์ชนิดต่างๆ (HZSM-5, HBeta, HMordenite และ HY ที่มี ซิลิกอน/อะลูมิเนียม = 13-500) ในฮีเลียม (อัตราการไหล 30 มล./นาที) ที่อุณหภูมิ 275-400 °C จากการทดลองพบว่าได้อะโครลีนและอะซีทอลเป็นผลิตภัณฑ์ปฐมภูมิ ซึ่งบางส่วนสามารถเกิดปฏิกิริยาต่อโดยผ่าน surface oxygenate pools ได้เป็นผลิตภัณฑ์ทุติยภูมิ ได้แก่ อะซิทาลดีไฮด์ โพรพิโอนาลดีไฮด์ ไพรูวาลดีไฮด์ สารอินทรีย์โครงสร้างแบบวงไม่อิ่มตัวที่มีออกซิเจนประกอบ และโค้ก โดย surface oxygenate pools นั้นจะแตกสลายได้มากขึ้นที่อุณหภูมิสูง นอกจากนี้รูพรุนขนาดกลางของ HZSM-5 สามารถยับยั้งการเกิดผลิตภัณฑ์ทุติยภูมิได้ดีโดยการใช้ HZSM-5 ที่มี ซิลิกอน/อะลูมิเนียม=13 เป็นตัวเร่งปฏิกิริยาที่อุณหภูมิ 300 °C จะสามารถเปลี่ยนกลีเซอรอลได้ทั้งหมดและคัดสรรต่ออะโครลีน 81%

ในลำดับถัดไปทำการศึกษาการออกซิเดชั่นของผลิตภัณฑ์ที่ได้จากการขจัดน้ำออกจากกลีเซอรอลบนตัวเร่งปฏิกิริยาโลหะออกไซด์ผสมวานาเดียม-โมลิบดีนัมบนตัวรองรับกรดซิลิซิค (โลหะออกไซด์ผสม 20-100% โดยน้ำหนัก และวานาเดียม/โมลิบดีนัม=0.2-2) ในบรรยากาศที่มี O_2 (ความดันย่อยของ O_2 = 0.05-0.20 บรรยากาศ) โดยใช้ระบบเบดแยกและเบดผสม จากการทดลองพบว่าระบบเบดแยกให้ความคัดสรรต่อสาร C_3 ที่มีออกซิเจนเป็นองค์ประกอบมากกว่า อะโครลีนและอะซิทาลดีไฮด์จากการขจัดน้ำจะเกิดการออกซิเดชั่นในเบดออกไซด์ผสมได้เป็นกรดอะครีลิกและกรดอะซิติกตามลำดับ ในขณะที่อะซีทอลจะสลายตัวเป็นกรดอะซิติก ตัวเร่งปฏิกิริยาที่มีโลหะออกไซด์ผสม 45% และวานาเดียม/โมลิบดีนัม=0.3 จะมีการกระจายตัวเหมาะสมและมีความคัดสรรต่อกรดอะครีลิคสูง ผลจาก XRD ระบุว่า V-Mo-O เฮกซะโกนอล ออโธรอมบิก และ ไตรคลินิก เป็นวัฏภาคที่ว่องไว โดยสามารถเปลี่ยนอะโครลีนได้ 48 % และคัดสรรต่อกรดอะครีลิคสูงสุด 98% ที่ความดันย่อยของ O_2 = 0.20 บรรยากาศ

Thesis Title	Conversion of glycerol to acrylic acid over zeolite and $VMoO_x$/silicic acid catalysts in a double bed system
Student	Mr. Ayut Witsuthammakul
Student ID	50068001
Degree	Master of Science
Program	Petrochemicals and Hydrocarbon Chemistry
Thesis Advisor	Assoc. Prof. Dr. Tawan Sooknoi

Abstract

The catalytic conversion of glycerol to acrylic acid was achieved by the subsequent oxidation of glycerol dehydrated products. The experiment was conducted in a fixed bed reactor. The product effluent was analyzed by GC-FID. Initially, the glycerol dehydration to acrolein was studied with various acidic zeolites (HZSM-5, HBeta, HMordenite and HY at Si/Al=13-500) under flow of helium (30 $ml.min^{-1}$) at 275-400 °C. It was found that over the acid zeolites, acrolein and acetol are generated as primary products. A part of them further react to secondary products (acetaldehyde, propionaldehyde, pyruvaldehyde, cyclic unsaturated oxygenate compounds and coke) via the surface oxygenate pools that can be cracked drastically at higher temperature. The used of medium pore (HZSM-5) can inhibit the formation of such secondary products. Hence, the high selectivity to acrolein (81 %) with complete conversion was obtained when HZSM-5 (Si/Al=13) was used at 300 °C.

Subsequently, the oxidation of dehydrated products over the vanadium-molybdenum oxides on silicic acid support (20-100 wt% mixed oxides loading and V/Mo=0.2-2) was investigated in atmosphere of O_2 (0.05-0.20 atm of O_2 partial pressure). The catalysts were compared in separated and mixed bed system. It was found that the separated system is highly selective for oxygenate C_3. In the mixed oxides bed, the acrolein and acetaldehyde from dehydration step can be oxidized to acrylic and acetic acid respectively. Meanwhile, the acetol is decomposed to acetic acid. The catalyst with 45 % mixed oxides and V/Mo=0.3 provide good dispersion and high selectivity to acrylic acid. The XRD shows that the V-Mo-O hexagonal, orthorhombic and triclinic is an active component. The maximum 98 % selectivity to acrylic acid with 48 % acrolein conversion can be achieved at 0.20 atm of O_2 partial pressure.

ACKNOWLEDGEMENTS

For the thesis completion, the author would like to appreciate my advisor, Assoc. Prof. Dr. Tawan Sooknoi for knowledge in catalysis, skill coaching, suggestion of the results, experimental instrument and fund. He is also grateful to examination committees including Asst. Prof. Dr. Vanchat Chuenchom, Dr. Montree Thongkam and Asst. Prof. Dr. Siriporn Jongpatiwut for judgment and valuable comments.

The work place and public utility are supported by his institute (King Mongkut's Institute of Technology Ladkrabang).

Unforgettable, he would like to thank all teachers and his work group for the impressive help and guidance.

Finally, he would like to appreciate his deceased parents who give the smart brain and strong body to use in this work.

Ayut Witsuthammakul

CONTENTS

CONTENTS (Continued)

CONTENTS (Continued)

LIST OF TABLES

LIST OF TABLES (Continued)

APPENDIXES

LIST OF TABLES (Continued)

LIST OF TABLES (Continued)

LIST OF FIGURES

Figure **Page**

CHAPTER 2

LIST OF FIGURES (Continued)

LIST OF FIGURES (Continued)

APPENDIXES

LIST OF FIGURES (Continued)

CHAPTER 1

INTRODUCTION

1.1 Motivation

Approximately two-third of high-value organic chemical intermediates contain oxygenates including aldehydes, ketones, alcohols and anhydrides [1]. Acrylic acid and its derivatives are among the most important oxygenated petrochemicals used mainly in coating industry. Selective oxidation was employed for production of acrylic acid via partial oxidation of propane and propylene to acrolein [2-4] or direct oxidation using MoVTeNbO [5] and vanadyl pyrophosphate [6]. Although these processes are currently successful, propane and propylene are unrenewable resources. While the goal of modern petrochemical industry focus on sustainable development, the use of alternative renewable source is more appropriate.

With this view, glycerol which is produced as parallel products from biodiesel production [7, 8] becomes over supplied. Several attempts have been done to make use of glycerol such as in polymer additives [9, 10] and cosmetics [11]. Nevertheless; it is also worth utilizing glycerol for alternative resource for production of oxygenated chemical namely acrylic acid.

It was known that high oxygen content in glycerol molecule could be easily eliminated by dehydration to form acrolein [12, 13]. This intermediate can be subsequently oxidized to acrylic acid. However, acrolein possesses handle difficulty due to low boiling point and self polymerization. It would be nice to integrate the dehydration and oxidation processes for the direct conversion of glycerol to acrylic acid. Such approach would open sustainable way to provide useful oxygenated C_3 petrochemicals especially acrylic acid from renewable sources.

1.2 Objectives

The main objective of this thesis is to convert glycerol to acrylic acid by integration of dehydration and oxidation processes. In addition, there are some specific objectives of the study as follow:

1.2.1 To accomplish high acrolein production from glycerol dehydration over acid catalyst.

1.2.2 To obtain appropriate catalyst for subsequent oxidation of glycerol dehydrated products.

1.2.3 To understand effect of temperature, contact time, O_2 partial pressure, glycerol concentration.

1.3 Scope of study

This thesis is divided into two parts which relate to each other.

1.3.1 Dehydration of glycerol

1) Modify and characterization the zeolites namely H ZSM-5, H Beta, H Mordenite, H Y
2) Study on effect of W/F from 29-295 $g.h.mol^{-1}$
3) Study on effect of temperature ranging from 275 to 400 ^{o}C
4) Study on effect of Si/Al of zeolites from 13 to 500
5) Study on effect of glycerol concentration in the range of 10 to 50 wt%

1.3.2 Subsequent oxidation of glycerol dehydrated products

1) Prepare and characterization of vanadium-molybdenum mixed oxides catalyst
2) Study on effect of vanadium to molybdenum molar ratio (0.2-2) and loading on silicic acid support (20-100%)
3) Study on effect of contact time for the mixed oxides bed between W/F=59 to 295
4) Study on effect of oxygen partial pressure from 0.05 to 0.20 atm

1.4 Expected result

This research can provide appropriate catalyst and reaction conditions for highly selective acrylic acid production from glycerol.

CHAPTER 2

LITERATURE REVIEWS AND THEORY

2.1 Glycerol [14]

2.1.1 Properties of Glycerol

Glycerol or 1, 2, 3-propanetriol (Figure 2.1) is colorless, odorless, viscous liquid with sweet taste that obtain from natural and petrochemical feedstocks. The general physic and chemical properties are given in Table 2.1. Glycerol is applied to more than 1500 end uses such as ingredient in cosmetics and pharmaceuticals, polymer synthesis, foodstuffs and detergents (Figure 2.2) due to its high stability under normal storage condition, compatibility with many other chemical materials, non-irritant and well known environment friendly.

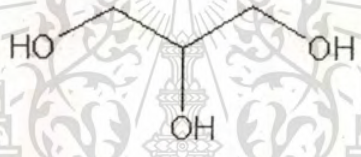

Figure 2.1 Structure of glycerol

Table 2.1 Physicochemical properties of glycerol at 20 °C

Chemical formula	$C_3H_5(OH)_3$
Molecular mass	92.09382 g/mol
Density	1.261 g/mL
Viscosity	1.5 Pa.s
Melting point	18.2 °C
Boiling point	290 °C
Food energy	4.32 kcal/g
Flash point	160 °C (closed cup)
Surface tension	64.00 mN/m
Temperature coefficient	-0.0598 mN/mK

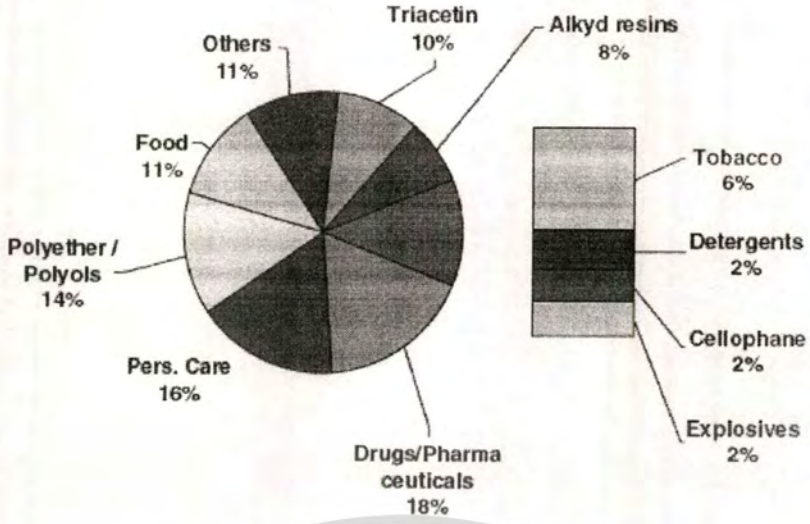

Figure 2.2 Markets for glycerol (volumes and industrial use)

2.1.2 Production of Glycerol

Glycerol is obtained as co-product from biodiesel production. Trans-esterification between vegetable oil (triglyceride) and methanol which is catalyzed by base, KOH, result in fatty acid methylester (biodiesel) and glycerol as shown in Figure 2.3. At equilibrium, stoichiometry of the process is given below

100 kg oil + 10.5 kg MeOH = 100 kg biodiesel + 10.5 kg glycerol

After reaction, the glycerol-methanol solution which is heavier than fatty acid methylester runs off from the reactor at bottom.

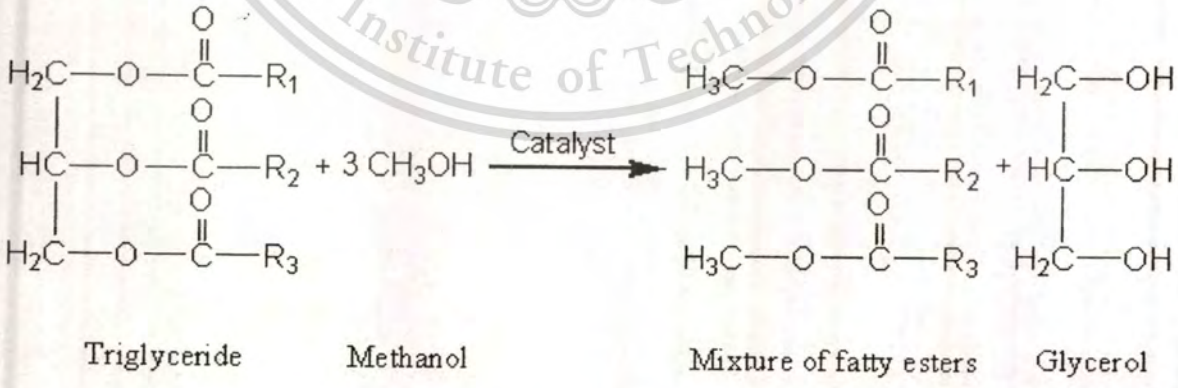

Figure 2.3 Acylglycerol trans-esterification with methanol

Moreover, glycerol is also obtained from hydrolysis of fats and oils in soap and fatty acid manufacturing. Thus, it is not surprise that over supply of glycerol become hot topic in industrial.

2.2 Catalysis [15]

Most of chemical processes need catalyst. Today, catalysts do not only help reaction drive easily but also help reaction drive specifically. They play important role in many chemical industries for examples the synthesis of sulfuric acid, the conversion of ammonia to nitric acid and catalytic hydrogenation. A definition of catalysis that still valid today is due to Ostwald (1985): "a catalyst accelerates a chemical reaction without effecting the position of equilibrium." While it was formerly assumed that the catalyst remained unchanged in the course of reaction, it is now known that the catalyst involve in chemical bonding with reactant during chemical process. Thus, catalyst work as cycle: it bonds with reactant to one form then product is released and the catalyst is back to the initial state (Figure 2.4). The intermediate of catalyst (Cat-R) is highly reactive and difficult to be detected.

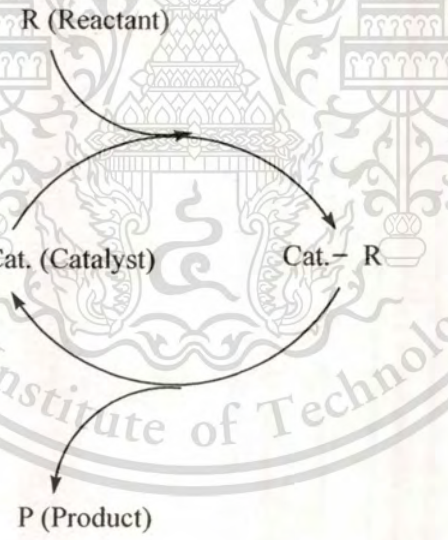

Figure 2.4 Catalytic cycle

In theory, catalyst would not be consumed but this is not true in practice. There are other competitive reactions cause chemical change of the catalyst and its activity become lower (called deactivation). Thus, catalyst must be regenerated.

2.2.1 Catalysts Classification

The catalysts can be classified by many criteria, i.e. states, structures, acid-base, compositions and applications. However, state which they act is most preferable classification. They can be divided into two main groups (Figure 2.5): heterogeneous and homogeneous catalysts. There are also intermediate forms known as heterogenized homogeneous catalysts (immobilized catalysts) such as homogeneous catalysts attached to support and biocatalysts (enzymes).

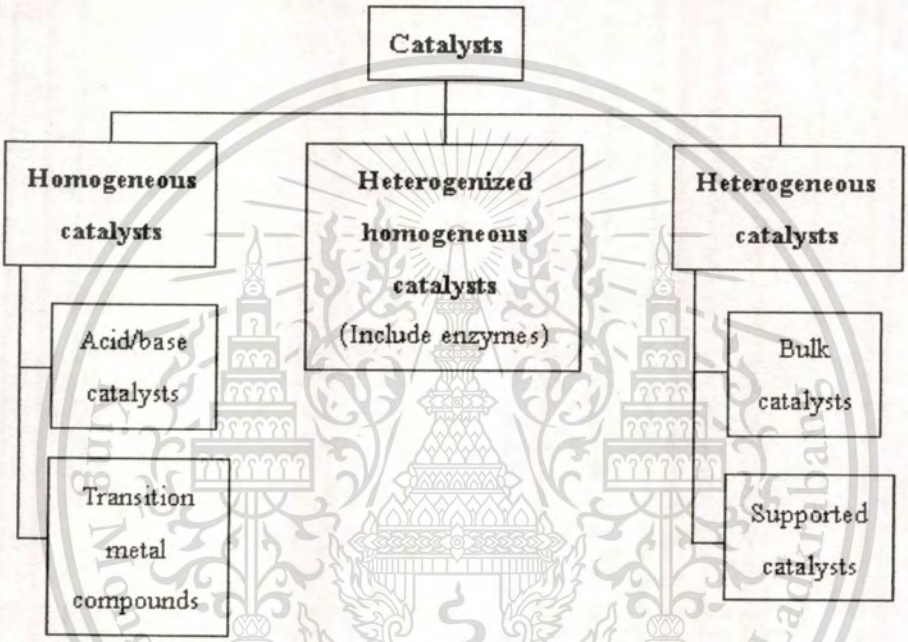

Figure 2.5 Catalysts classification

Catalytic processes take place between two phases are classified as heterogeneous catalysis. Only surface of the catalysts are active. In contrast, homogeneous catalysis takes place in uniform phase. They have higher degree of dispersion than the heterogeneous catalysts and all catalyst molecules can be active sites. Each kinds of catalyst have advantage and disadvantage as comparison in Table 2.2

Table 2.2 Comparison of homogeneous and heterogeneous catalysts

	Homogeneous catalysis	**Heterogeneous catalysis**
Effectivity		
Active centers	all metal atoms	only surface atoms
Concentration	low	high
Selectivity	higher	lower
Diffusion problems	practically absent	present (mass transfer controlled reaction)
Reaction conditions	mild (50-200 °C)	server (often > 250 °C)
Applicability	limited	wide
Activity loss	irreversible reaction with products (cluster formation); poisoning	sinter of the metal crystallites; poisoning
Catalyst properties		
Structure/stoichiometry	defined	undefined
Modification possibilities	high	low
Thermal stability	low	high
Catalyst separation	Sometimes laborious (chemical decomposition, distillation, extraction)	Fixed- bed: unnecessary suspension: filtration
Catalyst recycling	possible	unnecessary (fixed-bed) or easy (suspension)
Cost of catalyst losses	high	low

2.2.2 Action Mode of Catalyst

Suitable of catalyst depend on these three properties that is activity, selectivity and stability of catalysts (deactivation behavior).

Activity

Activity is a measure of how fast one or more reaction proceed in the presence of catalyst. Activity can be defined in term of kinetics or more practical viewpoints, e.g. reaction rate (r), rate constant (k) and activation energy (E_a).

In practice, instantly measures of activity (conversion under constant reaction condition, space velocity for a given constant conversion, space-time yield and temperature required for a given conversion) are often sufficient for determine catalyst suitability such as comparative among catalysts, process optimization, and deactivation study.

The conversion (X_A) is the ratio of the amount of reactant A that is reacted to the amount of reactant A that is introduced into reactor. For a batch reactor:

$$X_A = \frac{n_{A,0} - n_A}{n_{A,0}} \quad \text{(mol/mol or \%)}$$

where, $n_{A,,0}$: amount of reactant at initial time

n_A : amount of reactant at end point

Catalysts are often operated in continuous process, which conversion attained at constant space velocities or contact times are compared. The space velocity is ratio of volume flow rate (V_0) to catalyst mass (m_{cat}):

$$Space\ velocity = \frac{V_0}{m_{cat}} \quad (m^3\ kg^{-1}\ s^{-1})$$

Figure 2.6 compares two catalysts with difference conversions at given space velocity, catalyst A better than catalyst B.

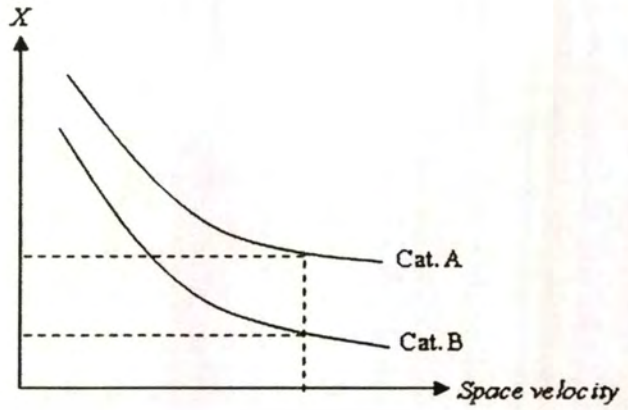

Figure 2.6 Catalyst activities comparison

Sometime performance of reactor relate to catalyst mass or volume so different reactor design and size can be compared to each other. This value is known as space-time yield (*STY*):

$$STY = \frac{Desired\ product\ quantity}{Catalyst\ volume \cdot time} \quad (\text{mol } L^{-1} h^{-1})$$

Another measurement of catalyst activity is "turn over number" (*TON*) that is defined as number of reactant molecules react per active center. In case of homogeneous catalyst, TON can be determined directly because all catalyst molecules present in solution. For heterogeneous catalyst, it is complicate to measure because only surface molecules of catalyst are active centers and it depend on area of catalyst surface. However the active centers can be determined indirectly by chemisorption methods in which the measurements require great care.

Selectivity

During operation, not only desired reaction happens in process but there are side-reactions occur simultaneously. In Figure 2.7, sometime a reactant converts to two or more products called parallel reaction and sometime a product further react to other product called sequential reaction. These phenomenons give undesired products (P_1, P_2).

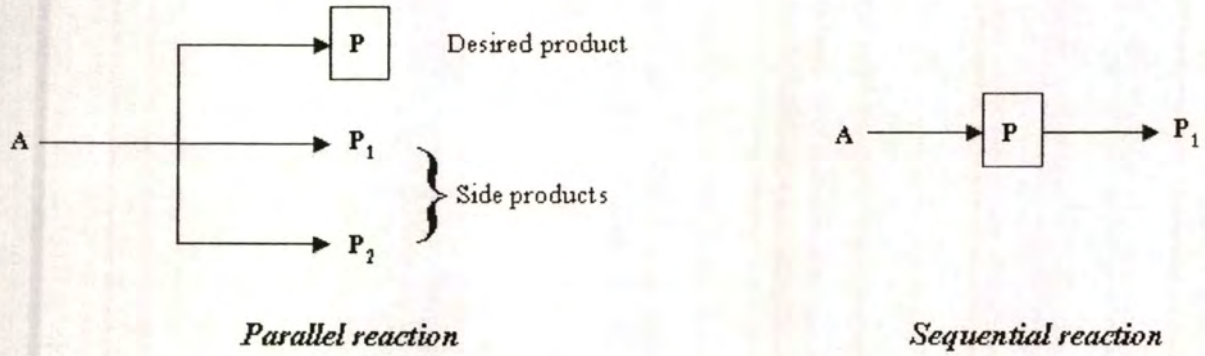

Figure 2.7 Parallel and sequential reaction

If consider only desire product (P), the selectivity (S_P) of reaction is defined as ratio of desired product to the amount of reactant that is converted to all products (or conversion). This quantity compares between reactant and product, so the stoichiometric coefficients (v_i) must be taken into account which gives rise to following equation:

$$S_P = \frac{n_P / \nu_P}{(n_{A,0} - n_A) / |\nu_A|} \quad \text{(mol/mol or \%)}$$

where, $n_{A,0}$: amount of reactant at initial time

n_A : amount of reactant at end point

ν_i : stoichiometric coefficients

Stability

The chemical, thermal and mechanical stability of catalyst determine lifetime of the catalytic process. They are influenced by several factors including decomposition, coking and poisoning. Catalyst deactivation can be followed by measuring activity and selectivity during processing time. The catalyst lifetime can be extended by regenerating the deactivated catalysts. The total lifetime is an important consideration for economic of the process and process possibility.

Today, the efficient use of reactant and energy is major important. For various reasons, priority of considerations is in order of following sequence:

Selectivity > Stability > Activity

2.3 Dehydration of Alcohols [16]

Dehydration of alcohols over solid catalysts gives alkenes by intra-molecular elimination or yield ethers by intermolecular elimination. It seems like elimination reactions but lost molecule is water. The catalysts used can be acidic, basic or bi-functional acid-base ones. Complication of reaction can be arisen by side-reactions (dehydrogenation, decomposition and transformation of intermediates and products).

2.3.1 Synthesis of Alkenes

When monohydric alcohols suffer dehydration, alkenes can be formed by the loss of water through β (or 1, 2-) elimination. Selective products are obtained as terminal alkenes (α olefin) when primary alcohols are dehydrated by appropriate solid catalysts. In contrast, either 1- or 2- alkenes can be produced by secondary alcohols dehydration. The reactivity of alcohols are as following sequence [16]

Tertiary > Secondary > Primary

From Figure 2.8 mechanistic studies of dehydration is established over acidic oxides follow two major routes. The single step mechanism (concerted E2) results in alkenes according Saytzev's rule (more substituted alkene isomers, product 1). The two-step mechanism, it is called E1 elimination which starts with $^{-}$OH removal. Because carbocation is generated as intermediates, it can be rearranged to a stable form which give rise to mixture of isomeric alkenes (product 3, 4). For basic oxide, E1cB mechanism initials by proton removal from β carbon. Its formation is usually in line with Hofmann rule (form of less substituted alkenes, product 2)

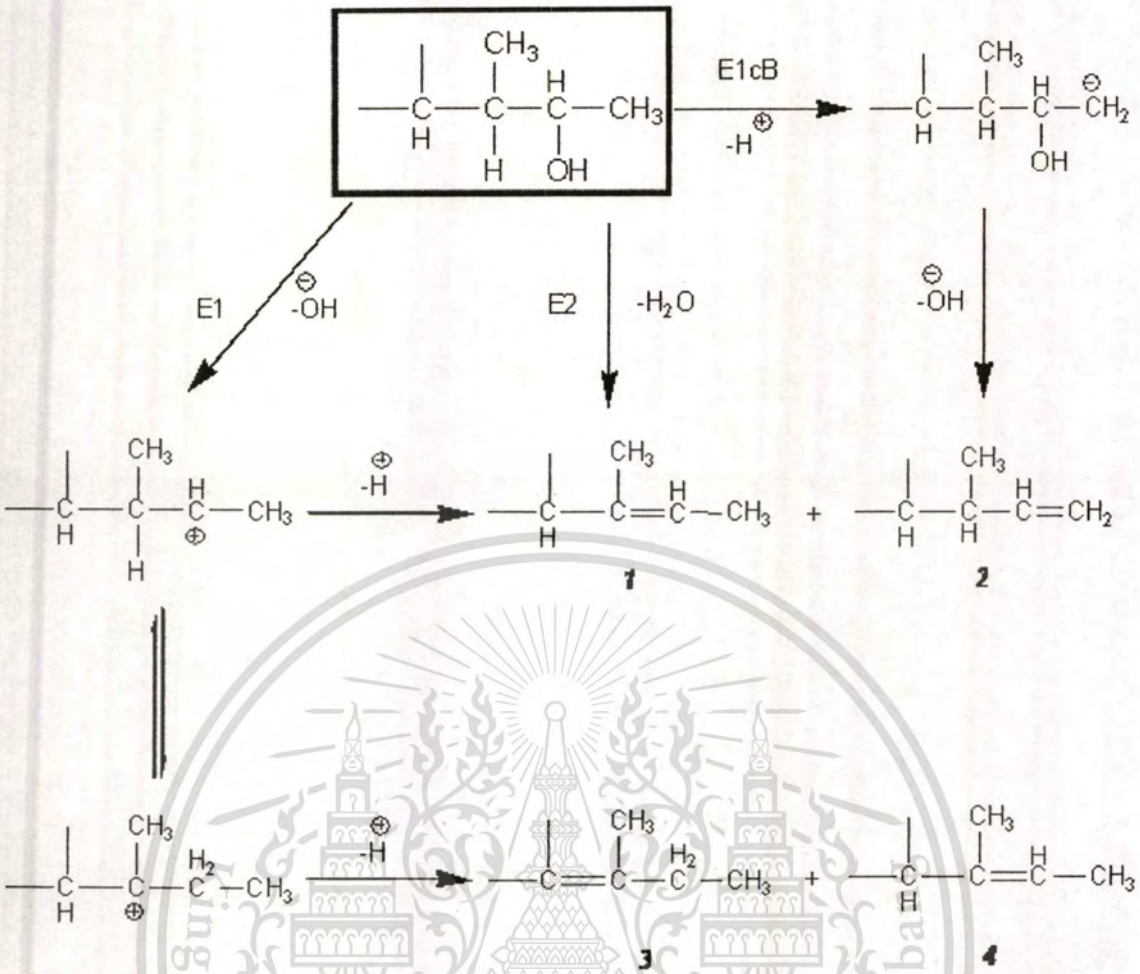

Figure 2.8 Routes of dehydration

As described above, the use of acidic oxides results in Saytzeff orientation alkenes [16]. This means that secondary 2-alkanols would transform to 2-alkenes. A catalyst that operated selectively is alumina treated with alkaline metal cations, ammonia or organic bases. Such treatment is necessary because pure strongly acidic alumina can promote carbocations rearrangement and double bond migration. The appropriate catalyst characteristic is illustrated in Figure 2.9.

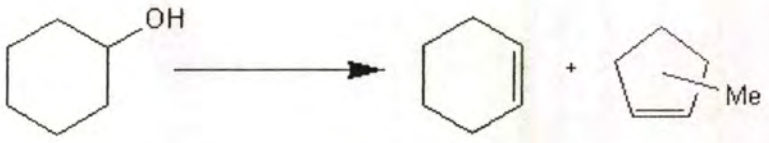

	Temperature (K)	Conversion (%)	Selectivity (%)	
Al_2O_3 with 1%K	683	95	100	0
pure Al_2O_3	623	95	89	11
	693	99	40	60

Figure 2.9 The cyclohexanol dehydration by pure alumina and potassium treated alumina

In contrast with alumina, thoria (thorium dioxide) is specified to be typical E1cB catalyst which converts 2-alkanols to 1-alkenes. The studies in lanthanide and alkaline earth are carried out with various alcohols. It was suggested that selectivity depends on the relative strength and concentration of acidic and basic centers. The E1cB mechanism is known to be associated with dehydrogenation (removed hydrogen gas). It was observed that dehydration activity increased with covalent characteristic of metal-oxygen bond while ionic characteristic one enhances dehydrogenation activity.

Numerous studies are performed with molecular sieves as dehydration catalysts. Despite they are highly reactive, they cannot transform complicated structure alcohols. For the reason, these give none selective product. Influence of E1 mechanism which generate reactive carbocationic intermediates followed by rearrangement and inter and intra molecular parallel reaction, result in mixture of alkene isomer products and ethers. However, some specific structural alcohols can be transformed selectively. For example, 1-phenyl-1-ethanol is converted to styrene with 95% yield over HZSM-5 zeolite at 493 K. Ethers formation occur when α-(*p*-tolyl) ethanol is reacted over HY zeolite. Low concentration of reactant in zeolite pores is required to prevent inter molecular reaction.

2.3.2 Dehydration of Polyols

A classical dehydration of polyol is glycerol transformation to acrolein in the presence of acid such as fused $KHSO_2$ powder (see 2.3.3). Recently, increased attention focus on dehydration

of renewable polyols and biomasses which is sustainable sources. Hexose and fructose dehydrations to 5-hydroxymethylfurfural (HMF) are apparent example (Figure 2.10). This compound can be used as starting materials for various fine chemicals and polymers.

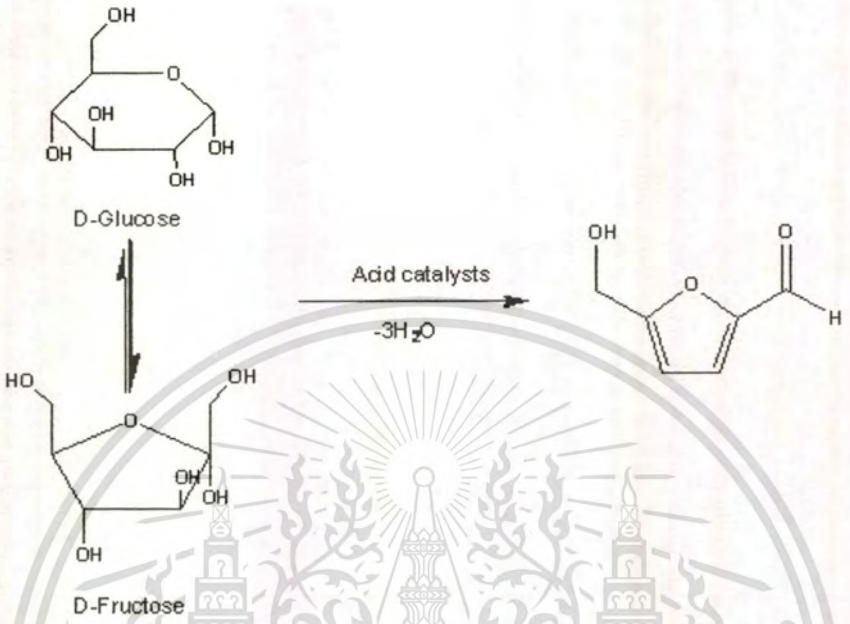

Figure 2.10 Dehydration of glucose or fructose to 5-hydroxymethylfurfural

Dehydrations usually proceed in aqueous media with continuous extraction. Strong acids such as ion-exchange resins and zeolites have been studied. Zeolites are selective catalysts [16] because side reactions and C-C cleavage are less important. Moreover, they are regenerated easily and can be operated at high temperature. Moredenite has excellence characteristic due to shape selectivity and low mesoporosity. Heterogeneous niobium catalysts (niobic acid, H_3PO_4 treated niobic acid and niobium phosphate) have recently been found to be selective catalysts [16].

2.3.3 Dehydration of Glycerol to Acrolein [14]

Acrolein is an important intermediate for chemical industry which can be obtained from dehydration of glycerol (Figure 2.11). It is an explosive and toxic chemical of which handling requires the highest safety standard.

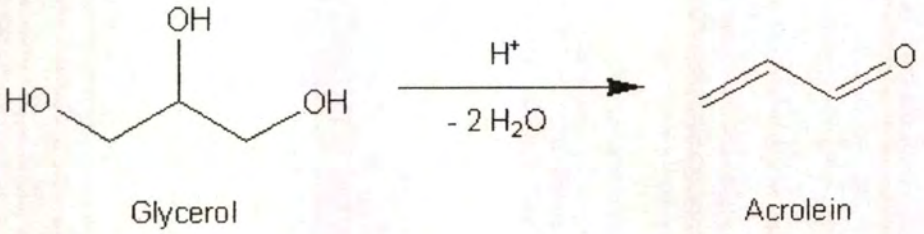

Figure 2.11 Acid-induced dehydration of glycerol to acrolein

When glycerol is protonated the energy barrier for dehydration is greatly reduced (from about 60 to 20 $kJ.mol^{-1}$). With this reason, dehydration of glycerol to acrolein is carried out under acidic condition. As the dehydration flavors at high temperature, it is necessary to provide sufficient heat to shift glycerol dehydration. The reaction can be proceeded both gas and liquid phase over acid catalyst.

In manufacturing, dehydration of glycerol to acrolein is carried out in gas phase process at atmospheric pressure. Typical reactor is a 85 cm long tube X 6 mm inside diameter with a ground solid tungstate zirconia (ZrO_2-WO_3) catalyst that is placed in heated chamber maintain at 300 $^{\circ}C$. The glycerol is fed into reactor in a form of 20 wt% aqueous solution at flow rate 12 mL/h^{-1}. The conversion is 84% and yield 35% acrolein with by-product hydroxypropanone (14%), propanaldehyde (8%) and acetaldehyde (4%).

2.4 Zeolites

2.4.1 Composition and Structure of Zeolites [1, 15]

Zeolites are solid crystalline of aluminosilicates which consist of SiO_4 and AlO_4^- tetrahedral, and interlinked to be three dimension network of porous structure. They can be built by nature or synthesis. Inside of zeolites pore have metals or other cations which balance negative charge from the anionic framework resulting from aluminium containing. The general formula of zeolite is given below:

$$M_v(AlO_2)_x(SiO_2)_y.zH_2O$$

where M are metal cations

The composition of zeolites are identified by the Si/Al atomic ratio or by molar ratio M

$$M = SiO_2 / Al_2O_3$$

The zeolites growth can be shown in Figure 2.12. The SiO_4 and AlO_4^- tetrahedra which is defined as primary units are polymerized to planar secondary units then evolve to complex three dimension unit called polyhedra e.g. cube, hexagonal and octahedral. These polyhedra are ultimately arranged in many connection modes to form porous (cages and channels) structure of zeolites such as sodalite cage and supercage.

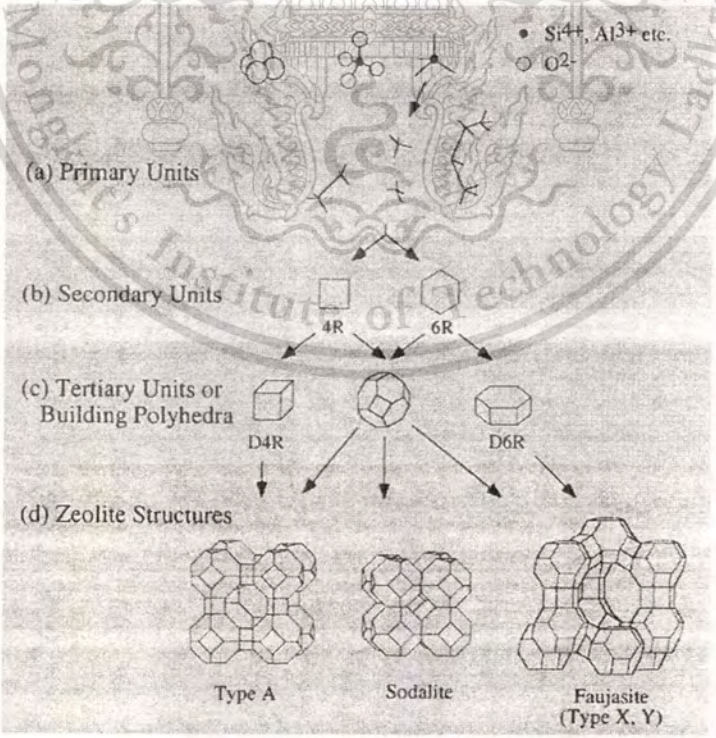

Figure 2.12 Formation of three common zeolites from primary units [1]

The pore of zeolites can be oriented in one, two or three dimension (Figure 2.13) and aperture of pore depend on number of T-atom composition (Si, Al or other metals; see Table 2.3). The pore size can be changed by exchanging the cation in zeolites: for example, the aperture size of zeolites A can be modified to be 3, 3.8 and 4.3 A^{o} when use K^{+}, Na^{+} and Ca^{2+} as balancing cation respectively.

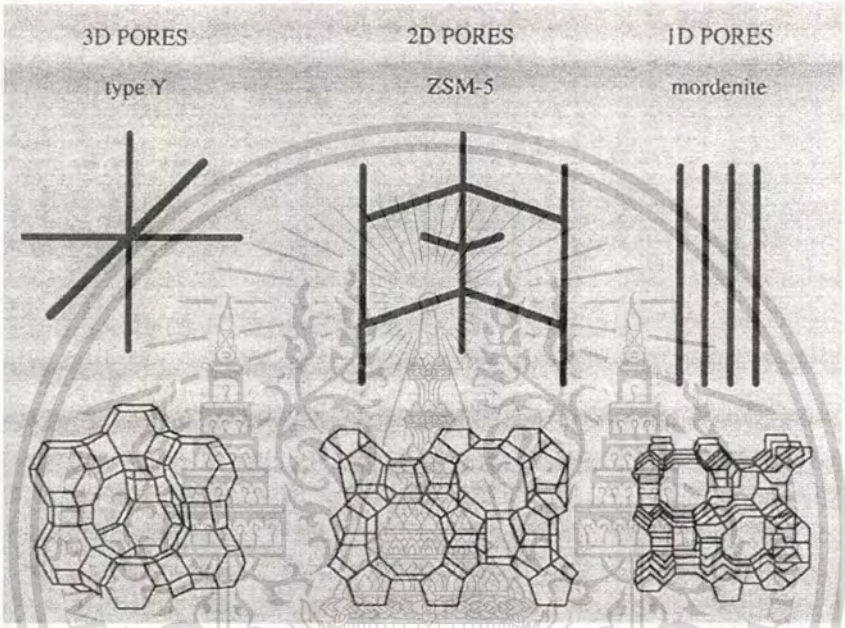

Figure 2.13 Three commercial zeolites of difference dimensionalities [1]

Table 2.3 Zeolites classified by window size [17]

Types	**Small**	**Medium**	**Large**	**Extra large**	**Mesopore**
Pore size (nm)	0.4-0.5	0.5-0.6	0.7-0.8	1.0-1.4	>2.0
T-atom	8	10	12	14-20	Variable
	Zeolite A	ZSM-5	Faujasite	CIT-5	MCM-41
	Chabasite	Theta-1	Cancrinite	VPI-5	MCM-48
	Rho	Ferrierite	Mordenite	Cloverite	
	Erionite	ZSM-11	Zeolite L		
	Zeolite P	ZSM-23	Offretite		
	Analcime		Beta		
	Philipsite		Gmelinite		

2.4.2 Adsorption Property and Kinetic Diameter

Despite the molecular sizes can be determined from molecular weight, in fact, diameter of molecules are bigger than those calculation because they are not static but always vibrate and rotate. The appropriate way to determine the relationship between molecular size and zeolite pore is considered through kinetic diameter of the molecules; diameter of molecules include its movement, rotation and vibration (so kinetic diameter must be larger than static diameter). In addition, determination of kinetic diameter is also based on several factors such as molecular weight, shape of molecule (i.e. sphere and cylinder) and temperature. Kinetic diameter extremely effect to adsorption property of zeolite for example, in Figure 2.14, *n*-hexane is best adsorbed by silicalite due to smallest cross-section cylinder shape and symmetrical linear motion. While, *o*-Xylene is least adsorbed because the benzene-like structure and steric constrain from two branches make it the largest kinetic diameter.

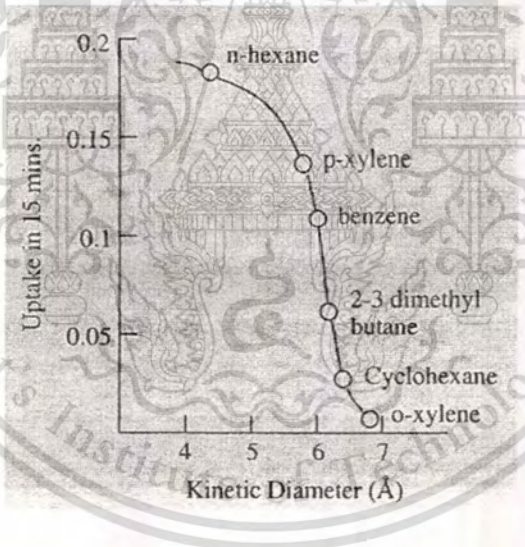

Figure 2.14 Decrease in sorption rate of silicalite with increasing kinetic diameter [1]

Due to their high surface area, zeolites have high capacity for molecular adsorption that small enough to diffuse pass aperture of pore (see Table 2.4 for largest adsorbed molecules). While too large molecules are logically excluded to pass into the pore, too small molecules can penetrate the pores but weak adsorption occur. For example, although both N_2 and O_2 penetrate the pore of 4A zeolite, the larger molecular size N_2 diffuse more slowly than O_2. Thus, O_2 adsorbs more rapidly than N_2 but larger amount of N_2 is retained at equilibrium (see Figure 2.15). This

fact brings about to commercial used of 4A for N_2 and O_2 separation from air. However, the adsorbed amount is function of several factors such as aperture size of pore, temperature, pressure, polarity and acidity which give more complex consideration.

Table 2.4 Pore diameter, ring size and largest molecules adsorbed of zeolites [1]

Zeolites	Pore diameter (°A)	T-atom per rings	Largest molecules adsorbed
Small pore			
3A	3.0	8	H_2O, NH_3
4A	3.8	8	N_2, C_2H_6
5A	4.3	8	*n*-alkanes, alkenes
Medium pore			
Pentasil (e.g.ZSM-5)	5.1 x 5.6	10	CCl_4, m-xylene
Large pore			
Faujasite (X, Y)	7.4	12	$(C_4H_9)_3N$, naphthalenes
ITG-21	7.4	12	$(C_4H_9)_3N$, naphthalenes
ALPO-VPI (e.g.VPI-5)	10-15	18	tris(isopropyl)benzene
Cloverite	17-18	20	model enzymes

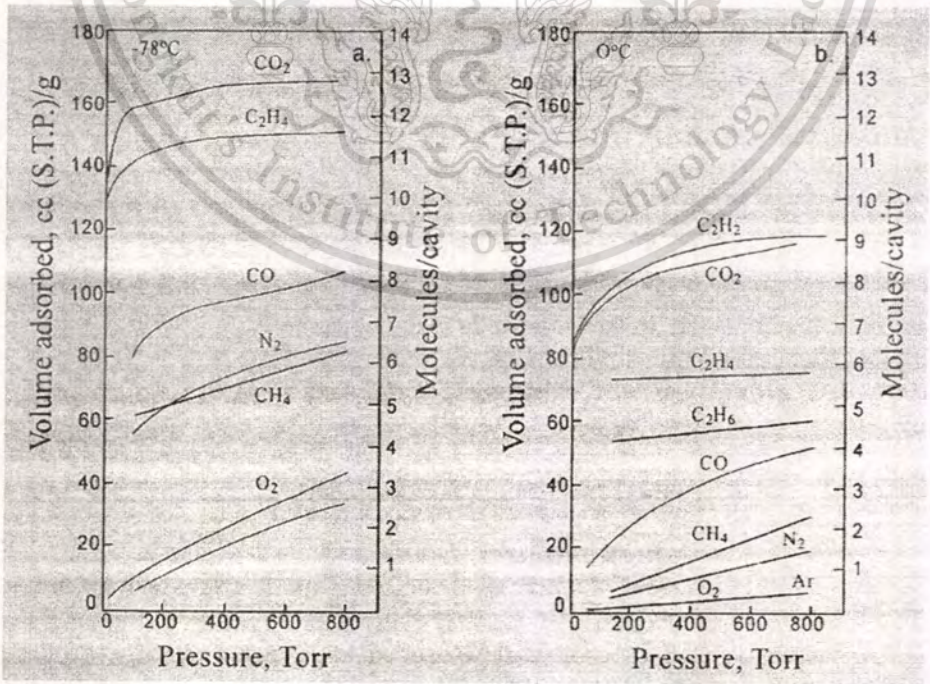

Figure 2.15 Adsorption isotherm on 4A zeolite at -78 °C and 0 °C [1]

2.4.3 Catalytic Properties of Zeolites [15]

Since chemist worldwide have prepared and modified numerous zeolites, the potential for fine chemicals and organic intermediates invoke them to innovate economically process and replace the old one because of following advantage over conventional catalysts:

- Precisely define crystalline and arrangement of SiO_2 and AlO_4^- make them good reproducibility in production.

- Due to the shape selectivity, only molecules that smaller than pore diameter of the zeolite undergo reaction.

- Tunable active site by synthesis or ion exchange

- At temperature above 300 °C, some zeolites such as pentasils and Y have acid strength comparable to mineral acids.

- Active metal ion catalysts can be incorporated by ion exchange or impregnation. Moreover, metal site can be generated by reduction such modified catalysts.

- The zeolites are thermally stable up to 600 °C and can be easily regenerated by combustion.

- They can be used at reaction temperature above 150 °C which is interested for reaction whose thermodynamic equilibrium lies on product side at high temperatures.

Shape Selectivity

Due to well-define of zeolite pore system, the accessibility of pore for molecules are controlled by geometric and steric restriction. The shape selectivity of zeolite is based on interaction between reactant and pore system which is divided into three types

(1) Reactant selectivity

Only reactants with proper size and shape can penetrate to inside of pore system and undergo reaction at the active sites. The reactants which are larger than pore can not react. For example, on HZSM-5 (Figure 2.16), *n*-heptane is more prefer for cracking (relative rate = 1.00) than dimethylhexane (relative rate = 0.09).

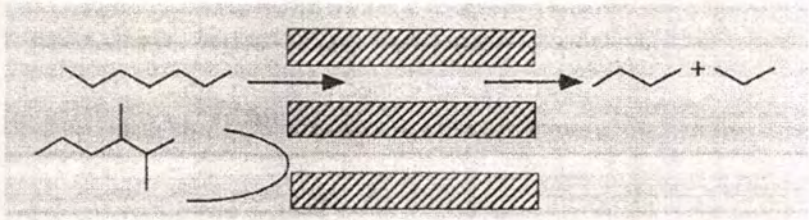

Figure 2.16 Reactant selectivity for cracking of straight chain and branch C_7 [1]

(2) Product Selectivity

Product selectivity predominate when reactants diffusion to the inside of pore are possible. Only products with suitable shape and size which can exit from pore system are formed. The well-know example of product selectivity is methylation of toluene on ZSM-5 (Figure 2.17). The three isomers o-, *m*-, *p*- are formed in pore. Although the thermodynamic equilibrium has 24% flavors for desired product *p*-xylene, the process elevate to 90 % selectivity with zeolite catalyst. This is because the diffusion rate of slimmer *p*-xylene is 10^4 faster than other two isomers. With this reason, *p*-xylene move out of pore to be desire product while two bigger isomers are still inside and their isomer are changed until reach *p*-xylene and move out.

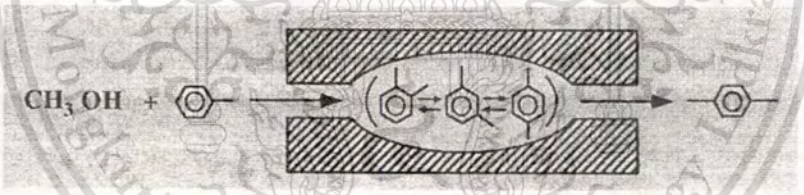

Figure 2.17 Product selectivity for *p*-xylene over *ortho* and *metha* forms [1]

(3) Restricted Transition State Selectivity

In pore system of zeolite, when reaction proceed via intermediates, only ones that have geometrical fit to the zeolite cavity can be formed during catalysis. In practice, it difficult to distinguish restricted transition state selectivity from product selectivity. A good example for this case is disproportionation of *m*-xylene to toluene and trimethyl benzene in the large pore zeolite Y (Figure 2.18). The fit shape intermediate (bottom way) is flavor while bulky intermediate (top way) take no reaction. Thus, the product from catalytic reaction consist mainly of the unsymmetrical 1, 2, 4-trimethylbenzene.

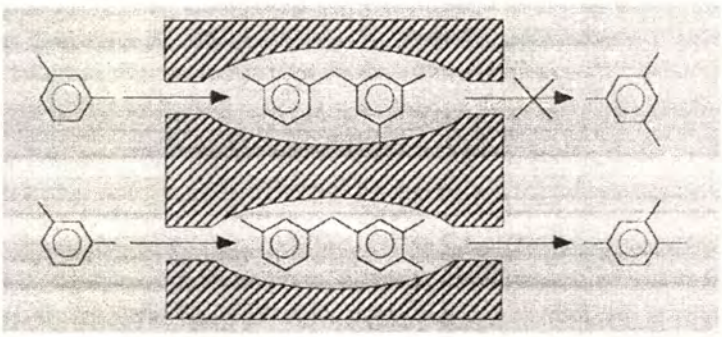

Figure 2.18 Restricted transition state selectivity for the formation of 1, 2, 4, trimethylbenzene from *m*-xylene [1]

Acidic Property of Zeolites

Zeolites in H form are solid acid catalysts. The acid strength (power of acid) can be varied over wide range by modification (i.e. ion exchange and dealumination). The direct replacement of alkaline metal ions by treatment with mineral acids can be applied only high silica content zeolites. The appropriate method is the exchange of alkaline metal ion by NH_4^+ ions then eliminate NH_3 by calcinations in air which results in proton balancing cation at negative framework (AlO_4^-) (Figure 2.19).

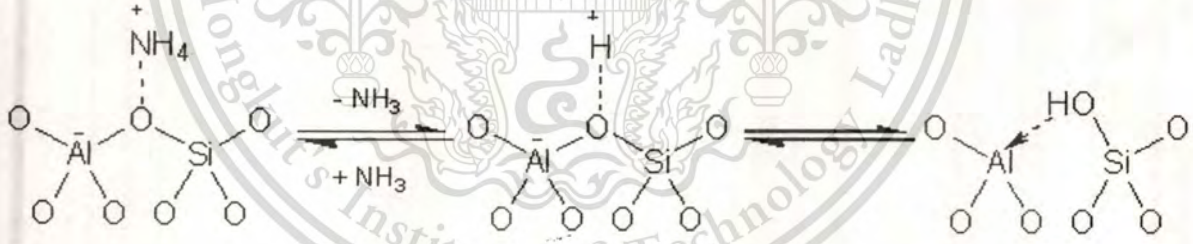

Figure 2.19 H-form zeolites production and their polarization [15]

Infrared investigation show that balancing protons are mainly in silanol form but still have high acid strength due to the effect of polarization with unsaturated aluminium center. These Brønsted acid centers are generally catalytic sites of H form zeolites.

The strong acidic property of zeolites can be modified to weak and moderate acid site by ion exchange with others cations. Acidic property is changed due to difference charges between cation and zeolite framework (hardness-softness property) and associated polarizing power of ions. The order of acid strength are given below

H form >> La form > Mg form > Ca form > Sr form > Ba form > Na form

Another consideration on acidic property is the Si/Al ratio that can be classified according to Table 2.5. Because acidity (quantity of acid) of zeolites is based on amount of H^+, acidity reverse variation to Si/Al ratio (amount of H^+; equal to Al content in zeolite). However, high aluminium in structure increase the negative charge density in pore structure and reduce the acid strength cause by increasing force between H^+ and the negative framework. Thus, acidity has reverse relationship to the acid strength like describe in Figure 2.20 but acid strength rise until Si/Al ~ 15 because the effect of neighbor negative framework was reduced when site approximatity is increased.

Table 2.5 Classification of acidic zeolites according to increasing Si/Al ratio [15]

Si/Al ratio	Zeolite	Acid/base properties
Low (1-1.5)	A	relatively low stability of lattice
	X	low stability in acids
		high stability in bases
		high concentration of acid groups of medium strength
Medium (2-5)	erionite	
	chabazite	
	clinoptilolite	
	mordenite	
	Y	
High (ca.10 to ∞)	ZSM-5	relatively high stability of lattice
	dealuminated erionite	high stability in acids
	mordenite	low stability in bases
	Y	low concentration of acid groups of high strength

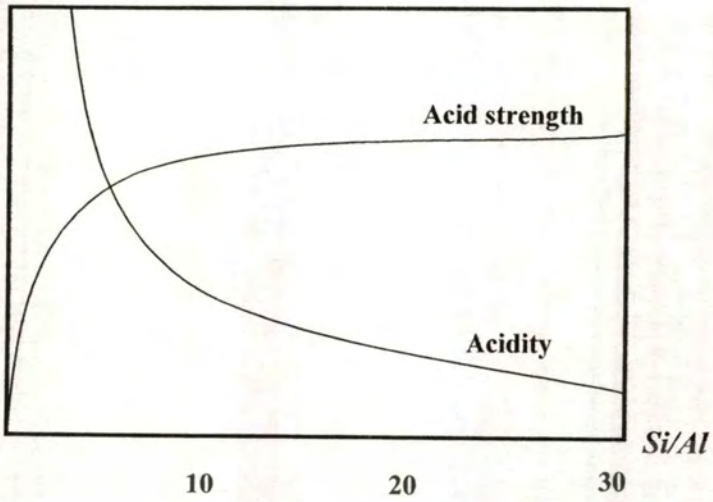

Figure 2.20 Relationship between acidity or acid strength and Si/Al ratio [17]

When H-zeolites are heated to high temperature (>500 °C), waters are released from the zeolites leading to defect of frameworks. These defects are electron deficient sites so they can act as Lewis acid catalyst (Figure 2.21). This is very strong acid site that can be used as catalyst for carbocation generation from alkanes in cracking process.

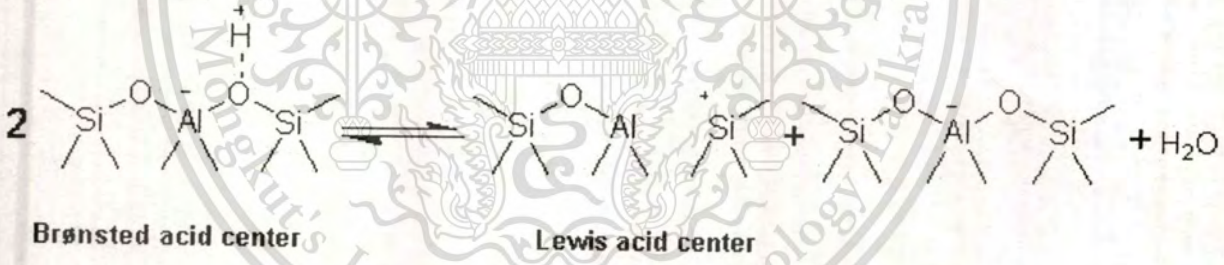

Figure 2.21 Dehydration of Brønsted acid center to Lewis acid center [15]

Figure 2.22 shows the transformation of Brønsted to Lewis acid centers of H-Y zeolite as function of calcination temperature by monitoring of IR spectroscopic measurement on pyridine adsorption.

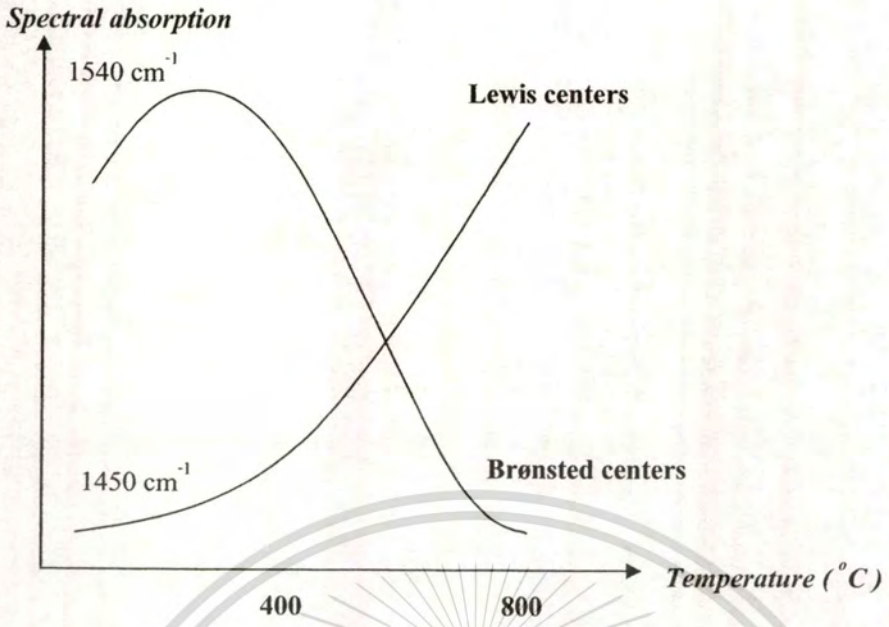

Figure 2.22 Calcination of an H-Y zeolite: equilibrium between Brønsted and Lewis acid centers [15]

2.5 Selective Oxidations [1]

Selective oxidation can be classified into two categories (see Figure 2.23): one is electrophilic oxidations which proceed via activation of dioxygen to electrophilic forms such as O_2^- or O^- and other is nucleophilic oxidation which hydrocarbons are activated to react with nucleophilic oxygen (O^{2-}).

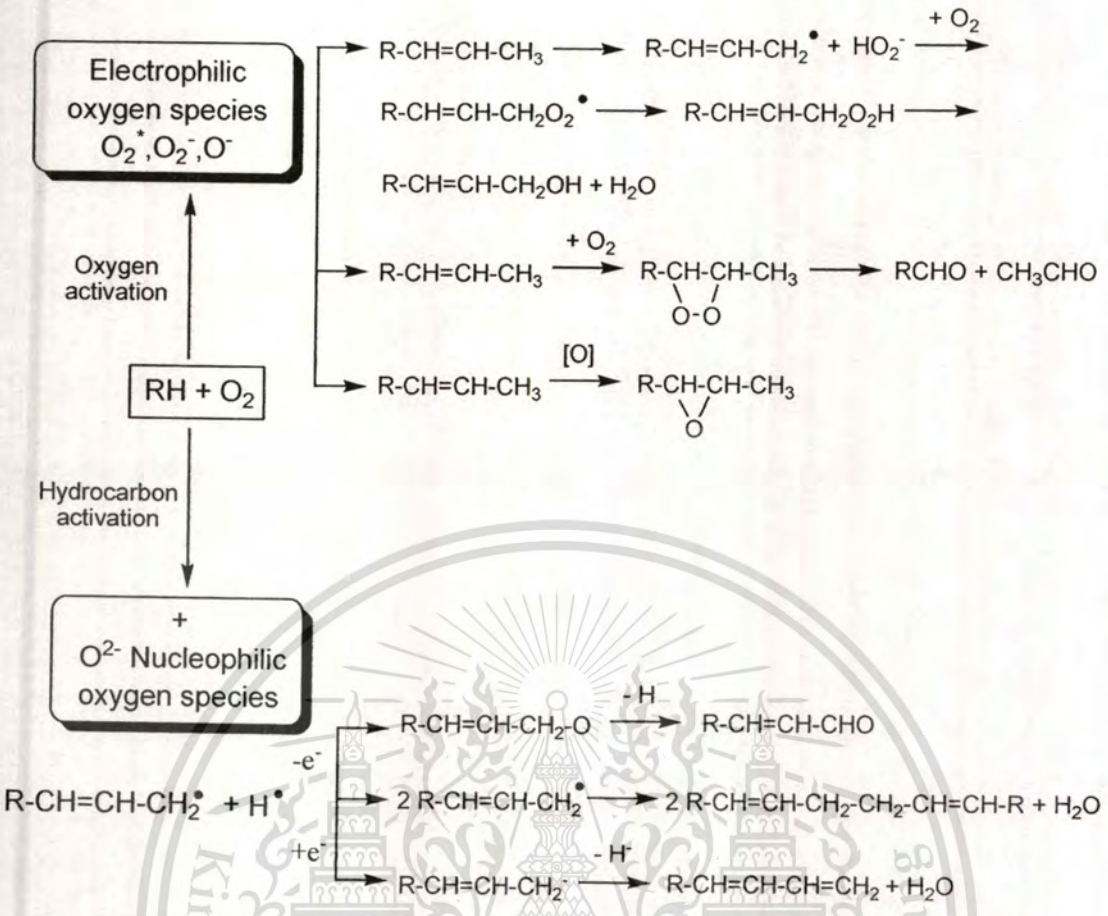

Figure 2.23 Electrophilic and nucleophilic mechanisms for catalytic oxidation of hydrocarbons

Electrophilic oxidations include i) atomic oxygen radicals addition to double bond to form epoxides, ii) homolytic cleavage by oxygen radicals to form alkyl radicals then react with oxygens to form hydroperoxides iii) double bond cleavage of alkenes to form two aldehydes iv) total oxidation: readily cleavage of all C-C and C-H bonds to form carbon dioxide and water.

Nucleophilic oxidations covers i) hydrogen abstraction of alkanes to form alkenes or dienes such as oxidative dehydrogenation ii) hydrogen abstraction of alkanes followed by nucleophilic addition of hetero atoms such as oxygen, sulfur, nitrogen or chlorine to form hetero molecules such as aldehydes, ketones and alcohols. In case of oxygen addition, while electrophilic oxidations attack pi-bond of alkenes, nucleophilic oxidations can protect them. The nucleophilic reactants may be obtained from gas phase additive (e.g. N from NH_3 or Cl from HCl). In case of oxygen, an O^{2-} can be provided from reduction of oxygen in lattice of catalysts by the reactant. After that vacant oxygen is compensated by re-oxidation of the lattice by oxygen

in gas phase. This redox mechanism was postulated by Mars and van Krevelen in 1954. The cycle of mechanism can be described as follow:

1) When reactant contacts a $M_1^{n+}O^{2-}$ site, a hydrogen atom is abstracted from reactant by lattice oxygen.

2) The oxygen gives one electron per hydrogen abstracted to lattice to form water.

3) The product alkene and water desorb from surface of catalyst result in oxygen vacant site.

4) The lattice cation M_1^{n+} is reduced to M_2^{m+}.

The oxygen vacancy is filled and the reduced cation is reoxidized by migration of lattice oxygen from another M_2^{m+} which is reoxidized by oxygen from gas phase. Sometime, this process can be repeated more than once in same molecule.

Example of hydrocarbon oxidations classified by reaction type (nucleophilic and electrophilic) and elementary transformation with suitable catalyst are shown in Table 2.6

Table 2.6 Chemistry of heterogeneous oxidation of hydrocarbons [1]

Electrophilic oxidation		**Nucleophilic oxidation**	
Reaction type	**Catalyst**	**Reaction type**	**Catalyst**
Double bond fission		*Without introduction of the hetero atom*	
- Oxidation of alkenes to oxides	Ag_2O	- Oxidative dehydrogenation of alkanes and alkenes to dienes	$BiPO_4$
- Oxydehydration of alkenes to saturated ketones	SnO_2-MoO_3	- Oxidative dehydrogenation and dehydrocyclization of alkenes	$BiPO_4$
C-C bond fission		*With introduction of the hetero atom*	
- Oxidation of alkenes to saturated aldehydes	V_2O_5	*Introduction of hetero atom into hydrocarbon chain*	
- Oxidation of aromatics to anhydrides and acids with ring rupture	V_2O_5-MoO_3	(I) Introduction of oxygen	
Total oxidation to $CO_2 + H_2O$	Co_3O_4,	- Oxidation of alkenes to unsaturated aldehydes and ketones	Bi_2O_3-MoO_3
	$CuCo_2O_4$,	- Oxidation of alkylaromatics to aldehydes	V_2O_5-TiO_2
	$CuCr_2O_4$	(II) Introduction of nitrogen- ammoxidation of alkenes to nitriles	Bi_3O_3-MoO_3
		Introduction of hetero atom into acyl group	
		(I) Oxidation of aldehydes to acids	NiMoO4
		(II) Oxidation of alkylaromatics to anhydrides	V_2O_5-TiO_2

2.5.1 Adsorption over Redox Oxide Surfaces [18]

On redox catalysts, chemisorptions phenomenon take place on solid surfaces. The surface of metal oxides can be considered to two types of active site; a positive charge including the metal cations and a negative charge including the oxygen anion. However, several oxides in redox catalysts have metal or metalloid cations connect with anionic oxygen in form of coordinative bond (not ionic). For example, vanadia and molybdena exist in compound as complex anions

which represent by VO_3^- and $Mo_7O_{24}^{6-}$ respectively. Thus their surface possess V=O and Mo=O functional groups which are important in many catalytic reactions.

If an oxide surface is considered to be a piece of the cleaved bulk solid, the surface metal centers will surround by neighbor oxygens and will have unsaturated coordinate bond (i.e. Mo=O). This is driving force for the chemisorption species to relieve the coordinative unsaturated from metal centers as shown in Figure 2.24. It is a mode of methanol chemisorption over molybdenum oxide.

Figure 2.24 Chemisorption of methanol over molybdena surface

Other interested example is oxegen molecule (O_2). It has three electron pairs in outer bonding orbitals and two unpaired electrons in two antibonding π^* orbitals. The O_2 species is initially attached to reduced metal site such as V (IV) by coordinative binding. After that, the electron density is transferred toward O_2 and enters the π^* orbitals result in weakness of the oxygen-oxygen bond until bond dissociated (Figure 2.25). This cooperative action involves more than one reduced sites.

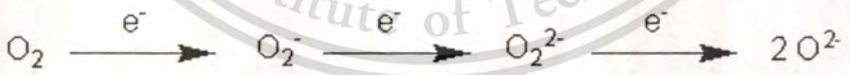

Figure 2.25 Cleavage step of adsorbed oxygen molecule on metal oxide surface

Key feature of redox catalysts is metal or metalloid centers on the surfaces that can be easily changed their oxidation state. However, the solid must preserve overall electrical charge neutrally so it necessary to gain or loss oxygen from lattice concurrently.

2.5.2 Oxidation Reaction on Redox Catalysts [18]

Redox catalysts can be defined as catalysts which able to operate both oxidation and reduction sequentially at surface. Two possible mechanism of oxidation over surface of catalysts can be described below:

A) $\frac{1}{2} O_2$ (g) ⟶ O (ads)

X (ads) + O (ads) ⟶ Products

B) X (ads) + O (lattice) ⟶ Products + Lattice vacancy

$\frac{1}{2} O_2$ (g) + Lattice vacancy ⟶ O (lattice)

where, X = reactant

Differences between two mechanisms are source of oxygen react. In A, oxygen has better adsorption than X then X reacts to remove excess adsorbed oxygen. For B, X reacts with oxygen in lattice of metal oxides (called reduction) result in oxygen vacancies in lattices. After that the lattices are filled by gas phase oxygen (called oxidation). When X are organics reactant, mechanism A tent to be deep oxidation and produce carbon oxides and water which has no utility in industrial However, mechanism B gives selective oxidation that generates various partial oxidation of organic molecules such as carbonyl and unsaturated compounds which is valuable chemicals. It conforms to Mars-van Krevelen mechanism which is described earlier.

Most of the selective oxidation catalysts formally contain full or empty outer *d*-orbital such as Mo^{6+} ($4d^0$), V^{5+} ($3d^0$) and Sb^{5+} or Sn^{4+} (both $4d^{10}$). The oxide of such elements have ability to release associated lattice oxygen (formally O^{2-}) for incorporation into organic adsorbates. with compensating reduction of metal centers to preserve formal electrical neutrality. The structure of these metal oxides is not ionic lattice which are separated between metal cations and oxide anions but they are coordination bonds between metal and oxygen.

The structure of vanadia surface can be represented as Figure 2.26. The corresponding to Mars-van Krevelen mechanism proceed through oxidation of organic species using oxygen from V=O group. This results in reduction of V(V) pairs to V(IV). After that the oxygen in gas phase can reoxidize V(IV) centers to V(V) and V=O groups are rebuilded subsequently. The bond strength of V=O is approximately 300 kJ mol^{-1} which allow oxygen atom to be changeable. Prove of Mars-van Krevelen mechanism had been test by oxygen isotopes [18]. The oxidation of butane over

vanadia ($V_2{}^{16}O_5$) with ${}^{18}O_2$ (g) is found that only ${}^{16}O$ appear in the initial products. This result shows that oxygens which react with reactant are oxygens from vanadia, not from the gas phase oxygens.

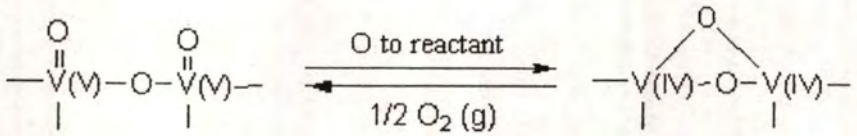

Figure 2.26 The surface of vanadia act as redox catalyst for oxidation reaction [18]

Vanadia catalyst can be promoted by adding potassium salt. For example, in the methanol oxidation to formaldehyde, the 85% selectivity on pure vanadia can be elevated to 97% when 10-20 wt% of potassium sulfate was added. There is also an increase in the rate at specified temperature. It can be explained that potassium species on surface donate electron density to the oxide. It decrease strength of V=O coordinative bond which depend on electron density that transfer from O to V. This phenomenon measure that the performance of selective oxidation catalysts is strongly related to an ability to release lattice oxygen.

Most of selective oxidation catalysts are mixed oxide of metals or metalloids. The basic component is a transition metal oxide in groups V, VI or VII in periodic table because they have ability to do the nucleophilic addition of their lattice oxygen. The most common metal oxides for this role are vanadium or molybdenum oxide while antimony pentoxide is used sometimes. The other component is oxide of lower oxidation state number metals such as iron(II), bismuth (III) or uranium (IV). These lower valent centers act as active site for dissociative adsorption of organic reactants (see Figure 2.27). Table 2.7 gives example of reactants, mixed oxide catalysts and products of selective oxidations.

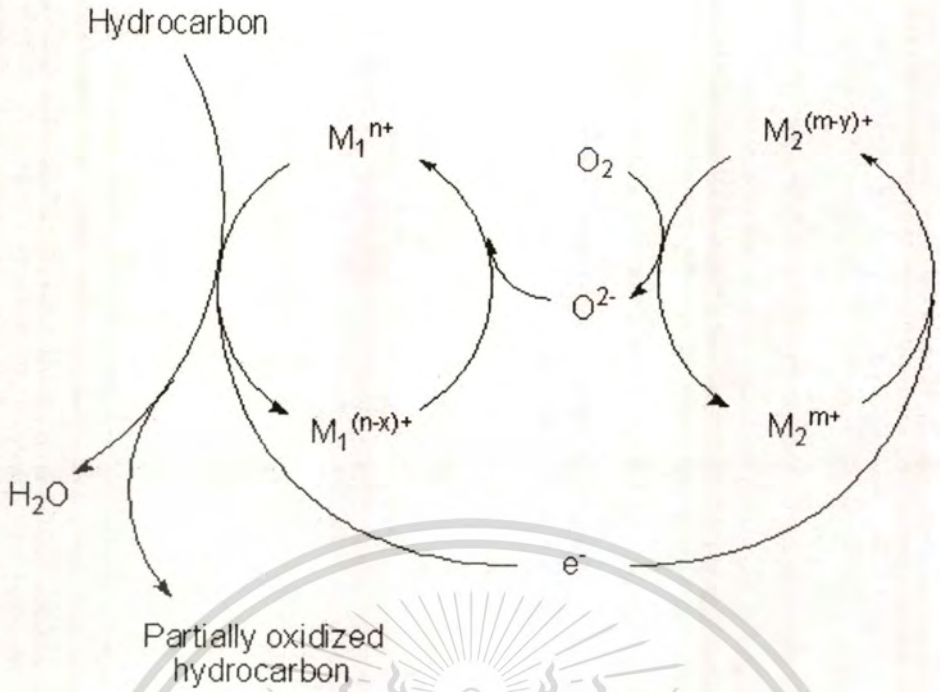

Figure 2.27 Schematic representations of surface-catalyzed partial oxidations; M_1 and M_2 represent the two metals in mixed metal oxide catalyst [19]

Table 2.7 Examples of selective oxidation processes catalyzed by chemically mixed oxides in the presence of molecular oxygen [18]

Reactant	Major product	Catalyst component	Typical temperature (K)
Propylene	Acrolein	Bi_2O_3, MoO_3	650
		UO_2, Sb_2O_5	
Isobutene (+water)	Acetone	UO_2, MoO_3	600
		SnO_2, MoO_3	
Methanol	Formaldehyde	Fe_2O_3, MoO_3	653
Acrolein	Acrylic acid	V_2O_5, MoO_3	673
1-Butene	Butadiene	CdO, MoO_3 (2%TeO_2)	683
1-Butene	Maleic anhydride	CoO, MoO_3	753

In mixed oxide system, both metal oxides have co-operative work between each structure which may be well understood by examining the mechanism of selective oxidation of propylene

to acrolein over the mixed oxide of bismuth and molybdenum. The action of each units can be described as shown in Table 2.8.

Table 2.8 Action of structural units of chemically mixed oxides of bismuth and molybdenum in the selective oxidation of propylene [18]

Unit	Action
Bi-O-Mo	Dissociative chemisorption of propylene to form the allylic radical by abstraction of the α-hydrogen atom
Bi center	Chemisorption of allylic radical
Mo center	Supply of lattice oxygen for insertion into allylic radical
Bi-O-Bi	Chemisorption of oxygen from the gas phase to replenish lattice oxygen at the molybdenum center, achieve through solid state diffusion of oxide ions

2.6 Literature Reviews

Despite the chemistry of how to obtain acrolein from glycerol dehydration is known for a long time, such process was seriously attended due to widely expansion of biodiesel production that generate large amount of glycerol. The simple dehydration of glycerol is homogeneous process. In 2006, Masaru Watanabe *et al.* used sulfuric acid as catalyst for continuous gas phase dehydration at supercritical condition of water. They obtained 74 mol% yield of acrolein with 81 % selectivity and found that high pressure can readily enhance both glycerol conversion and selectivity to acrolein. In addition, an increase in sulfuric acid concentration promotes acrolein selectivity and slightly improves glycerol conversion [13].

Nowadays, the trends of research lie on heterogeneous catalysis due to feasibility for industrial processes. Various acidic oxides were tested in gas phase dehydration without pressure. However, the common acid oxides such as Al_2O_3 (37 mol% selectivity), SiO_2/Al_2O_3 (30%) and TiO_2 (16%) did not provide satisfied selectivity to acrolein [20]. In 2007, Nb_2O_5 was studied by Song-Hai Chai *et al.* They reported that the high calcination temperature could decrease the catalyst surface area and acid strength, which result in a drop of activity. Their catalyst deactivated after 3 hours on stream, while selectivity to acrolein remained constant (51 mol%) [12].

WO_3/ZrO_2 was found that be highly active catalyst since 2005. Later in 2009, WO_3/ZrO_2 activity was tested by Arga Ulgen and Wolfgang Hoelderich and 75% selectivity to acrolein with 100 % conversion of glycerol were obtained. They announced that high loading of WO_3 gave better selectivity to acrolein but took no effect for glycerol conversion. The basic sites in ZrO_2 decreased selectivity to acrolein. However, those basic sites could be removed by calcination at 600 °C. The inter-molecular dehydration that gave oligomer was preferable at temperature below 240 °C. In addition, the presence of oxygen (< 7%) enchants selectivity to acrolein but slightly reduce glycerol conversion [21].

Recently, phosphorus compound including Al_2O_3-PO_4, TiO_2-PO_4, SAPO-11 and SAPO-34 were tested by Wladimir Suprun *et al.* Although a similar selectivity were obtained as previous works, they proposed interesting reaction pathways for the formation of by-products. Furans were generated from acetol and cyclic oxygenated C_6 derivatives were produced from two intermediates; 3-HPA and oligomerized glycerol. In addition, they also found that coke could be preferably deposited at high temperature [22].

Zeolites are also known as superior acid catalysts for many petrochemical processes including dehydration of alcohols. ZSM-5 and Y zeolites were tested by Avelino Corma *et al.* in 2008 with two type reactors; fixed bed and fluidized bed. They concluded that oxygenated compounds could not be operated at high temperature (500-720 °C) because glycerol were decomposed to cracking products including CO, CO_2, C_1-C_4 alkanes, ethylene, propylene and acetaldehyde. At low temperature (290-350 °C), 62% selectivity to acrolein was obtained when ZSM-5 was used. They also found that high concentration of glycerol led to coking and secondary products from hydrogen transfer. While the presence of water reduced coke in zeolites pore. The selectivity to acrolein from the reaction in fixed bed reactor was also lower than that of fluidize bed. However, this could be compensated by increasing catalyst to feed ratio [23].

Most preferred catalysts at present are heteropoly acids. Eriko Tsukuda *et al.* introduced silica supported silicotungstic acids (HSiW) that successfully reach 86% selectivity to acrolein with 98% glycerol conversion. However, this catalyst possessed low stability. In the same paper, phosphotungstic and phosphomolibdic acids were also tested but gave relatively poor performance, as compared to that of silicotungstic acid [20].

Hereafter, many researchers attempted to develop heteropoly acids on other supports. Ning Lili *et al.* reported that silicotungstic on activated carbon gave 75% selectivity to acrolein [24]. Hanan Atia used alumina supported and achieved 64% selectivity to acrolein when silicotungstic was active component [25]. Zirconia was also good support that provided 71% selectivity to acrolein as reported by Song-Hai Chai [26]. However, stability of catalysts were not improved.

Unlike the dehydration of glycerol, the oxidation of acrolein to acrylic acid has been widely investigated since 1970s. It was known as a part of propylene oxidation process [1, 27]. For selective oxidation of acrolein, MoO_3 and WO_3 alone were inactive while V_2O_5 was quite active but non-selective [28]. Most of the studies suggested that vanadium-molybdenum mixed oxides based (V-Mo oxides) were appropriate catalyst. Kitahara *et al.* reported that 17.8 wt% of MoO_3, V_2O_5 and Al_2O_3 (8:1:0.4 by mol) on spongy aluminium gave 85.7 % yield of acrylic acid with 97.3% acrolein conversion at temperature 573 K [29].

The performance of V-Mo oxides catalyst was improved with 30 wt% $MoVO_x$ supported on aerosil (SiO_2). The ratio of Mo:V was 5:1 by mol. Ethylenediamine was used as reducing agent. The catalyst was calcined at 453 K then annealed in air at 573 K. 100 % acrolein conversion and 96 % yield of acrylic acid were obtained [29].

It was suggested that the performance of catalyst strongly depended on amount of V^{4+} species. However, annealing in air at high temperature resulted in the loss of activity due to the loss of V^{4+} [29].

In general, selective oxidation competes against total combustion and the oxidation products could be further oxidized to CO_2 [30]. The reaction between acrolein and lattice oxygen in V-Mo oxides were investigated by TPR with MS detector. It was found that CO_2 could be minimized at temperature below 400 °C [31]. While acrylic acid could be selectively generated with low conversion at temperature between 300 and 450 °C (depend on Mo:V ratio) [32].

For industrial practice, the third or more metals are added as promoter to increase the production rate. It was found that alkaline additive including Cs, K and Na did not affect the selectivity but lower the activity. While weak acid and base or amphoteric oxide (i.e. CuO) could improve selectivity without dramatically change in the acid-base property of catalyst surface [29]. In 1990s, Copper and iron were combined to V-Mo oxides system by J. Tichy and J. Machek [33]. The oxide of $Mo_{12}V_3Cu_2Fe_{0.5}$ successfully gave 98.3 % to acrylic acid with 59 % acrolein conversion. Moreover, W-V-Mo oxides based catalysts were widely used. $Mo_9V_3W_{1.2}O_x$ gave nearly 100 % selectivity to acrylic acid with low total combustion during 3-8 hours on stream at 543 K [34]. Tungsten doped catalysts exhibited a long-term stability, as compared to tungsten-free V-Mo oxides. XAS measurement indicates that tungsten did not participate in the redox process [28]. TPR of $Mo_9V_2W_{1.2}O_x$ showed that the initial temperature of selective oxidation took place at ~ 150 °C which is lower than that of V-Mo oxides. However the initial combustion temperature was decreased to ~ 200 °C [35]. In addition, P_2O_5-MoO_3 oxides were also used as catalyst for selective oxidation with Mo/P of 4.5-24.5. However, it was found that selectivity to acrylic acid (maximum ~ 75 %) was lower than that obtained from V-Mo oxides based catalysts [36].

CHAPTER 3

EXPERIMENTAL

3.1 Chemicals

1. Glycerol USP grade (>99.5%); Union Chemical 1986 Co.,Ltd.
2. Distillated water
3. Air zero grade; Praxair
4. Nitrogen 99.999%; Praxair
5. Helium 99.999%; Praxair
6. HZSM-5 (Si/Al=12.5); Zeochem (Zeocat PZ-2/25H)
7. NH_4^+ZSM-5 (Si/Al=28); Zeolyst (CBV 5524G)
8. NH_4^+ZSM-5 (Si/Al=180); Zeolyst (CBV 28014)
9. HZSM-5 (Si/Al=250); Zeochem (Zeocat PZ-2/500H)
10. HZSM-5 (Si/Al=500); Zeochem (Zeocat PZ-2/1000H)
11. NH_4^+Beta (Si/Al=14); Tohso Co.,Ltd (HSZ930NHA)
12. HMordenite (Si/Al=15); Tohso Co.,Ltd. (HSZ660HOA)
13. HY (Si/Al=100); Tohso Co.,Ltd. (HSZ390HUA)
14. Ammonium molybdate powder ($(NH_4)_6Mo_7O_{24}.4H_2O$); APS Ajax Fine Chem
15. Ammonium metavanadate (NH_4VO_3); APS Asia Pacific Specialty Chemicals Limited
16. Silicic acid (for the preparation of lipid chromatography); BDH Chemicals Ltd.
17. Hydroxyacetone >95%; Sigma-Aldrich

3.2 Apparatuses

1. Syringe pump; Razel (A-99)
2. 10 ml gas tight syringe with a foot-long needle; Hamilton Company USA
3. Tube furnace; Carbolite (MFT 12/25/250)
4. Glass trap
5. Glass tube reactor with glass rod and glass wool
6. Bubble flow meter
7. Septum
8. Vials

9. Circulator with cooling unit; Haake (K15)
10. Stainless steel tubes, connectors, valves and fittings; Swagelok
11. Teflon tubes and fittings; Swagelok
12. Mass flow controllers; Allborg (GFC17)

3.3 Experimental Procedures

3.3.1 Catalyst Preparation

All zeolites are calcined in a horizontal tube furnace which is flowed by 60 mL/min of air zero. The temperature is set to 500 °C with ramp rate of 1 °C/min, and held at that temperature for 5 hours. Zeolites are pressed into a disc at 3 tons then crushed and sieved into 600-850 micron (or 20-30 meshes) of USA standard sieve (ASTM E-11). The pellet zeolites are kept in dried plastic containers at room temperature.

The solution of V-Mo precursor was prepared as shown in Table 3.1. Ammonium molybdate and ammonium metavanadate precursors are dissolved in 150 mL of distillated water. The mixture is heated at 80 °C until total volume of solution is below 20 mL. The mixed precursor solution is adjusted to 20 cm^3 by distilled water addition then kept in plastic container.

Table 3.1 Weight of precursors and support for $VMoO_x$/Silicic acid preparation

Formular	V_2O_5+MoO_3 (wt%)	SiO_2 (wt%)	Mole ratio		Precursors weigh (g)		Support weight (g)
			V	Mo	NH_4VO_3	$(NH_4)_6Mo_7O_{24}4H_2O$	Silicic acid
1	43	57	1	5	0.31	2.34	2.85
2	43	57	1	3.3	0.44	2.21	2.85
3	43	57	1	1	1.07	1.62	2.85
4	43	57	3.3	1	1.87	0.85	2.85
5	10	90	1	3.3	0.03	0.17	1.44
6	20	80	1	3.3	0.07	0.34	1.37
7	28	72	1	3.3	0.10	0.52	1.29
8	35	65	1	3.3	0.14	0.69	1.21
9	48	52	1	3.3	0.20	1.03	1.06
10	69	31	1	3.3	0.34	1.72	0.76
11	100	0	1	3.3	0.44	2.21	0

The wetness impregnation method is applied for preparation of $VMoO_x$/silicic acid. The silicic acid powder, that is calcined in air zero (60 mL/min) at 500 °C for 5 hours, is weighted into plastic beaker as indicated in Table 3.1. The V-Mo precursor solution is elaborately dropped into support until wet. The mixture is then dried in oven at 80 °C. The process is repeated until all V-Mo precursor solution is consumed. The V-Mo on support is left to dry overnight.

After impregnation, the catalyst is calcined in a horizontal tube furnace under a flow of air zero (60 mL/min). The temperature is set at 300 °C with a ramp rate of 1 °C/min and held at that temperature for 5 hours. After that, the sample is pressed, crushed and sieved into 600-850 micron.

3.3.2 Characterization of Catalysts

1. Elemental Analysis

Elemental composition of catalyst is determined by a X-ray fluorescence spectrometer (XRF; Siemens SRS3400). The sample can be prepared by mixing 0.5 g of catalyst with 4.5 g of boric acid binder and ground in a ball-mill (Rock Lab grinder). The mixture is pressed into aluminium pan at 150 kN. The analysis can be done by placing a sample pan into a sample chamber. Lithium fluoride, pentaerythrite and W/Si multilayer are used as diffracting crystal and Rhodium is used as source for measurement at 50 kV, 60 mA.

2. Crystal Structure

Crystal structure of the catalyst is determined by a X-ray diffractometer (XRD; Siemens D8 Advance). CuKα is used as analytical X-ray source at 30 kV, 30 mA. The sample is prepared by spreading catalyst over sample holder and placed into the instrument. The sample is scanned from $2\theta = 5$ to 80 with 1sec/step time and 0.04 2θ/step increment.

3. Surface Area

Surface area of the catalyst is measured by a gas absorption analyzer (Quantachrome Autosorb-1). Nitrogen (N_2) is used as probe molecules. The sample is prepared by weighting approximately 0.02-0.05 g of the catalyst into a sample cell. Before testing, the surface of catalyst is cleaned by outgasing at 280 °C. The sample cell is moved to the analysis station. Adsorption isotherm is measured in a pressure range of 0.05-0.30 P/P_0 at 70 K.

4. Morphology and Surface Composition

Field emission spectrometry (FE-SEM; Hitachi S-4800) is applied for determining catalyst morphology. The sample is prepared by dispersing the catalyst sample on a carbon tape of an SEM stub. Then, it is coated with gold by ion sputtering. The stub is transferred to instrument and electron image is analyzed at 20 kV and 10^{-1} mbar

Deep surface composition of V-Mo oxides on silicic acid is instantly quantified using energy-dispersive X-ray spectroscopy (SEM-EDX). The probe of SEM is commanded to scan for the elements in the selected area and mapping of elements is also digitally generated.

3.3.3 Catalytic Performance Testing

1. Reaction Testing

(1) Dehydration of Glycerol to Acrolein

The zeolite pellets are packed into the glass reactor (6 mm of inside diameter) and covered by glass wool as an insert shown in Figure 3.1 (enlargement of reactor). The catalyst bed is borne by a glass rod. The glass beads are loaded on top of the bed to facilitate feed flow dispersion.

The catalytic testing rig is also illustrated in Figure 3.1. The reactor is positioned at the center of a vertical tube furnace. Helium is used as carrier gas. The gas flows are controlled by mass flow controllers and checked by bubble flow meter. Before activity testing, the catalyst is activated by heating at 1 °C/min to 500 °C and held at that temperature for 5 hours under the stream of air zero (30 mL/min). The reactor is cooled to the reaction temperature (275-400 °C) and purged with carrier gas (30 mL/min) for half an hour. After that, glycerol solution (10-50 wt%) is fed into reactor by a syringe pump at 1.7 mmol/h. The reaction is operated for 7 hours on stream. The product effluents are trapped at 5 °C and collected hourly.

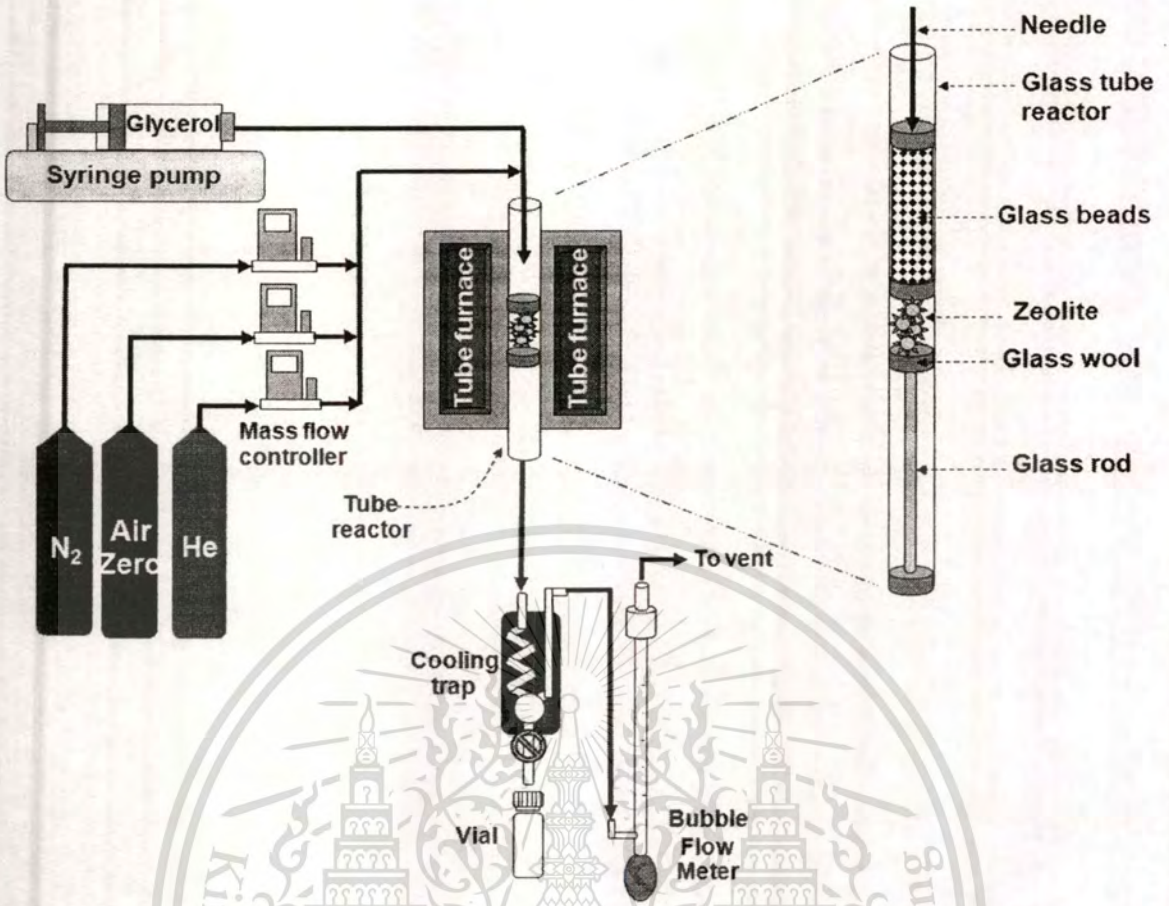

Figure 3.1 Schematic of catalytic testing rig and reactor for glycerol dehydration

(2) Subsequent Oxidation of Glycerol Dehydrated Products

The zeolite pellets and the $VMoO_x$/silicic acid pellets are sequentially packed in two-bed reactor as shown in Figure 3.2. Each bed is screened by glass wool. The glass rod is inserted under the $VMoO_x$/silicic acid bed. The glass beads are introduced as flow dispersing media on top of the catalyst bed.

The two-bed tubular down flow reactor is placed within vertical tube furnace as explained previously. Two mass flow controllers are applied for gas mixing. Air zero diluted with nitrogen is used as oxygen source. The catalysts are activated at 1 °C/min to 300 °C and held at that temperature for 5 hours in air zero (30 mL/min) prior to testing. After that, the catalysts are purged for half an hour under 30 mL/min of reactant gas (5-20 vol% of O_2). Glycerol solution (10 wt%) are fed into the reactor by a syringe pump at a flow rate of 1.7 mmol/h. The reaction is operated for 7 hours on stream. The products are trapped at 5 °C and collected hourly.

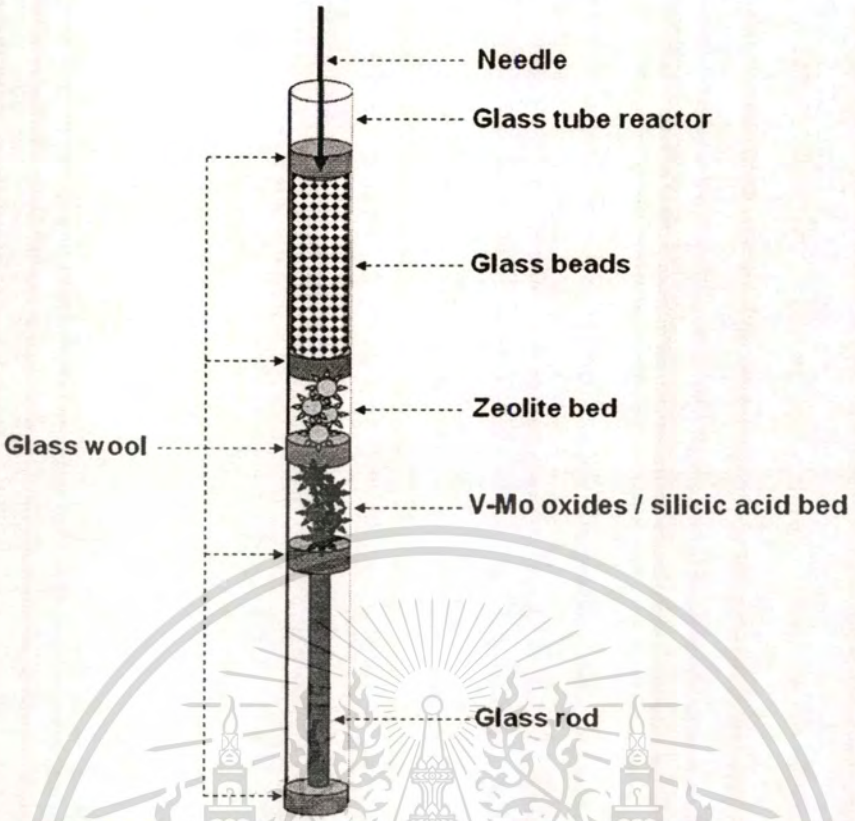

Figure 3.2 Reactor scheme for subsequent oxidation of glycerol dehydrated products

2. Products analysis

Product distribution is identified by a gas chromatograph equipped with mass detector (GC-MS Agilent 6890). DB-Wax (0.52 mm X 30 m) is used as a separating column. The collected products are diluted to 10 wt% in *n*-propanol.

Products are quantified by gas chromatograph equipped with flame ionized detector (GC-FID Variant CP-3800). EC-Wax (0.25 mm X 30 m) is used as a separating column. The products are mixed with equal weight of *n*-propanol as internal standard. The mixture is injected at 0.1 µl and 200 of split ratio.

CHAPTER 4

RESULTS AND DISCUSSION

4.1 Characterization of Catalysts

4.1.1 Elementals Analysis

The silicon-aluminium molar ratio of the zeolites that were used as first bed catalyst, was informed by the manufacturers. It is shown in Table 4.1. In this study, they are titled by framework (silicon/aluminium ratio), for example, Zeocat PZ-2/25H is designated as HZSM-5 (13).

Table 4.1 The silicon-aluminium molar ratio and surface area of zeolites used in this study

Name	Trade name	Silicon/Aluminium	Surface area (m^2/g)
HZSM-5 (13)	Zeocat PZ-2/25H	13	352
HZSM-5 (28)	CBV 5524G	28	466
HZSM-5 (180)	CBV 28014	180	482
HZSM-5 (250)	Zeocat PZ-2/500H	250	376
HZSM-5 (500)	Zeocat PZ-2/1000H	500	349
HBeta (14)	HSZ930NHA	14	523
HMordenite (15)	HSZ660HOA	15	454
HY (100)	HSZ390HUA	100	713

The vanadium-molybdenum molar ratio and vanadium-molybdenum oxides content of the second bed vanadium-molybdenum oxides was determined by X-ray fluorescence spectroscopy. The results are shown in Table 4.2. The samples are designated as xVMo(y) when x is the loading of vanadium-molybdenum oxides on silicic acid support and y is vanadium/molybdenum molar ratio. All catalysts are calcined at 300 °C for 5 hours prior to analysis.

Table 4.2 The vanadium-molybdenum molar ratio and vanadium-molybdenum oxides content of vanadium-molybdenum oxides catalysts used in this study

Name	wt%			V_2O_5+ MoO_3	V/Mo	Surface area
	V_2O_5	MoO_3	SiO_2	(wt%)	(by mole)	(m^2/g)
45VMo(0.2)	4.85	41.9	53.2	46.8	0.18	187
45VMo(0.3)	6.40	38.8	54.8	45.2	0.26	193
45VMo(0.6)	11.6	30.0	58.4	41.6	0.61	211
45VMo(2)	23.1	17.4	59.5	40.5	2.1	240
20VMo(0.3)	3.09	19.3	77.4	22.4	0.25	283
30VMo(0.3)	3.96	25.6	70.2	29.6	0.24	206
40VMo(0.3)	5.36	33.5	61.0	38.9	0.25	201
50VMo(0.3)	7.37	45.4	47.2	52.7	0.26	158
75VMo(0.3)	10.9	63.4	25.6	74.3	0.27	91.4
100VMo(0.3)	14.8	85.3	0.00	100	0.27	37.9
SiO_2	0.00	0.00	100	0.00	-	492

4.1.2 Surface Area

Surface area of all catalysts (zeolites and vanadium-molybdenum oxides on silicic acid) was analyzed by nitrogen adsorption technique and calculated by Brunauer-Emmet-Teller (BET) equation. The results are also shown in Table 4.1 and Table 4.2. All zeolites possess high surface area. While, the surface are of vanadium-molybdenum oxide catalysts markedly decrease when the mixed oxides content is increased.

4.1.3 Crystal Structure

The diffraction pattern of catalysts (zeolites and vanadium-molybdenum oxides on silicic acid) was obtained by X-ray powder diffraction technique (XRD). The CuKα was used as radiation source. The XRD patterns are shown in Figure 4.1-4.4. The 2θ angle of the catalysts diffraction pattern was compared with 2θ angle of the reference diffraction pattern to identify their crystal structure.

For zeolite catalysts, it can be seen that the diffraction pattern of all zeolites used in this study are similar to their reference diffraction pattern (Apendix A) [37]. Hence, the structures of the zeolites are confirmed.

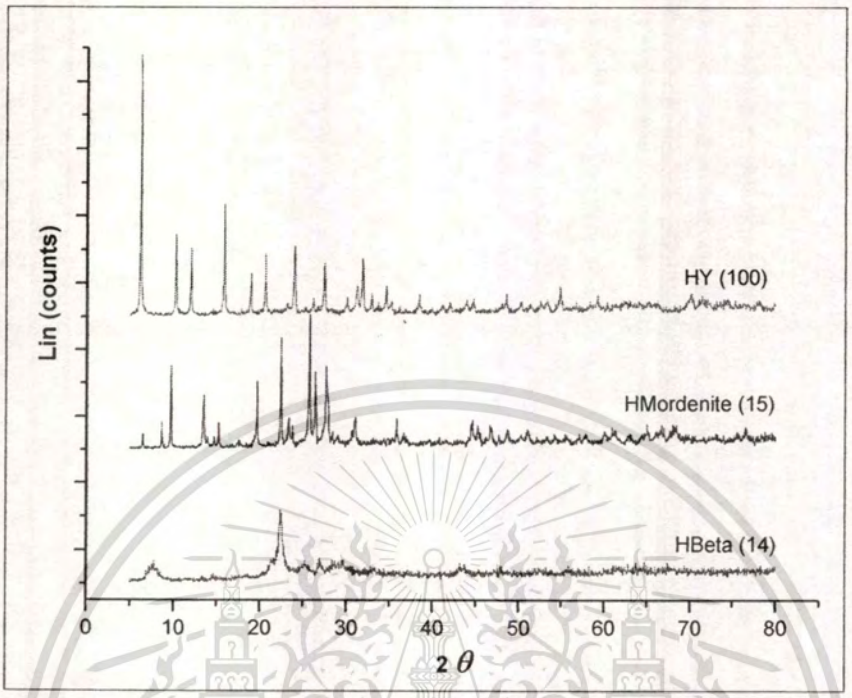

Figure 4.1 X-ray diffraction patterns of HBeta, HMordenite and HY

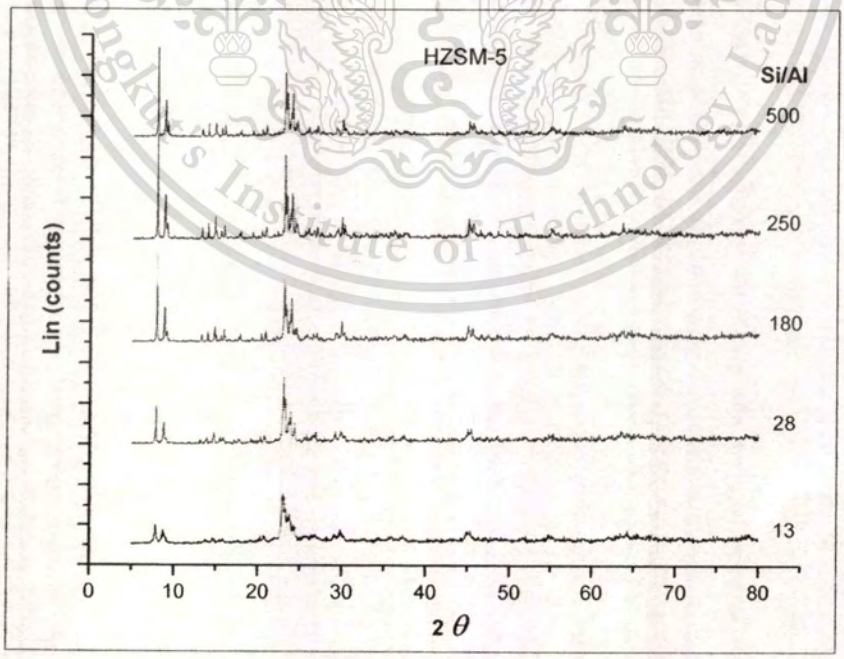

Figure 4.2 X-ray diffraction patterns of HZSM-5

For the vanadium-molybdenum oxides catalysts, the silicic acid support shows only amorphous phase (Figure 4.3). While, the bulk vanadium-molybdenum oxides (V/Mo=0.3) exhibits two phases including V-Mo-O hexagonal [38, 39] and α-MoO_3 [40]. The presence of α-MoO_3 indicates that the molybdenum is in excess for this sample.

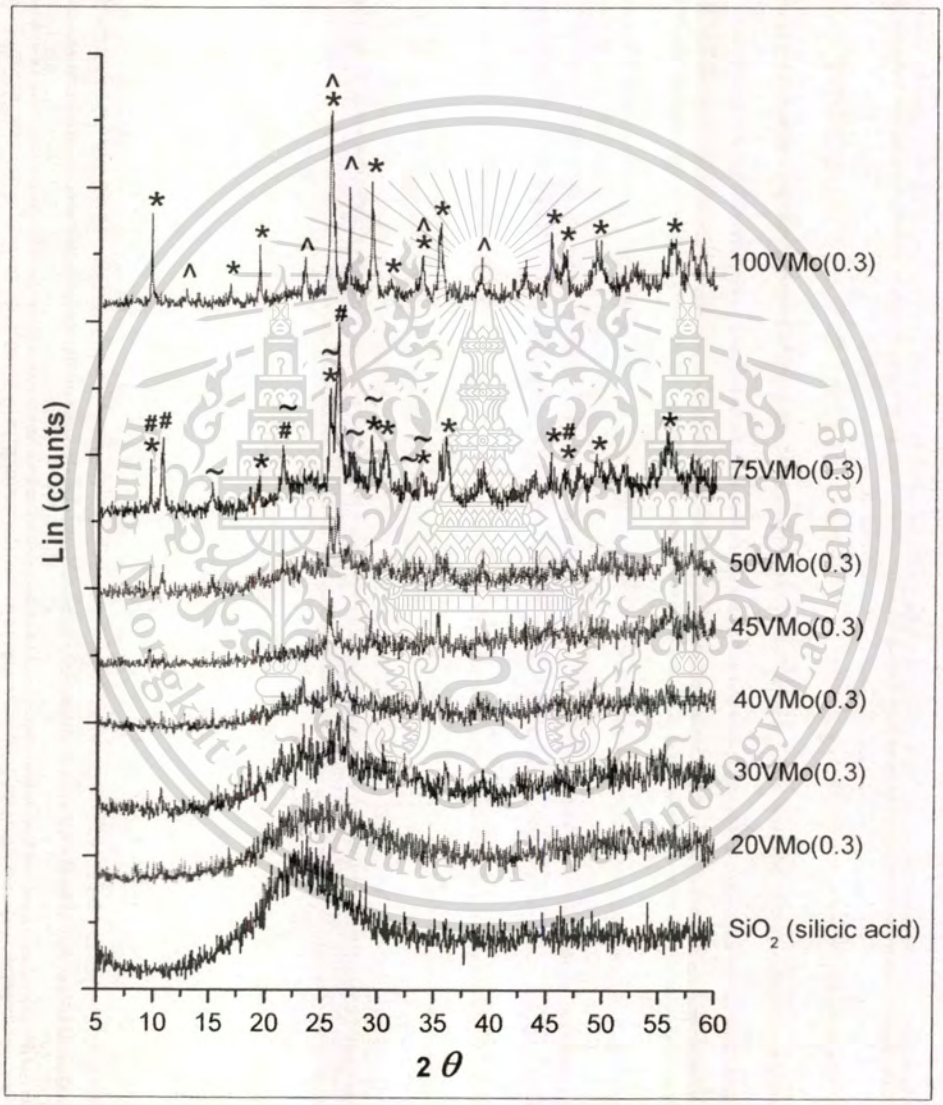

Figure 4.3 X-ray diffraction patterns of various vanadium-molybdenum oxides loaded on silicic acid support at V/Mo = 0.3; ^ = α-MoO_3 (orthorhombic), * = V-Mo-O hexagonal, # = V-Mo-O orthorhombic, ~ = V-Mo-O triclinic

However, when the mixed oxides (20 - 40 wt%) are increasingly loaded on the support, only very weak intensity of V-Mo-O hexagonal can be observed. Since the mixed oxides always exist in crystal form, the relatively small intensity of the mixed oxides phase, as compared to the bulk one, indicates that the mixed oxides are well dispersed. Moreover, the disappearance of α-MoO_3 pattern suggests that it is highly dispersed on silicic acid support. At higher than 45 wt% loading, the V-Mo-O hexagonal and V-Mo-O orthorhombic [41] was revealed and the V-Mo-O triclinic [39, 42] is additionally observed. It can be seen that various phases of V-Mo-O were formed on the silicic acid support and the crystalinity increase with the mixed oxides loading.

At 45 wt% loading, phase was changed when the V/Mo molar ratio was varied as seen in Figure 4.4. The catalyst with V/Mo = 0.2 shows that the excess α-MoO_3 is formed with V-Mo-O hexagonal and V-Mo-O orthorhombic. When the vanadium is increased to the ratio of 0.3, only mix oxides phase of V-Mo-O hexagonal and V-Mo-O orthorhombic can be observed. This indicates that the increase in vanadium can diminish the formation of α-MoO_3. However, the intensity of the V-Mo-O hexagonal and V-Mo-O orthorhombic decrease continuously and disappear at V/Mo = 0.6. This might be due to the effect of SiO_2 support that possess strong interaction with V^{5+} [43]. When the vanadium is increased, the interaction between support and mixed oxide was increased. Hence, the dispersion of mixed oxide is improved and the crystal size becomes smaller. Once the V/Mo is increased to two, the diffraction pattern reveals only vanadium oxide phase [44]. This suggests that the increase in vanadium content also increases the V_2O_5 formation. However, the intensity is very weak and observed only for high vanadium content catalyst due to high dispersion of V_2O_5 on SiO_2 support.

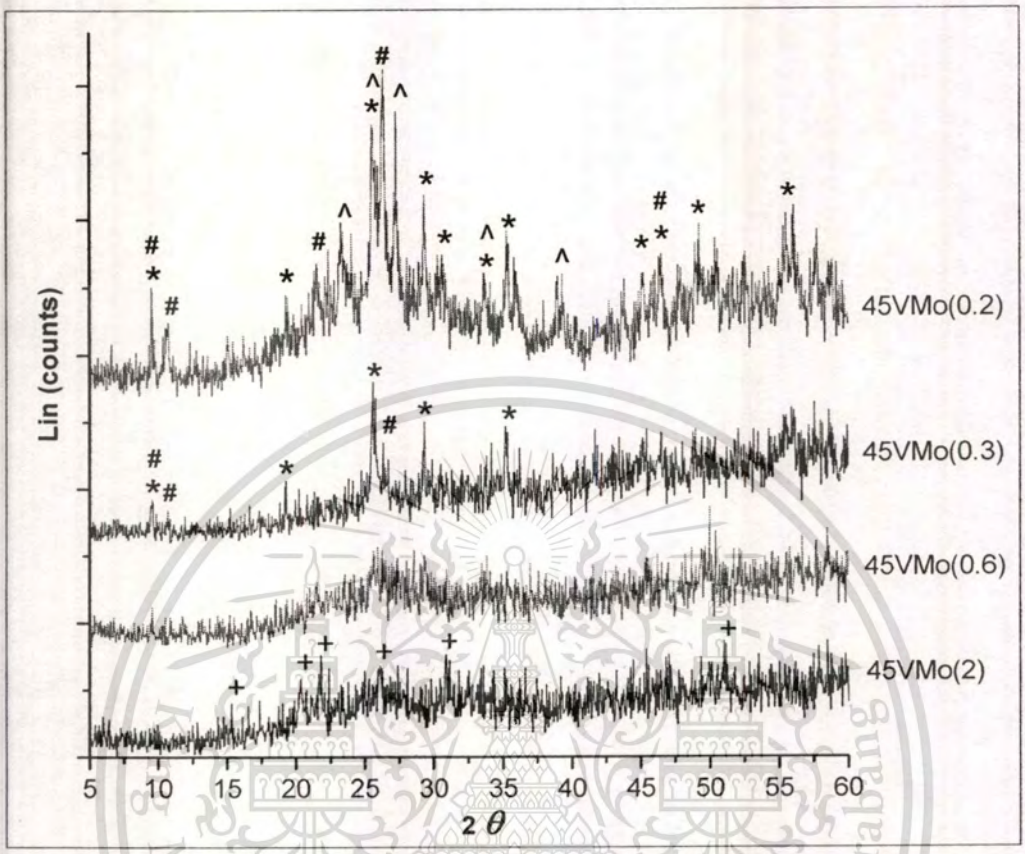

Figure 4.4 X-ray diffraction patterns of catalysts with various V/Mo molar ratios at 45 wt% of vanadium-molybdenum oxide on silicic acid; ^ = α-MoO_3 (orthorhombic), * = V-Mo-O hexagonal, # = V-Mo-O orthorhombic, + = V_2O_5 (orthorhombic)

4.1.4 Morphology and Surface Composition of Vanadium-Molybdenum Oxides on Silicic Acid Support

The morphology of vanadium-molybdenum oxides on silicic acid with V/Mo of 0.2, 0.3 and 0.6 is determined by field emission spectrometry (FE-SEM) as shown in Figure 4.5. It can be seen that the metal oxides clusters are deposited on the silicic acid surface.

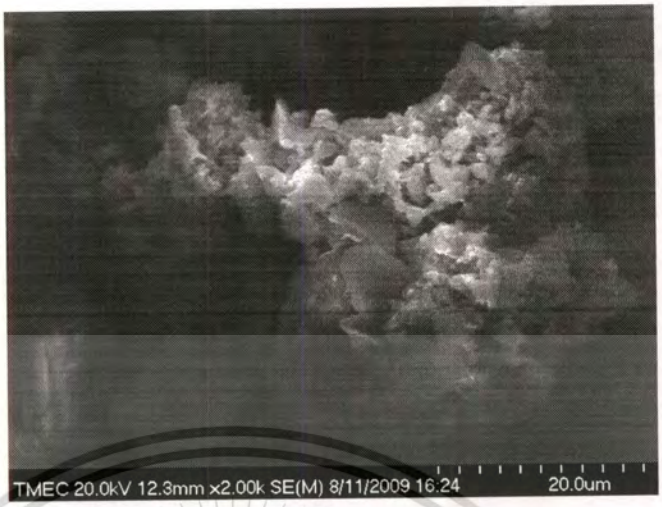

a) 45VMo(0.2)

b) 45VMo(0.3)

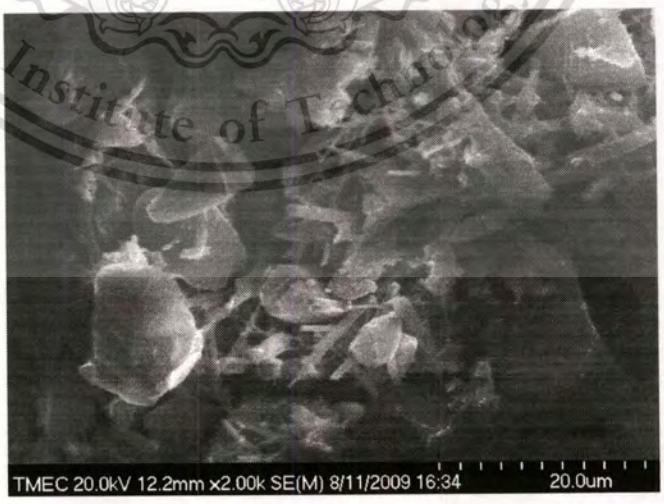

c) 45VMo(0.6)

Figure 4.5 SEM image of 45 wt% vanadium-molybdenum oxide on silicic acid support at V/Mo = 0.2, 0.3 and 0.6

The energy dispersive analysis of such catalysts are also determined to obtain the vanadium and molybdenum dispersion (Figure 4.6). It can be seen that the molybdenum (blue dots) is non-uniformly dispersed on silicic acid surface (SiO_2). This indicates that the interaction between molybdenum and silicic acid are relatively low. Meanwhile, the vanadium (yellow dots) has good dispersion on the silicic acid surface. Moreover, the vanadium is also thoroughly dispersed among molybdenum. It is likely that that the vanadium is co-exist with molybdenum to form the mixed oxides. However, when vanadium content is increased, the isolate vanadium is increasingly observed. This result supports the formation of V_2O_5 phase when vanadium content is increased as dicussed in 4.1.3.

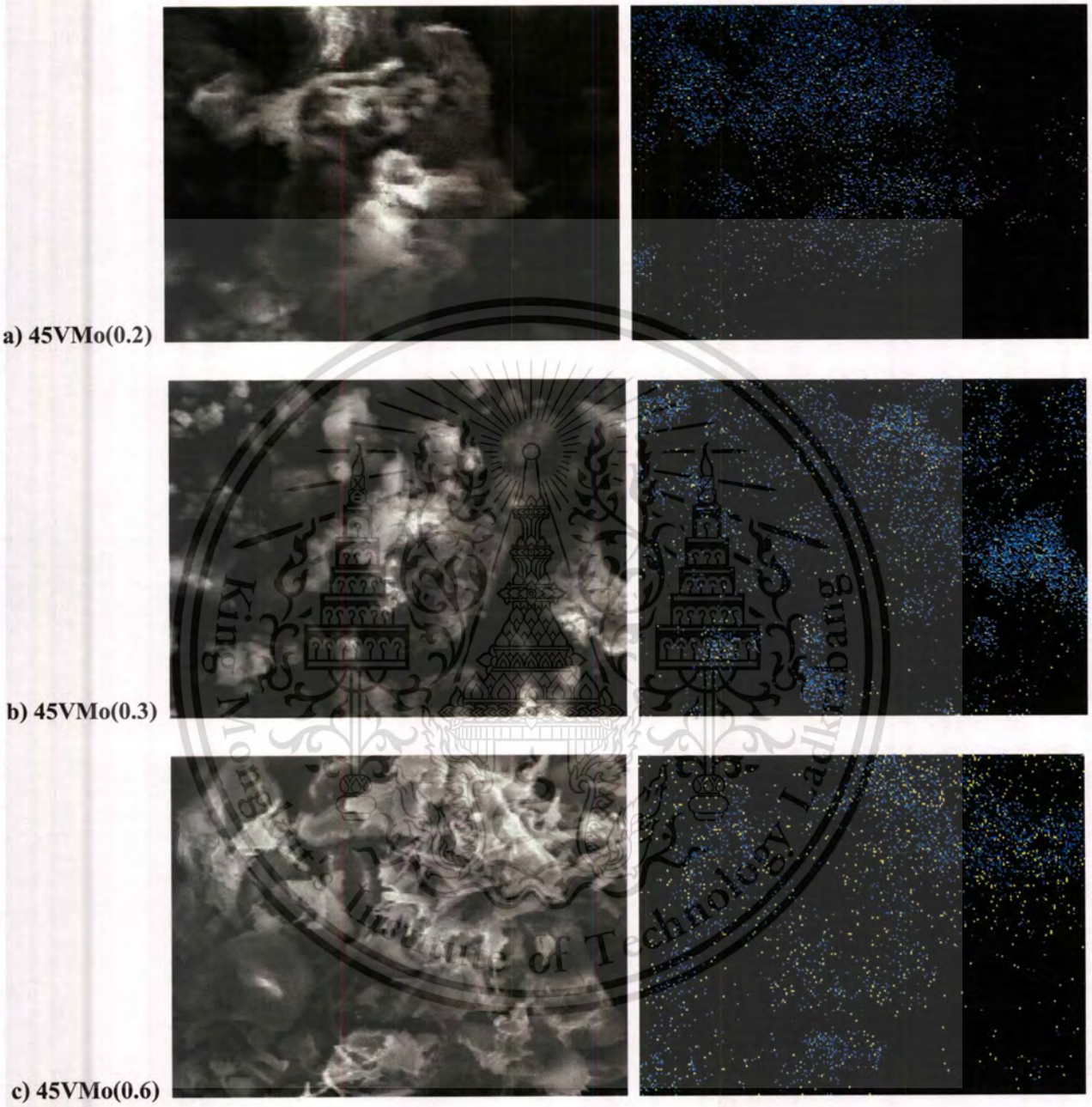

Figure 4.6 SEM-EDX image of 45 wt% vanadium-molybdenum oxide on silicic acid support at Mo/V = 2, 4 and 6; yellow points represent the vanadium and blue points represent the molybdenum

4.2 Dehydration of Glycerol to Acrolein

4.2.1 Effect of Zeolite Contact Time

The contact time of dehydration were studied in range of 29 to 295 g.h.mol^{-1}. The results (Figure 4.7) show that glycerol conversion dramatically increases when contact time is increased. The complete conversion is observed at contact time over 58 g.h.mol^{-1}. It is noted that the amount of catalyst used may well be in excess. In this study, the contact time that provides the complete conversion is required because the unreact glycerol can interfere the oxidation of the dehydrate products in the second bed.

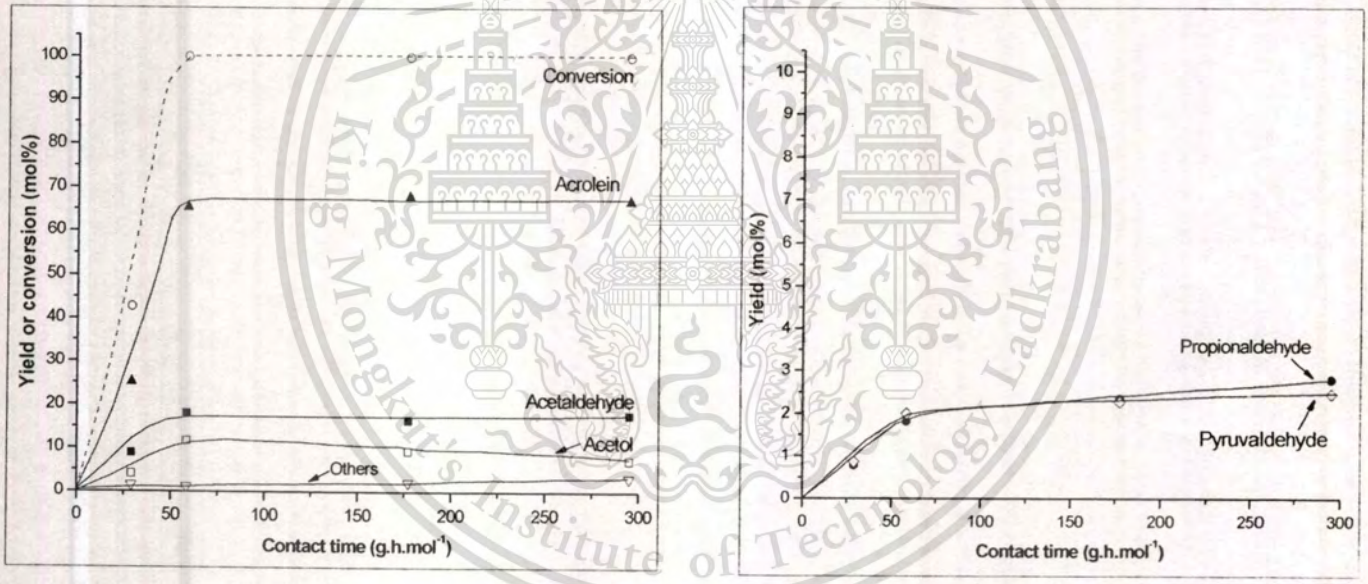

Figure 4.7 The yield and conversion of glycerol dehydration over HZSM-5 (102) as function of contact time

** Reaction conditions; Catalyst: HZSM-5 (180), Temperature: 350 °C, Feed: 1.7 mmol.h^{-1} of glycerol at 10 wt%, Carier gas: 30 ml.min^{-1} of helium; left is major products and right is minor products; the results average between fifth and seventh hour on stream*

It can be seen from Figure 4.7 that the yield of acrolein, acetol and acetaldehyde proportionally increase with the glycerol conversion and reach 67, 12 and 17 mol% at 100 mol% glycerol conversion, respectively. This indicates that acrolein, acetol and acetaldehyde are generated in parallel. It is known that acrolein is generated via double dehydration of glycerol. The first dehydration takes place at the secondary hydroxyl resulting in an intermediate called 3-hydroxypropionaldehyde (3-HPA). This intermediate is then re-adsorbed and the second dehydration takes place immediately at the primary hydroxyl resulting in unsaturated aldehyde. It was also reported by *Tsukuda E. et al* [20] that 3-HPA can be decomposed to acetaldehyde and formaldehyde. The formaldehyde co-product is then decomposed to carbon monoxide as observed in the gas product. In addition, acetol is produced in parallel from dehydration of glycerol at one of the primary hydroxyls resulting in hydroxy ketone compound.

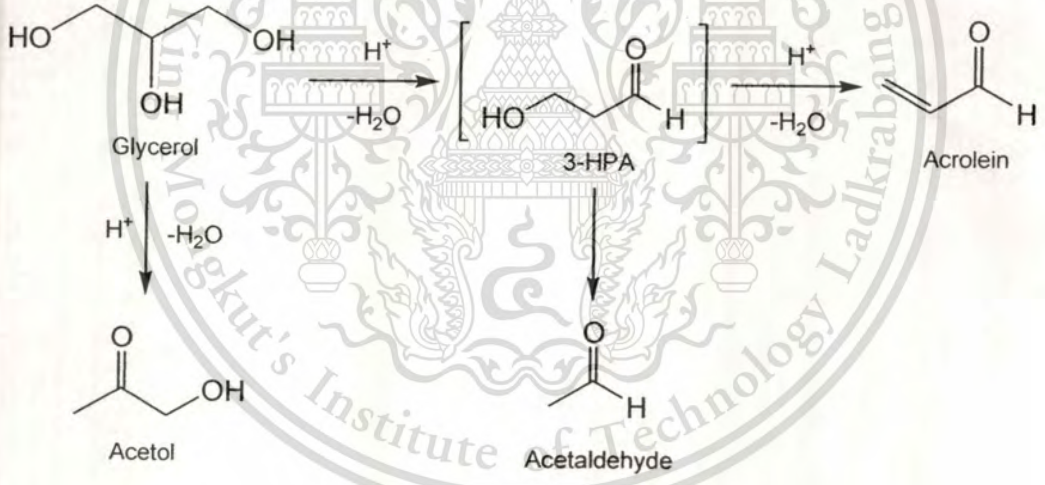

When the excess catalyst is used, the acrolein and acetaldehyde yield do not change. However, the acetol yield decreases gradually (Figure 4.7). This indicates that acetol can be further reacted to form secondary products. Since acetol is more reactive, as compared to acrolein and acetaldehyde, it is likely that the acetol is condensed or oligomerized to higher molecular weight when the catalyst is in excess. In consistence with this view, other products with higher molecular weight thoroughly increase with a decrease in acetol yield. The GC-MS identify that other products are cyclic unsaturated oxygenate compounds as shown below,

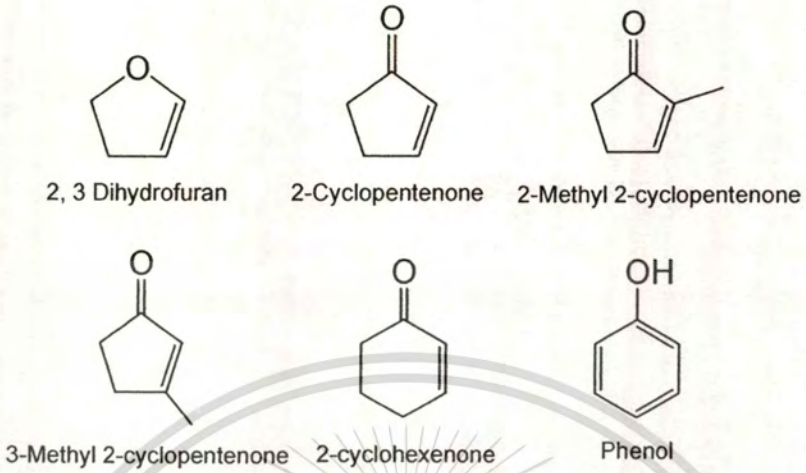

Formation of higher molecular weight oxygenates can be confirmed by the reaction of acetol over HZSM-5 (Table 4.3). When 10 wt% of acetol was fed, a significant yield of other products can be observed. This suggests that acetol can form a "surface oxygenate pool" that can be fragmented to cyclic oxygenated compound. As the reaction proceed, the surface oxygenate pool can evolved to coke which is the cause of the rapid catalyst deactivation as observed from Figure 4.8. In the support view, high coke deposit up to 5.2 wt% of used catalyst is found in the acetol conversion.

Table 4.3 The acetol conversion over HZSM-5 (180)

Products	**Yield** (mol%)	**Selectivity** (mol%)
Acetaldehyde	1.63	6.28
Propionaldehyde	1.10	4.21
Acetone	1.93	7.44
Phenol	2.29	8.82
Others	18.81	72.35

** Reaction conditions; Catalyst: HZSM-5 (180), Contact time: 142 g.h.mol^{-1}, Temperature: 350 ^{o}C, Feed: 2.1 mmol.h^{-1} of acetol at 10 wt%, Carier gas: 30 ml.min^{-1} of helium; the results average between fifth and seventh hour on stream; only 26 mol% acetol is converted*

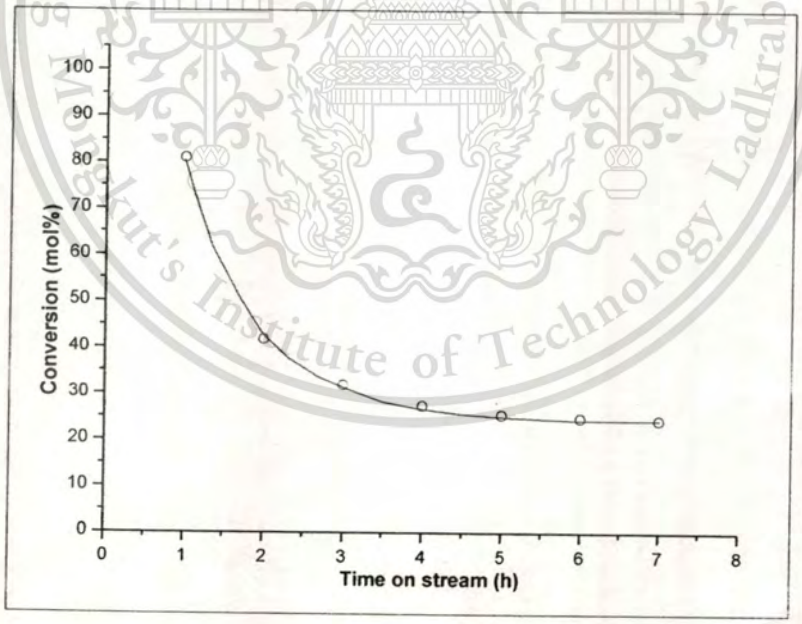

Figure 4.8 The acetol conversion over HZSM-5 (180) as function of time on stream

** The conditions are same as Table 4.3*

In addition to the three major products discussed earlier, pyruvaldehyde and propionaldehyde were somewhat equally found as minor products (approximately 2 mol%). It is suggested that the bi-molecular hydrogen transfers yield pyruvaldehyde and propionaldehyde from the reaction of acetol and acrolein.

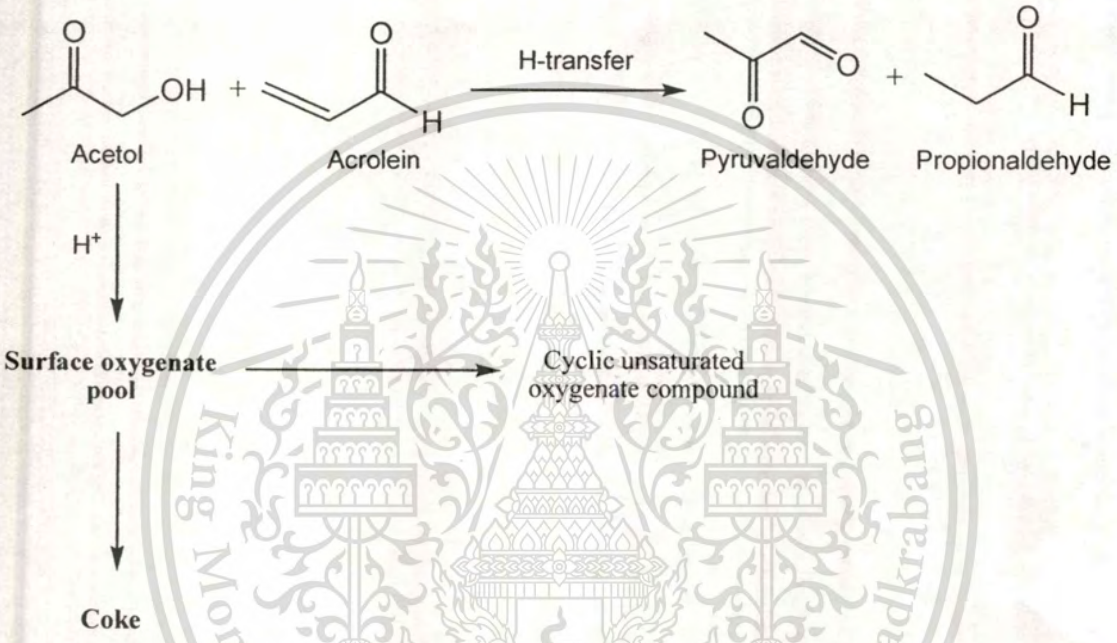

4.2.2 Effect of Zeolite Frameworks

The effect of zeolite structures on dehydration was investigated over HZSM-5, HBeta, HMordenite and HY. The result (Table 4.4) shows that the glycerol conversion is in the order of; HZSM-5 (13) > HBeta (14) > HMordenite (15) for high aluminium zeolites and HZSM-5 (180) > HY (100) for high silica ones. No drop in conversion can be observed over HZSM-5 (13) and HZSM-5 (180) during seven hours on stream (Figure 4.9). Other catalysts show a severe deactivation after certain time on stream. The catalyst with higher stability also give higher conversion. Since the products including acrolein, acetol and acetaldehyde are strongly adsorbed and highly reactive, they can undergo secondary reaction including condensation and oligomerisation to form larger oxygenate pools on the surface. These surface oxygenate pools determine stability of the catalysts because they can evolve to coke deposit. Thermal degradation study of the used catalysts (Table 4.5) confirms that hard coke was found for all catalysts. For the HZSM-5, a medium pore zeolite, condensation or oligomerisation of products to form surface oxygenate pools are somewhat restricted, as compared to that in HBeta and HMordenite. Moreover, the two dimensional pore system facilitates the mass transfer of the products to diffuse out of the pore. Accordingly, the coke is gradually accumulated and the catalyst is relatively stable. Although the deactivation was not observed during seven hours on stream, it is believed that the HZSM-5 (13) and HZSM-5 (180) are continually deactivated as seen from the coke deposits. The excess acid sites keep the 100% conversion despite part of catalyst bed gradually loss their active site.

Table 4.4 The products selectivity and conversion of glycerol dehydration over HZSM-5, HBeta, HMordenite and HY

Catalyst	Conversion	Selectivity (mol%)							
(Si/Al)	(mol%)	Acetaldehyde	Propionaldehyde	Acrolein	Pyruvaldehyde	Acetol	Acetic acid	Propanoic acid	Others
HZSM-5 (13)	100.0	5.71	2.19	81.10	0.64	10.11	0	0	0.25
HBeta (14)	90.66	13.95	2.72	63.97	2.29	10.50	2.38	0.14	4.04
HMordenite (15)	10.57	7.44	1.52	67.25	3.43	10.27	2.55	2.85	4.68
HZSM-5 (180)	100.0	6.23	2.67	78.24	1.40	10.28	0	0	2.59
HY (100)	5.79	25.79	3.26	41.09	5.17	8.09	1.10	0.84	14.67

** Reaction conditions; Contact time: 177 g.h.mol^{-1}, Temperature: 300 °C, Feed: 1.7 mmol.h^{-1} of glycerol at 10 wt%, Carrier gas: 30 ml.min^{-1} of helium; the results average between fifth and seventh hour on stream*

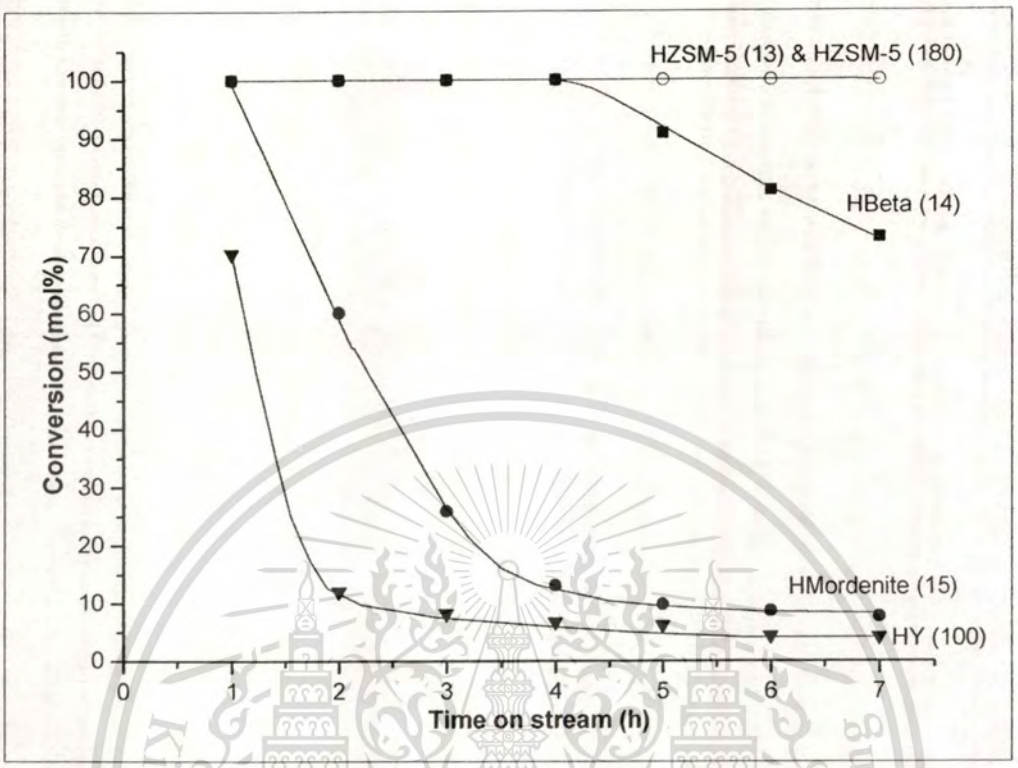

Figure 4.9 The glycerol conversion of HZSM-5, HBeta, HMordenite and HY as function of time on stream

** The conditions are same as Table 4.4*

Table 4.5 Thermo gravimetric analysis of various zeolites after seven hours on stream

Framework types	Coke (wt% of used catalyst)	Decomposition temperature (°C)
HZSM-5 (13)	11.8	556
HBeta (14)	23.7	524
HMordenite (15)	10.3	568

In contrast, condensation or oligomerisation of products in large pore HBeta and HMordenite is readily promoted. Larger extend of surface oxygenate pools can be formed covering the active sites of catalysts. The glycerol cannot be easily adsorbed and the dehydration is inhibited as seen by a lower conversion. Nevertheless, the three dimensional pore system of HBeta gives better mass transfer than one dimensional pore of HMordenite. The molecule has various alternative pathways to diffuse through the three dimension pore. On the other hand, the diffusion is limited in case of one dimension pore. Thus, the HBeta give better conversion although the coke deposition is higher. In case of HY, it has a large pocket within cage structure to promote condensation and oligomerisation of the products. The pool is formed easily and retain in the cage structure. Accordingly, the catalyst is rapidly deactivated. According to the result, the catalyst with appropriate pore size and rapid mass transfer would possess high activity and stability as seen in HZSM-5.

In addition to high conversion, the acrolein selectivity from HZSM-5 is higher than that of HBeta, HMordenite and HY. As described earlier, the mass transfer can be facilitated in HZSM-5 and the dehydrated acrolein can easily diffuse out from pore before further conversion to the secondary products. Moreover, the higher molecular weight oxygenates are restricted by the medium pore of HZSM-5. The oligomerisation of acrolein to surface oxygenate pool takes place somewhat rarely. In other words, the medium pore zeolite facilitates the formation of primary products and prevents them from the secondary reaction.

In contrast to the excellence acrolein selectivity obtained in HZSM-5, the selectivity to cyclic unsaturated oxygenate compounds (other products) from the HBeta, HMordenite and HY are significantly high. This is again because the pool is easily formed in large pore and undergo decomposition to cyclic unsaturated oxygenate compounds as discuss in 4.2.1. Since the cage structure of HY readily promotes the formation of pool, a very large quantity of cyclic unsaturated oxygenate compounds (15 mol%) was observed over this catalyst. It is also note that acetic acid and propanoic acid was found from the HBeta, HMordenite and HY, while this is not the case of HZSM-5.

Acetaldehyde is also produced from large pore zeolite, especially for HY and HBeta. It is likely that the acetaldehyde generation is directly related to the surface oxygenate pool as seen in

cyclic unsaturated oxygenate compounds. It is possible to consider the acetaldehyde as a fragment from surface oxygenate pool. As described in 4.2.1, the acetaldehyde is derived from 3-HPA. Moreover, the 3-HPA is highly reactive and can be further converted to larger oxygenate compound and coke over the acid catalysts [22]. Thus, it is believed that the 3-HPA can be further converted to surface oxygenate pool that can be fragmented to acetaldehyde and cyclic unsaturated oxygenate compounds.

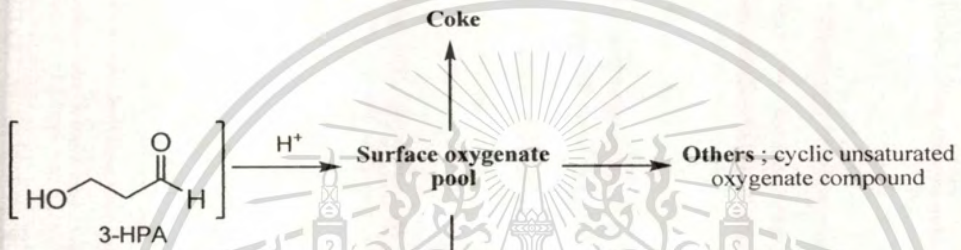

It can be seen that the surface oxygenate pool play important role in secondary reaction. Most of primary products can be transformed to the pools. Simultaneously, the pool is fragmented to secondary products and can evolve to coke deposit on catalyst. The overall reaction pathways for glycerol dehydration over acid zeolites can be illustrated as below.

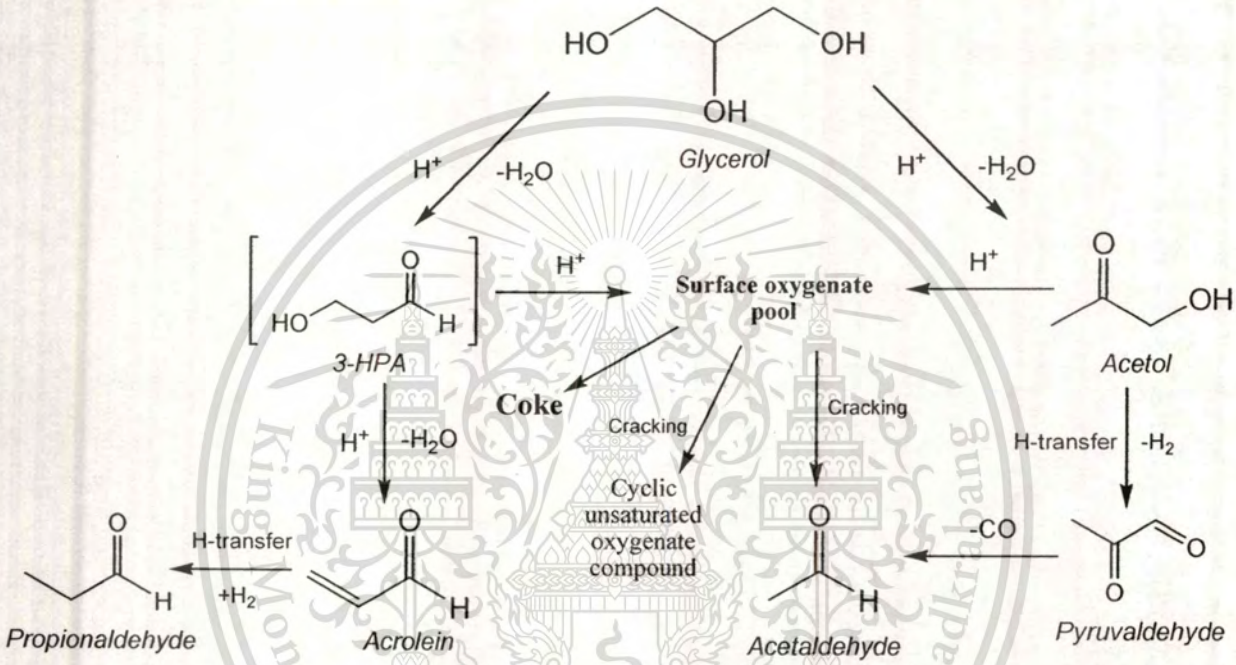

In this study, the HZSM-5 was used as catalyst due to the highest acrolein selectivity and stability.

4.2.3 Effect of Dehydration Temperature

Figure 4.10 shows result of the study in dehydration temperature (275 °C - 400 °C). It can be observed that the glycerol conversion increases with reaction temperature and reach 100 mol% at 300 °C. Theoretically, the elimination reactions, i.e. dehydrations are endothermic process. The reaction favors high temperature. Thus, together with kinetics consideration, the dehydration rate can be elevated by increasing the reaction temperature.

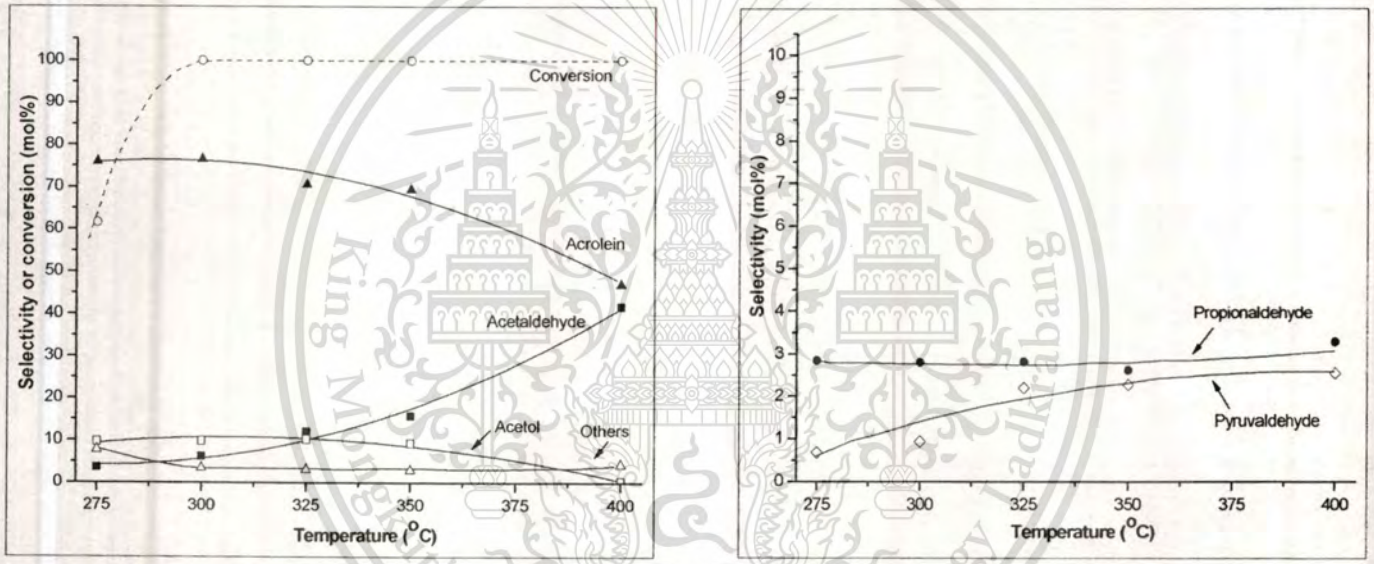

Figure 4.10 The selectivity and conversion of glycerol dehydration over HZSM-5 (180) as function of reaction temperature

** Reaction conditions; Catalyst: HZSM-5 (180), Contact time: 177 g.h.mol^{-1}, Feed: 1.7 mmol.h^{-1} of glycerol at 10 wt%, Carrier gas: 30 ml.min^{-1} of helium; left is major products and right is minor products; the results average between fifth and seventh hour on stream*

In contrast to the conversion, the selectivity to primary products including acrolein and acetol readily decrease when the reaction temperature is increased. This indicates that the primary products can be increasingly converted to secondary products at higher temperature, particularly

the surface oxygenate pool as proposed in 4.2.2. This can be confirmed by thermogravimetric analysis of used catalyst (Table 4.6). The results show that the coke deposits increase with the reaction temperature.

Table 4.6 Thermogravimetric analysis of zeolites at various dehydration temperatures after seven hours on stream

Dehydration temperature (°C)	Coke (wt% of used catalyst)	Decomposition temperature (°C)
300	5.9	450
325	6.2	530
400	7.1	542

Meanwhile, the acetaldehyde selectivity readily increases when the reaction temperature is increased. This is because at higher temperature, the cracking of surface oxygenate pool is drastically taken place according to its endothermic nature. Together with the kinetics consideration, the low molecular weight products particularly acetaldehyde is obtained.

In this study, 300 °C is chosen for reaction temperature because the high selectivity to acrolein can be obtained with a complete conversion. The acetaldehyde and cyclic unsaturated oxygenate compounds selectivity are reasonably low.

4.2.4 Effect of Aluminium Content in Zeolite

The effect of aluminium content in HZSM-5 was investigated between 0.07 and 2.33 mol% (Si/Al = 13-500). The results (Figure 4.11) show that the glycerol conversion drastically increases when increase the aluminium content in catalyst. This is because the increase in aluminium content result in the increase of acid concentration. The glycerol has higher opportunity to interact with the acid sites. Therefore, the catalyst with high acidity gives high activity. In addition, the complete conversion is observed when the aluminium content is over 0.18 mol%. This shows that the acid site may well be in excess for this contact time.

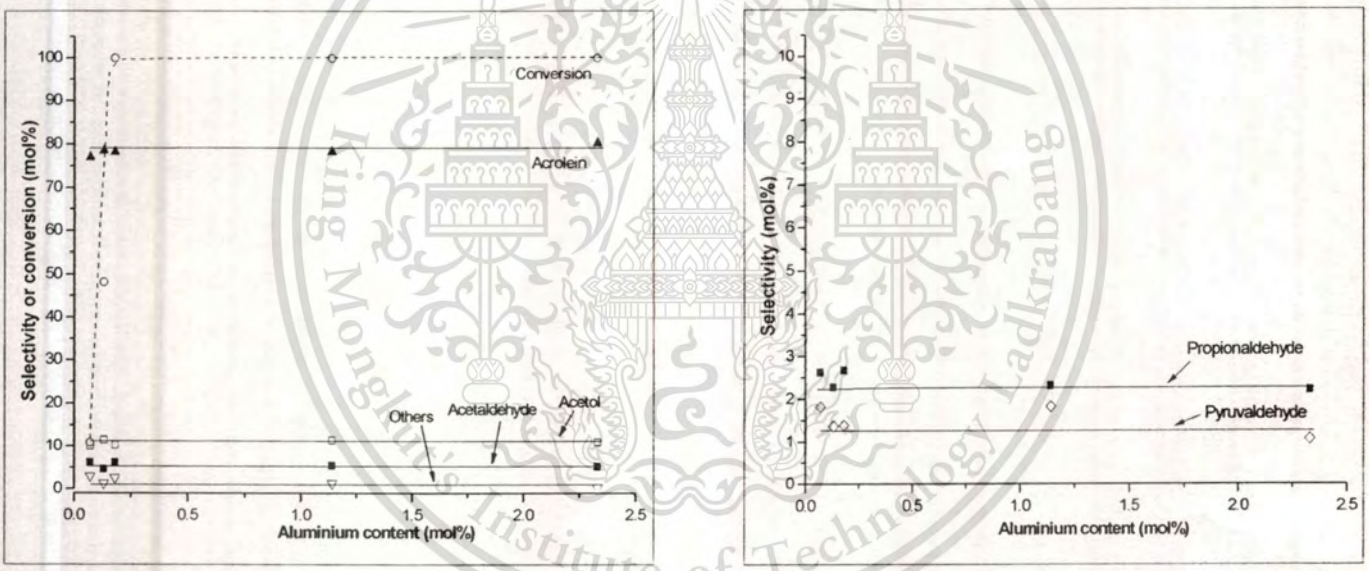

Figure 4.11 The selectivity and conversion of glycerol dehydration as function of aluminium content in HZSM-5

** Reaction condition; Catalyst: HZSM-5, Contact time: 177 g.h.mol^{-1}, Temperature 300 ^{o}C, Feed: 1.7 mmol.h^{-1} of glycerol at 10 wt%, Carrier gas: 30 ml.min^{-1} of helium; left is major products and right is minor products; the results average between fifth and seventh hour on stream*

In line with this view, the coke deposits on HZSM-5 also increase when the alumunium content is increased (Table 4.7). As discussed earlier, the increase in acidity results in the increase in activity for both dehydration and secondary reaction. This results in the increase of pool formation and coke deposit.

Table 4.7 Thermo gravimetric analysis of various Si/Al of HZSM-5 after seven hours on stream

Si/Al	Coke (wt% of catalyst)	Decomposition temperature (°C)
13	11.8	556
28	10.5	550
180	4.6	527
500	0	-

It is noted that the products selectivity does not change when increase the aluminium content of catalyst. As the 100 % conversion is required, the effect of aluminium content on products selectivity cannot be evaluated.

In this study, the HZSM-5 (13) was chosen because the catalyst has highest acidity among this study. The catalyst bed obtain from this catalyst is also thinnest that can prevent the trouble from the bed thickness when the second bed is added.

4.2.5 Effect of Glycerol Concentration

As the 100% conversion is required, the contact time with respect to the glycerol fed is fixed and the glycerol concentrations were varied between 10 and 50 wt%. The result in Figure 4.12 shows that the selectivity to the products does not significantly change when the feed concentration is in range of 10 – 30 wt%. However, the selectivity to acetol increases with the decrease of acrolein selectivity when the feed concentration is increased from 30 to 50 wt%. This indicates that at higher feed concentration, the glycerol molecules become closely interact on the surface. The hydrogen bond formations between glycerol molecules are relatively strong and the difference between primary and secondary hydroxyl group is eliminated. Both can be protonated and the dehydration at primary hydroxyl is proportionally increased. Therefore, the selectivity to acetol is increased and the selectivity to acrolein is decreased.

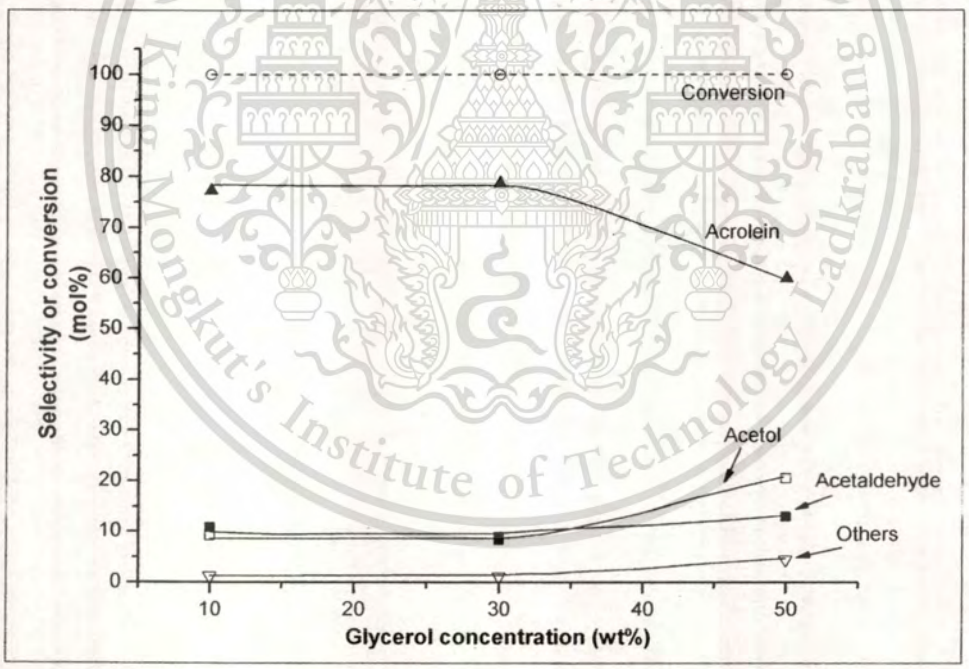

Figure 4.12 The selectivity and conversion of glycerol dehydration over HZSM-5 (13) as function of feed concentration

** Reaction condition; Catalyst: HZSM-5 (13), Contact time: 59 g.h.mol^{-1}, Temperature: 300 ^{o}C, Carrier gas: 30 ml.min^{-1} of helium; the results average between fifth and seventh hour on stream*

The feed concentration also significantly affects the surface oxygenate pool formation. This is seen as a function of acetaldehyde, cyclic unsaturated oxygenate compounds and the coke yields (Table 4.8) when the feed concentration is increased. A similar result is also reported by *Corma A. et al.* [23]. This indicates that at high feed concentration is fed, water concentration is reduced and the high polar products preferentially retain on the catalyst surface. This facilitates the condensation of the primary products to form the surface oxygenate pool and hence coke.

Table 4.8 Thermo gravimetric analysis of HZSM-5 (13) with the various feed concentration after seven hours on stream

Glycerol Concentration (wt%)	**Coke** (wt% of used catalyst)	**Decomposition temperature** (^{o}C)
10	12.8	510
30	12.8	515
50	13.5	528

To obtain high selectivity to acrolein, the glycerol concentration between 10 – 30 wt% was used. This also minimizes the formation of acetol. acetaldehyde and cyclic unsaturated oxygenate compounds.

4.3 Subsequent Oxidation of Glycerol Dehydrated Products

4.3.1 Separate versus Mix System

In section 4.2, we successfully obtained acrolein by the dehydration over HZSM-5. The vanadium-molybdenum oxides was hence included as catalyst for subsequent oxidation of acrolein to acrylic acid. In this study, a separate bed of HZSM-5 (13) and 45VMo(0.3) and physical mixture between HZSM-5 (13) and 45VMo(0.3) were comparatively studied. The results are presented in Figure 4.13.

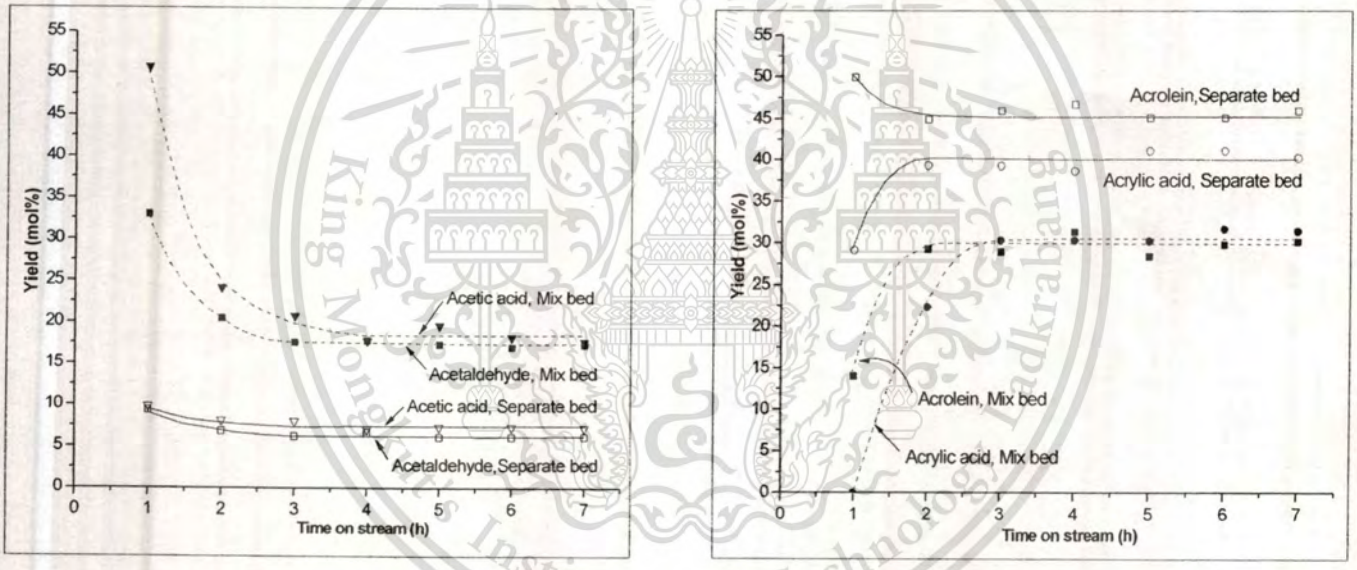

Figure 4.13 Comparative yields of separate and mix bed for subsequent oxidation of glycerol dehydrated products; Left: C_2 oxygenate, Right: C_3 oxygenate

** Reaction condition; Temperature: 300 °C, Feed: 1.7 mmol.h^{-1} of glycerol at 10 wt%, Carrier gas: 30 ml.min^{-1} of 20 vol% O_2 in N_2, Separate system catalyst: 1st bed: contact time: 88 g.h.mol^{-1}, catalyst: HZSM-5 (13), 2nd bed: contact time: 177 g.h.mol^{-1}, catalyst: 45 VMo(0.3), Mix system: contact time: 265 g.h.mol^{-1}, catalyst 1:2 (by wt) of HZSM-5 (13): 45 VMo(0.3)*

It can be seen that the acrylic acid is successfully obtained from both systems. This indicates that the vanadium-molybdenum oxides can be used for acrolein oxidation. However, the yield of C_2 products including acetaldehyde and acetic acid from mixed bed is much higher than that obtained from the separated bed. This might be because the acrylic acid could be decomposed to C_2 products over HZSM-5. Alternatively, it possible that the glycerol is dehydrogenated to higher ketone then decomposed to C_2 oxygenates immediately [45] since vanadium-molybdenum oxides was also active for oxidative dehydrogenation [46-48]. In addition, it can be seen that the acetol, which is minorly found in glycerol dehydration, disappear when the mixed oxides is added for both systems. This suggests that acetol can be decomposed presumably to C_2 products. For the C_3 oxygenate products, the separate system shows the excellence yield of acrolein and acrylic acid (86 mol% totally) while the mixed bed system give only 61 mol%. As the 87 mol% of acrolein is generated by the first bed (Table D21), the better ability to maintain the C_3 oxygenates can be obtained from the separate system with only 1 mol% lost of acrolein. Accordingly, the study in subsequent oxidation of glycerol dehydrated products lies on the separate system.

The result also shows that, the acrolein conversion and yield of products do not change at over seven hours on stream for both systems. Furthermore, no coke deposit on 45VMo(0.3) as observed by thermogravimatric method. This indicates that the vanadium-molybdenum oxides catalyst possesses good stability.

4.3.2 Effect of Contact Time

As the contact time of the first bed (HZSM-5 (13)) is fixed at 88 g.h.mol^{-1}, the subsequent oxidation of glycerol dehydrated products was studied with the contact time of second bed (45VMo(0.3)) between 58 and 295 g.h.mol^{-1}. It can be seen that, as the contact time is increased, yield of acrylic acid is increased together with a decrease in acrolein as shown in Figure 4.14.

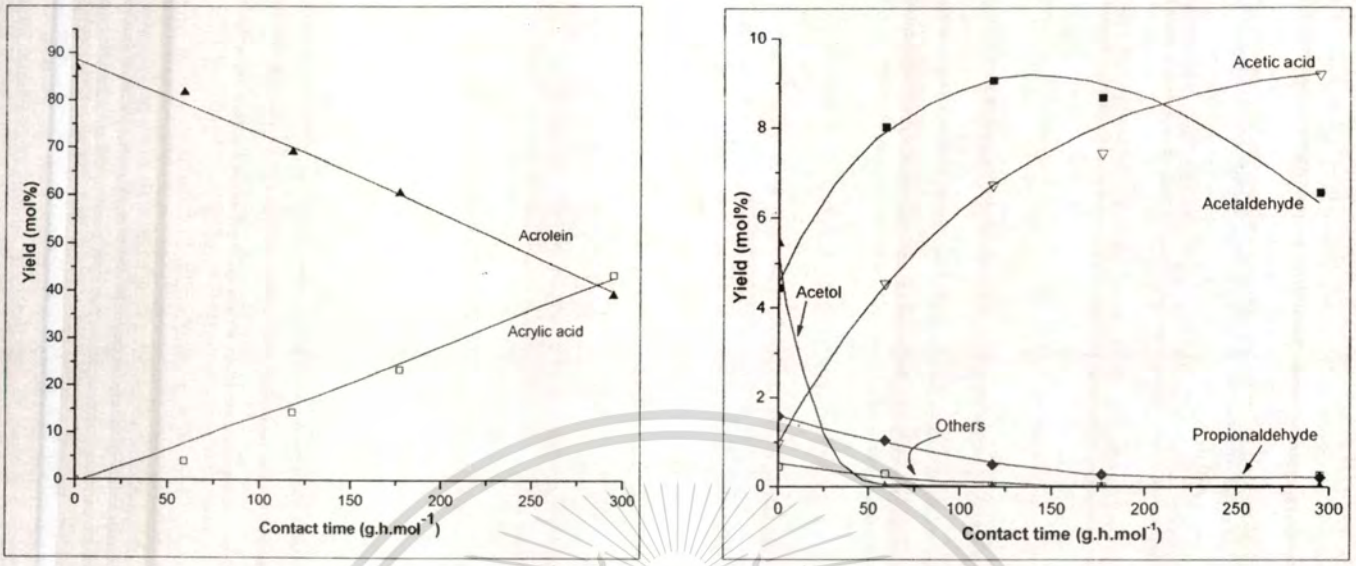

Figure 4.14 The yield from subsequent oxidation of glycerol dehydrated products as function of second bed contact time

** Reaction condition; Temperature: 300 °C, 1st bed: contact time: 88 g.h.mol^{-1}, catalyst: HZSM-5 (13), 2nd bed: catalyst: 45VMo(0.3), Feed: 1.7 mmol.h^{-1} of glycerol at 10 wt%, Carrier gas: 30 ml.min^{-1} of 10 vol% O_2 in N_2; left is major products and right is minor products; the results average between fifth and seventh hour on stream*

This suggests that the acrolein formed in the first bed can be successfully oxidized to acrylic acid. As the oxidation is facilitated by the lattice oxygen of V-Mo-O, the gas phase oxidation is diminished under the reaction condition and selectivity to acrylic acid is relatively high (90 mol% at 177 g.h.mol^{-1}).

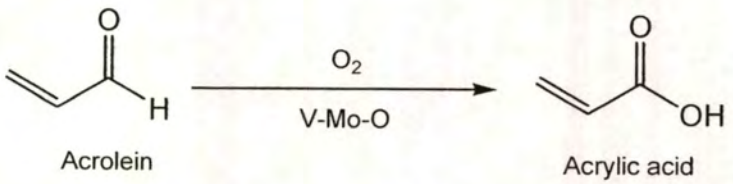

Acrolein Acrylic acid

Similar to the acrolein, the yield of acetol and other products also drop when the contact time is increased. This indicates that acetol and other products can be also decomposed over vanadium-molybdenum oxides. In line with this view, yield of acetaldehyde and acetic acid markedly increase presumably due to the decomposition of the acetol. This is confirmed by the reaction of acetol over 45VMo(0.3) (Table 4.9). It was found that acetic acid is observed as major product while acetaldehyde and pyruvaldehyde are minor ones.

Table 4.9 The acetol conversion over 45VMo(0.3)

Products	**Yield** (mol%)
Acetaldehyde	5.79
Pyruvaldehyde	2.04
Acetic acid	92.17

** Reaction condition; Contact time: 710 g.h.mol^{-1}, Temperature: 300 ^{o}C, Feed: 0.4 mmol.h^{-1} of acetol at 2 wt%; the results average between fifth and seventh hour on stream; 100 mol% acetol is converted*

It is suggested that the acetol can undergo oxidative dehydrogenation to pyruvaldehyde over vanadium-molybdenum oxide [49]. Then, pyruvaldehyde is thermally decomposed to acetaldehyde [48] and carbon monoxide. The gas stream was also analyzed to affirm the carbon monoxide generation and it was found to be equal to the mole of acetol introduced. The acetaldehyde produced can be readily oxidized to acetic acid as seen from subsequent oxidation of glycerol dehydrated products (Figure 4.14) that acetaldehyde decrease and acetic acid increase at contact time over 118 g.h.mol^{-1}.

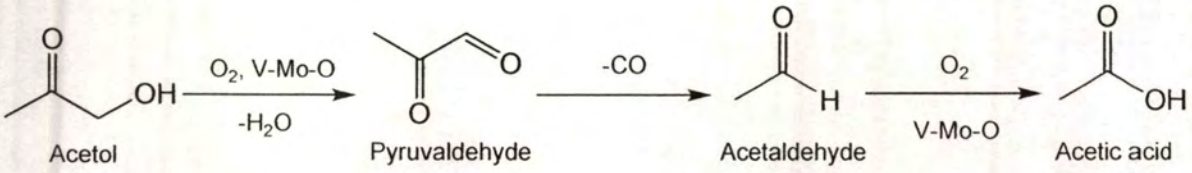

Moreover, the propionaldehyde also decreases with the increase of contact time. This possible that it can undergo oxidative dehydrogenation to acrolein and acrylic acid.

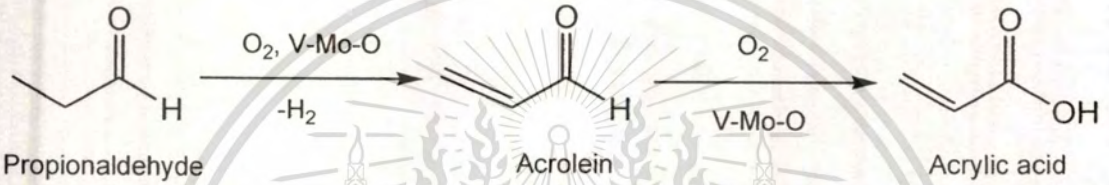

It can be seen that the final products from the selective oxidation of dehydrated glycerol over vanadium-molybdenum oxides are mainly acrylic acids and acetic acid with non-converted aldehydes (acrolein and acetaldehyde). The acetol can be transformed to acetic acid and carbon monoxide. The overall reaction networks of glycerol dehydration with subsequent oxidation were proposed as the scheme below

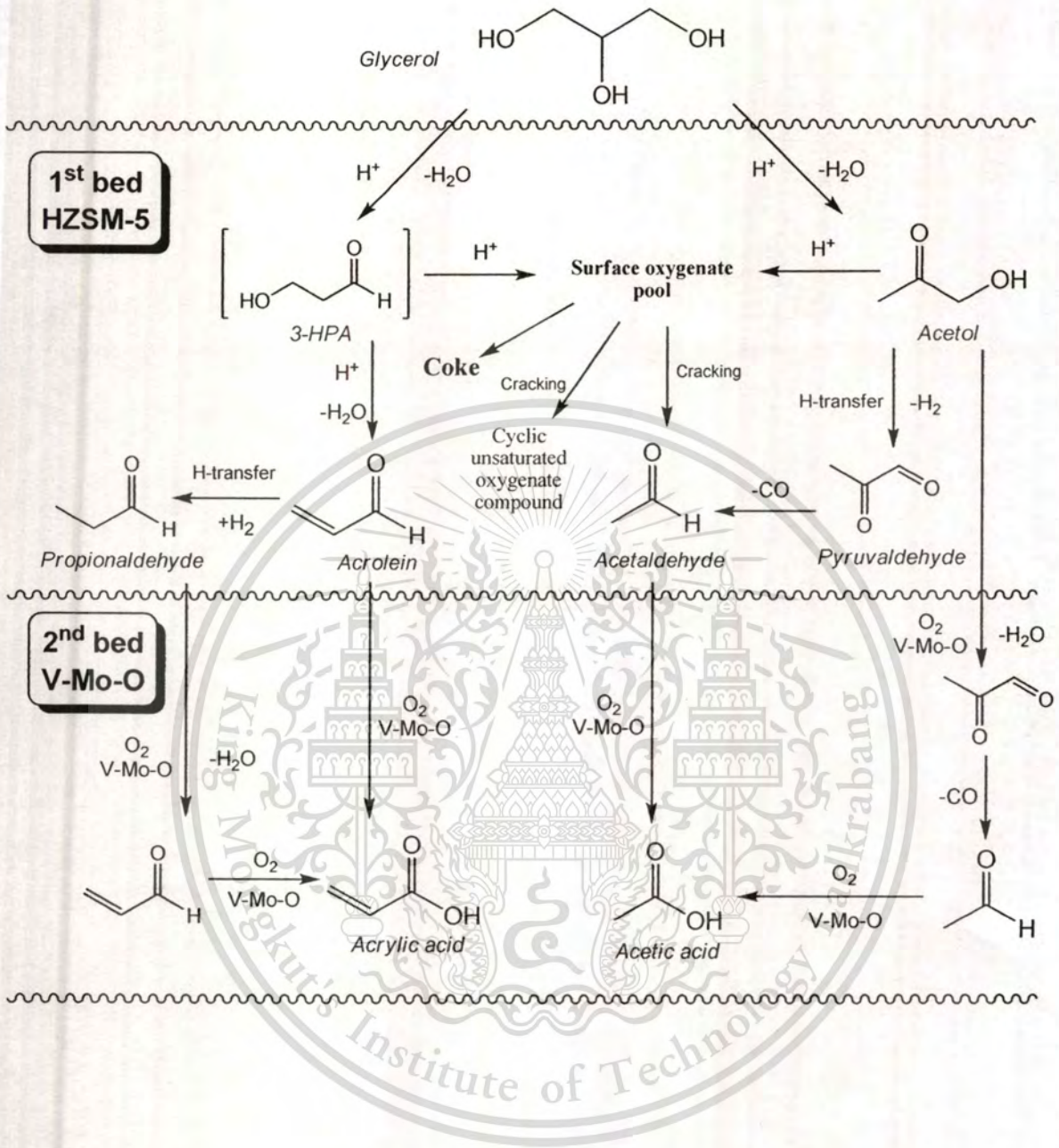

4.3.3 Effect of Vanadium-Molybdenum Oxides Loading on Silicic Acid

In this study, the V/Mo molar ratio of catalyst was fixed at 0.3 and loading of vanadium-molybdenum oxides on silicic acid was varied between 20 and 100 weight%. The result (Figure 4.15) shows that the acrolein conversion increases when the mixed oxides loading is increased from 20 – 50 wt%. As the catalyst loading of 20 – 50 % still possesses good dispersion of vanadium-molybdenum oxides on SiO_2 (Table 4.2), the increase in mixed oxides loading would increases the number of active sites. However, the acrolein conversion decrease gradually, when

the mixed metal oxides loading is higher than 48 wt%. This is due to agglomeration of the mixed oxides phase as seen by the increase crystallinity of the mixed oxides (XRD result, Figure 4.3). This results in the decrease in active surface of the catalyst which is also seen from the decrease in surface area (Table 4.2). Therefore, the catalyst possesses poor dispersion and its activity becomes less.

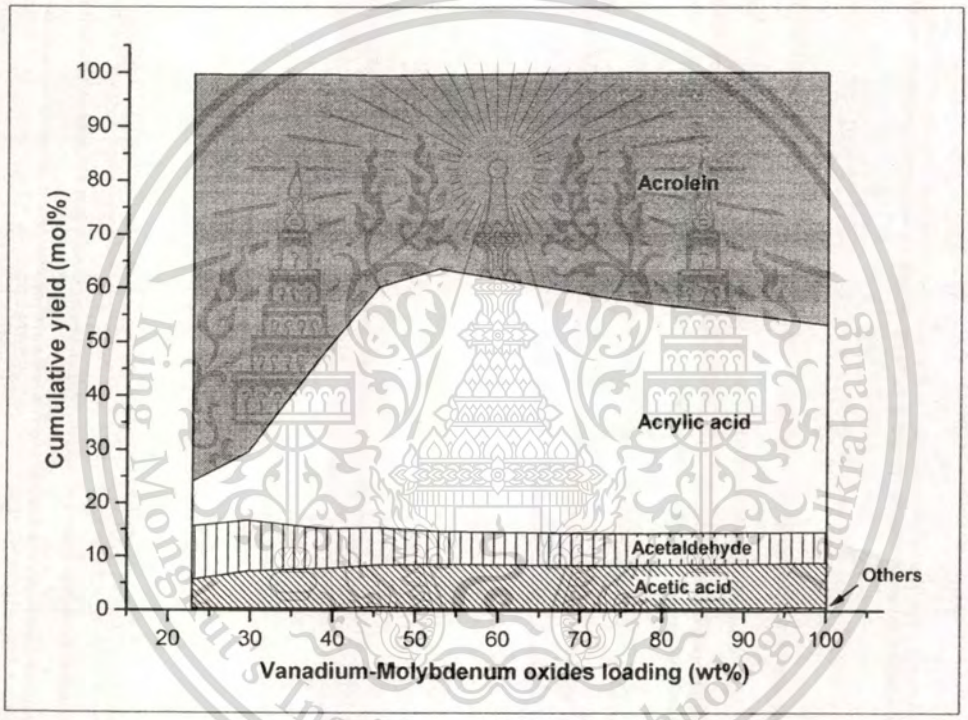

Figure 4.15 The cumulative yield for subsequent oxidation of glycerol dehydrated products as function of vanadium-molybdenum oxides loading on silicic acid

** Reaction condition; Temperature: 300 °C, 1st bed: contact time: 88 g.h.mol^{-1}, catalyst: HZSM-5 (13), 2nd bed: contact time: 295 g.h.mol^{-1}, catalyst: xVMo(0.3), Feed: 1.7 mmol.h^{-1} of glycerol at 10 wt%, Carrier gas: 30 ml.min^{-1} of 10 vol% O_2 in N_2; the results average between fifth and seventh hour on stream*

To obtain efficient catalyst, the dispersion of mixed oxides would be optimized by the turnover frequency (TOF) that can be calculated from the acrolein conversion in an hour (mol) over the amount of vanadium and molybdenum in catalyst (mol). The result is presented in Figure 4.16. It can be observed that the catalyst with 45 wt% mixed metal oxides loading provides maximum turnover frequency in the study range. With the reason, this catalyst will be used for the further tests.

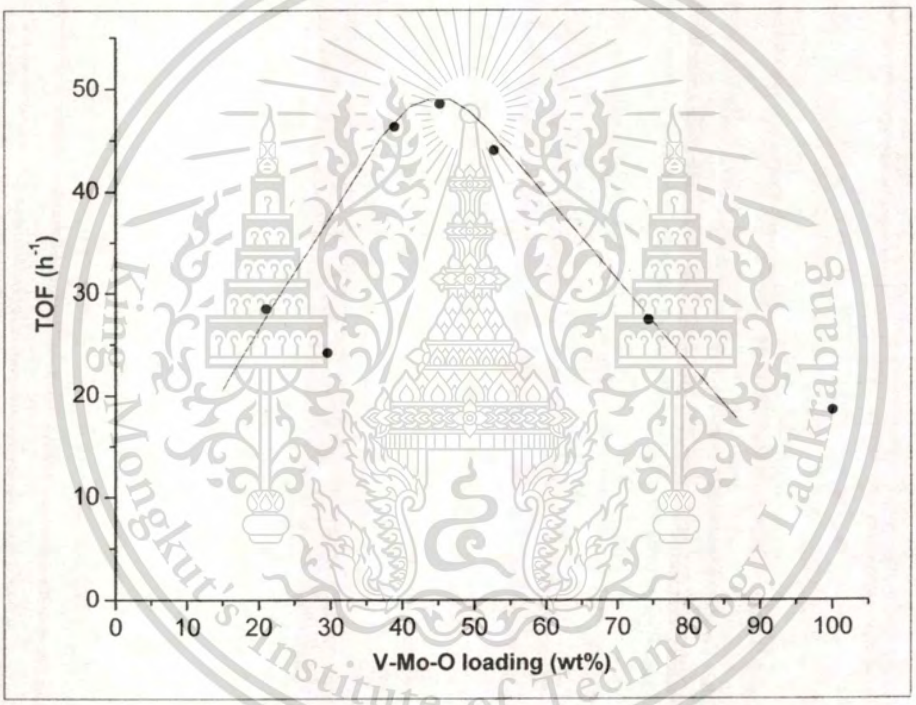

Figure 4.16 The turnover frequency of catalysts with various vanadium-molybdenum oxides loading on silicic acid

4.3.4 Effect of the Mixed Oxides Composition

The effect of mixed oxides composition was studied with 45 wt% mixed oxides loading. The results are presented in Figure 4.17. It can be seen that the acrolein conversion sharply increase when vanadium content is increased from 15 to 40 %.

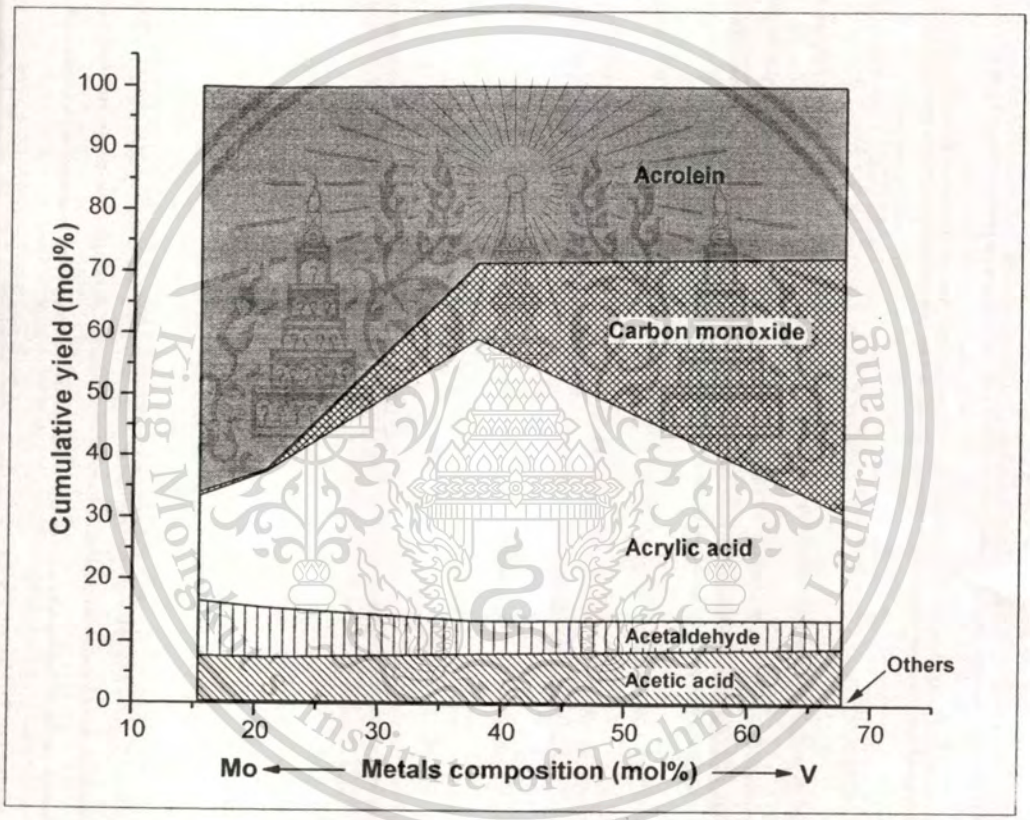

Figure 4.17 The cumulative yield for subsequent oxidation of glycerol dehydrated products as function of vanadium content in vanadium-molybdenum oxides catalyst

** Reaction condition; Temperature: 300 °C, 1st bed: contact time: 88 g.h.mol^{-1}, catalyst: HZSM-5 (13), 2nd bed: contact time: 177 g.h.mol^{-1}, catalyst: 45VMo(y), Feed: 1.7 mmol.h^{-1} of glycerol at 10 wt%, Carrier gas: 30 ml.min^{-1} of 10 vol% O_2 in N_2; the results average between fifth and seventh hour on stream*

In consistence with this result, the XRD patterns and SEM-EDX (Figure 4.4, 4.6) show that the mixed oxides (V-Mo-O hexagonal, V-Mo-O orthorhombic and V-Mo-O triclinic) is increased when the vanadium content is increased. These species is highly reactive for acrolein oxidation, as compared to α-MoO_3 [50]. However, the conversion of acrolein remain unchanged when vanadium content > 40 %. This is possible that when the molybdenum is decreased, the active mixed oxides phases cannot be additionally formed. The excess vanadium is contributed for the formation of V_2O_5.

Unlike the acrolein conversion, the carbon monoxide continuously increases when the vanadium content > 20 %. The selectivity to acrylic acid, that is derived from acrolein oxidation, continually decreases with the increase in vanadium content. The similar result was reported by *Kuznetsova T.G. et al.* [51]. when the V_2O_5 was used as catalyst. Hence, it is possible that the acrolein can be deeply oxidized to carbon monoxide over V_2O_5 that is increasingly observed from SEM-EDX (Figure 4.6) when vanadium content is increased. The deep oxidation is supported by gas product analysis as seen in Table 4.10. The catalyst with high vanadium content (70 %) generates the noticeable yield of carbon monoxide. The carbon dioxide was not detected despite gas phase O_2 is ~ 4 times in excess of the glycerol fed. Thus, it is suggested that the low vanadium catalyst could be used to avoid the deep oxidation.

Table 4.10 The gas product analysis from subsequent oxidation of glycerol dehydrated products over 45VMo (0.3) and 45VMo (2)

Catalyst	V/(V+Mo)	CO (mol% of glycerol)
45VMo (0.3)	0.21	0.6
45VMo (2)	0.68	37.9

* *The conditions are same as Figure 4.15*

A slight decrease in the total yield of C_2 oxygenates can also attribute to deep oxidation to carbon monoxide.

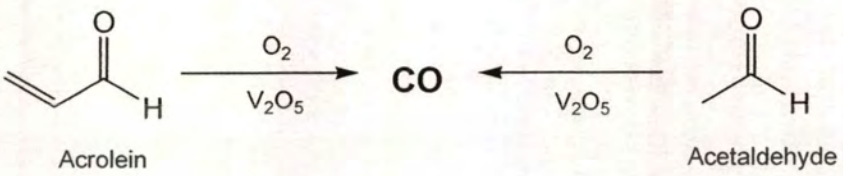

Acrolein Acetaldehyde

In this study, the vanadium-molybdenum oxide catalyst with low vanadium content (V/Mo = 0.3) is chosen because it provide reasonably activity and high acrylic acid selectivity without carbon monoxide formation.

4.3.5 Effect of Oxygen Partial Pressure

As the oxidation proceeds via the lattice oxygen, gas phase oxygen plays important role only in regeneration of oxygen vacant site in catalyst. Thus, the oxygen partial pressure could effects the rate of reaction. To investigate this effect, the oxygen partial pressure was varied between 0.05 and 0.20 atm. The result (Figure 4.18) shows that the acrolein conversion and yield of acrylic acid increase when the oxygen partial pressure is increased. In addition to the increase of conversion, the selectivity to acrylic acid also increases (up to 98 mol% at 0.20 atm of % O_2). This is because, as the oxidation rate is increased, the side reaction namely decomposition is inhibited. This is seen by the decrease in selectivity of the decomposed products including acetaldehyde and acetic acid at high oxygen partial pressure.

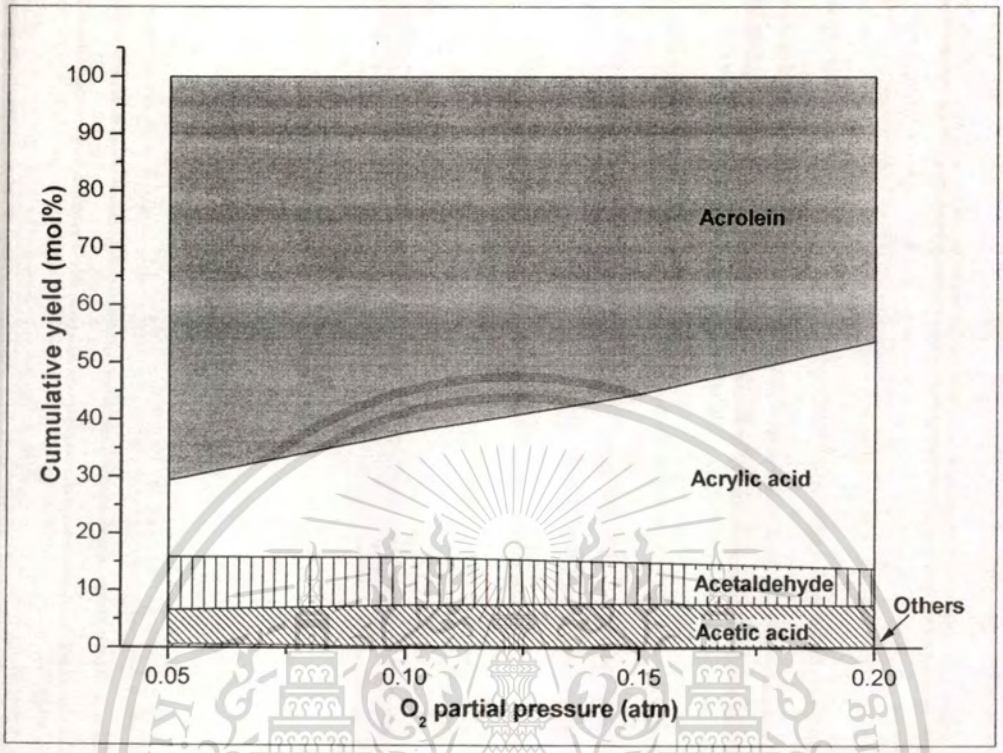

Figure 4.18 The cumulative yield for subsequent oxidation of glycerol dehydrated products as function of oxygen partial pressure

** Reaction condition; Temperature: 300 °C, 1st bed: contact time: 88 g.h.mol^{-1}, catalyst: HZSM-5 (13), 2nd bed: contact time: 177 g.h.mol^{-1}, catalyst: 45VMo(0.3), Feed: 1.7 mmol.h^{-1} of glycerol at 10 wt%, Carrier gas: 30 ml.min^{-1} of 5-20 vol% O_2 in N_2; the results average between fifth and seventh hour on stream*

According to the result, air can be economically used as oxidant for this reaction without producing the CO and CO_2.

CHAPTER 5

CONCLUSION AND SUGGESTION

5.1 Conclusion

The dehydration of glycerol catalyzed by acid zeolites was investigated. It was found that the acrolein and acetol are primarily produced, and they can further react to form "surface oxygenate pools". The pools are the source of secondary products i.e. acetaldehyde, propionaldehyde, pyruvaldehyde, cyclic unsaturated oxygenate compounds and coke that is the cause of catalyst deactivation. The HZSM-5 is appropriate catalyst among other catalysts used in this study (HBeta, HMordenite and HY). This is obtained from the medium two dimensional pore system that can inhibit the secondary reaction. Moreover, increase in catalyst acidity was found increase the total activity. A complete conversion with 81 % selectivity to acrolein was achieved by the catalyst with Si/Al = 13. However, the acrolein selectivity is drastically reduced at temperature > 300 °C because the pools are readily formed and cracked severely to acetaldehyde. In addition, the glycerol concentration $\leq$ 30 wt% could be fed to avoid the increase of acetol and coke formation.

Later, the vanadium-molybdenum oxides on silicic acid support was included to achieve the subsequent oxidation of glycerol dehydrated products. The blending of mixed oxide into HZSM-5 result to the decompose of glycerol and oxygenate C_3 products. While, the separate HZSM-5 / mixed oxides bed shows high selectivity to the C_3 products and was chosen as the test system. Over the mixed oxides, the acrolein and acetaldehyde obtained from first bed (HZSM-5) is successfully oxidized to acrylic acid and acetic acid respectively. Meanwhile, the acetol is decomposed to acetic acid. The increase in mixed oxides loading on silicic acid support can increase the active sites but the dispersion is decreased. The catalyst with ~ 45 wt% mixed oxide possesses the highest activity. Furthermore, the mixed oxides composition is also examined and found that the V-Mo-O hexagonal, V-Mo-O orthorhombic and V-Mo-O triclinic phases are active species for selective oxidation. The molybdenum rich catalyst possesses low activity due to the

formation of α-MoO_3. On the other hand, the vanadium rich catalyst shows the high activity but the low selective to acrylic acid due to the formation of V_2O_5 that promote the deep oxidation to CO. The mixed oxides with V/Mo ~ 0.3 is chosen because no deep oxidation is observed with an acceptable activity. However, the activity can be elevated with slightly increase in acrylic acid selectivity by increasing O_2 concentration. For the second bed, the 48 mol% conversion of acrolein and 98 mol% selectivity to acrylic acid was achieved when the 45VMo(0.3) was used at 0.20 atm of O_2 partial pressure.

5.1 Suggestion for Future Studies

5.1.1) The structures of surface oxygenate pools formed in zeolites would be identified to understand how can they undergo and inhibit their formation.

5.1.2) Due to the limit of reactor capacity in part of second bed, the complete acrolein conversion was not be achieved. For further study, new reactor could be design to support the experiment that possess the second bed contact time > 295 $g.h.mol^{-1}$.

5.1.3) As the alcohols (glycerol and acetol) can be decomposed over vanadium-molybdenum oxides, the test could be applied to the high molecular weight polyol such as glucose and fructose. The smaller oxygenate compounds are expected products.

5.1.4) The subsequent ammoxidation of glycerol dehydrated products can be expansively studied by including the ammonia into the feed. The acrylonitrile and acetonitrile are expected products. In addition, the vanadium-molybdenum oxides would be comparatively studied to the bismuth-molybdenum oxides that prefer for ammoxidation.

REFERENCES

[1] Bartholomew C.H., and Farrauto R.J., **Fundamentals of Industrial Catalytic Processes**, 2nd ed., John Wiley & Sons, Inc., New Jersy, 2005, 578-584, 606-609.

[2] Baerns M., Buyevskaya O.V., Kubik M., Maiti G., Ovsitser O., Seel O., **Catalytic partial oxidation of propane to acrolein**, Catalysis Today, 1997, 33, 85-96.

[3] Zhang X., Wan H., and Weng W., **Reaction pathways for selective oxidation of propane to acrolein over Ce-Ag-Mo-P-O catalysts**, Applied Catalysis A: General, 2009, 353, 24-31.

[4] Zhao C., and Wacsh I. E., **Selective oxidation of propylene over model supported V_2O_5 catalysts: Influence of surface vanadia coverage and oxide support**, Journal of Catalysis, 2008, 257, 181-189.

[5] Zheng W, Yu Z., Zhang P., Zhang Y., Fu H., Zhang X., Sun Q., Hu X., **Selective oxidation of propane to acrylic acid over mixed metal oxide catalysts**, Journal of Natural Gas Chemistry, 2008, 17, 191-194.

[6] Landi G., Lisi L., and Russo G., **Oxidation of propane and propylene to acrylic acid over vanadyl pyrophosphate**, Journal of Molecular Catalysis A: Chemical, 2005, 239,172-179.

[7] Liu Y., Wang L., **Biodiesel production from rapeseed deodorizer distillate in a packed column reactor**, Chemical Engineering and Processing, 2009, 48, 1152-1156.

[8] Demirbas A., **Biodiesel from waste cooking oil via base-catalytic and supercritical methanol transesterification**, Energy Conversion and Management, 2009, 50, 923-927.

[9] Shaw N.B., Monahan F.J., O'Riordan E.D., O'Sullivan M., **Effect of soya oil and glycerol on physical properties of composite WPI films**, Journal of Food Engineering, 2002, 51, 299-304.

[10] Deka H., and Karak N., **Bio-based hyperbranched polyurethanes for surface coating applications**, Progress in Organic Coatings, 2009.

[11] Bonet J., Costaa J., Sireb R., Reneaumeb J, Plesu E.A., Plesu V., Bozgac G., **Revalorization of glycerol: Comestible oil from biodiesel synthesis**, Food and Bioproducts Processing, 2009.

[12] Chai S. H., Wang H.P, Liang Y., Xu B.Q., **Sustainable production of acrolein: Gas-phase dehydration of glycerol over Nb_2O_5 catalyst**, Journal of Catalysis, 2007, 250, 342-349.

[13] Watanabe M., Iida T., Aizawa Y., Aida T.M., Inomata H., **Acrolein synthesis from glycerol in hot-compressed water**, Bioresource Technology, 2007, 98, 1285-1290.

[14] Pagliaro M., **The Future of Glycerol: New Uses of a Versatile Raw Material**, 1st ed., The Royal Society of Chemistry, Cambridge, 2008, 1-17, 54-59.

[15] Hagen J., **Industrial Catalysis: A Practical Approach**, 1st ed., Wiley-VCH, Weinheim, 1999, 1-11.

[16] Sheldon R.A., van Bekkum H., **Fine Chemicals through Heterogeneous Catalysis**, 2001, 295-304.

[17] Sooknoi T., **Zeolites and Related Microporous Materials**, 17, 50.

[18] Campbell I.M., **Catalysis at Surfaces**, 1st ed., Chapman and Hall Ltd, London, 1988, 168-174.

[19] Gates B.C., **Catalytic Chemistry**, 1st ed., John Wiley & Sons, Inc., USA, 1991, 403.

[20] Tsukuda E., Sato S., Takahashi R., Sodesawa T., **Production of acrolein from glycerol over silica-supported heteropoly acids**, Catalysis Communications, 2007, 8, 1349-1353.

[21] Ulgen A., Hoelderich W., **Conversion of Glycerol to Acrolein in the Presence of WO_3/ZrO_2 Catalysts**, Catal Lett, 2009, 131, 122-128.

[22] Suprun W., Lutecki M., Haber T., Papp H., **Acidic catalysts for the dehydration of glycerol: Activity and deactivation**, Journal of Molecular Catalysis A: Chemical, 2009, 309, 71-78.

[23] Corma A., Huber G.W., Sauvanaud L., O'Connor P., **Biomass to chemicals: Catalytic conversion of glycerol/water mixtures into acrolein, reaction network**, Journal of Catalysis, 2008, 257, 163-171.

[24] Lili N., Yunjie D., Weimiao C., Leifeng G., Ronghe L., Yuan L., Qin X., **Glycerol Dehydration to Acrolein over Activated Carbon-Supported Silicotungstic Acids**, Chinese Journal of Catalysis, 2008, 29(3), 212-214.

[25] Atia H., Armbruster U., Martin A., **Dehydration of glycerol in gas phase using heteropolyacid catalysts as active compounds**, Journal of Catalysis, 2008, 258, 71-82.

[26] Chai S.H., Wang H.P., Liang Y., Xu B.Q., **Sustainable production of acrolein: Preparation and characterization of zirconia-supported 12-tungstophosphoric acid catalyst for gas-phase dehydration of glycerol**, Applied Catalysis A: General, 2009, 353, 213-222.

[27] Grasselli R.K., **Advances and future trends in selective oxidation and ammoxidation catalysis**, Catalysis Today, 1999, 49, 141-153.

[28] Endres S., Kampe P., Kunert J., Drochner A., Vogel H., **The influence of tungsten on structure and activity of Mo–V–W-mixed oxide catalysts for acrolein oxidation**, Applied Catalysis A: General, 2007, 325, 237-243.

[29] Tichy J., **Oxidation of acrolein to acrylic acid over vanadium-molybdenum oxide catalysts**, Applied Catalysis A: General, 1997, 157, 363-385.

[30] Drochner A., Kampe P., Kunert J., Ott J., Vogel H., **Steady State Isotopic Transient Kinetic Analysis of the acrolein oxidation on Mo–V–W-mixed oxide catalysts**, Applied Catalysis A: General, 2005, 289, 74-83.

[31] Kunert J., Drochner A., Ott J., Vogel H., Fueβ H., **Synthesis of Mo/V mixed oxide catalysts via crystallisation and spray drying - a novel approach for controlled preparation of acrolein to acrylic acid catalysts**, Applied Catalysis A: General, 2004, 269, 53-61.

[32] Adams A. H., Haaβ F., Buhrmester T., Kunert J., Ott J., Vogel H., Fuess H., **Structure and reaction studies on vanadium molybdenum mixed oxides**, Journal of Molecular Catalysis A: Chemical, 2004, 216, 67–74.

[33] Tichy J., Machek J., **Oxidation of acrolein on a multicomponent oxide catalyst**, Catalysis Letters, 1992, 15, 401-404.

[34] Ovsitser O., Uchida Y., Mestl G., Weinberg G., Blume A., Jäger J., Dieterle M., Hibst H., Schlögl R., **Molybdenum oxide based partial oxidation catalyst Part 3. Structural changes of a MoVW mixed oxide catalyst during activation and relation to catalytic performance in acrolein oxidation**, Journal of Molecular Catalysis A: Chemical, 2002, 185, 291–303.

[35] Krauß K., Drochner A., Fehlings M., Kunert J., Vogel H., **Oxygen exchange at Mo/V mixed oxides A transient and 18O isotope study under technical conditions**, Journal of Molecular Catalysis A: Chemical, 2002, 177, 237–245.

[36] Bondareva V.M., Andrushkevieh T.V., Plyasova L.M., Maksimovskaya R.I., Chumachenko N.N., **Study of the P_2O_5 - MoO_3 system in acrolein oxidation**, Reaction Kinetic Catalysis Letters, 1998, 63, 201-206.

[37] International Zeolite Association, **Zeolite Powder Diffraction Patterns**, [Online], Available: http://izasc.ethz.ch/fmi/xsl/IZA-SC/xrd.xsl, (Retrieve: 8 May 2010).

[38] Inorganic Crystal Structure Database (ICSD) collection code: 073877.

[39] Roussela M., Boucharda M., Bordes-Richarda E., Karimb K., Al-Sayarib S., **Oxidation of ethane to ethylene and acetic acid by MoVNbO catalysts**, Catalysis Today, 2005, 99, 77–87

[40] Mathew S. M., Biradar A. V., Umbarkar S. B., Dongare M. K., **Regioselective nitration of cumene to 4-nitro cumene using nitric acid over solid acid catalyst**, Catalysis Communications, 2006, 7, 394–398.

[41] Woi P.M., Irmawati R., Taufiq-Yap Y.H., **Influence of organic species on the characteristics of Mo-V oxides**, The Malaysian Journal of Analytical Sciences, 2007, 11 (1), 160-165

[42] Katou T., Vitry D., Ueda W., **Hydrothermal synthesis of a new Mo–V–O complex metal oxide and its catalytic activity for the oxidation of propane**, Chemistry Letters, 2003, 32(11), 1028-1029.

[43] Gorshkova T. P., Tarasova D. V., Olenkova I. P., Maksimov N. G., Anufrienko V. F., **Influence of silica on the phase composition of vanadium-molybdenum oxides catalysts**, Reaction Kinetic Catalysis Letters, 1979, 12(4), 509-511.

[44] Crystallography Open Database (COD) entry: 1011291.

[45] Ai M., Motohashi A., Abe S., **Formation of pyruvaldehyde (2-oxopropanal) by oxidative dehydrogenation of propylene glycol**, Applied Catalysis A: General, 2003, 246, 97–102.

[46] Mitran G., Marcu I., Yuzhakova T., Sandulescu I., **Selective oxidation of isobutane on V-Mo-O mixed oxide catalysts**, Journal of Serbian Chemical Soceity, 2008, 73(1), 55-64.

[47] Roussel M., Bouchard M., Karim K., Al-Sayari S., Bordes-Richard E., **MoVO-based catalysts for the oxidation of ethane to ethylene and acetic acid Influence of niobium and/or palladium on physicochemical and catalytic properties**, Applied Catalysis A: General, 2006, 308, 62–74.

[48] Pless J. D., Bardin B. B., Kim H., Ko D., Smith M. T., Hammond R. R., Stair P. C., Poeppelmeier K. R., **Catalytic oxidative dehydrogenation of propane over Mg–V/Mo oxides**, Journal of Catalysis, 2004, 223, 419–431.

[49] Ai M., Ohdan K., **Formation of pyruvaldehyde (2-oxopropanal) by oxidative dehydrogenation of hydroxyacetone**, Bulletin of the Chemical Society of Japan, 1999, 72, 2143-2148.

[50] Andrushkevich T. V., Plyasova L. M., Kuznetsova G. G., Bondareva V. M., Gorshkova T. P., Olenkova I. P. Lebedeva N. I., **Catalytic properties of the vanadium-molybdenum oxide system for acrolein oxidation**, Reaction Kinetic Catalysis Letters, 1979, 12(4), 463-467.

[51] Kuznetsova T. G., Andrushkevich T. V., Gorshkova T. P., **Catalytic properties of V-Mo-O systems in acrolein oxidation**, Reaction Kinetic Catalysis Letters, 1986, 30(1), 149-156.

APPENDIXES

APPENDIX A

Reference X-ray Diffraction Patterns of Zeolites

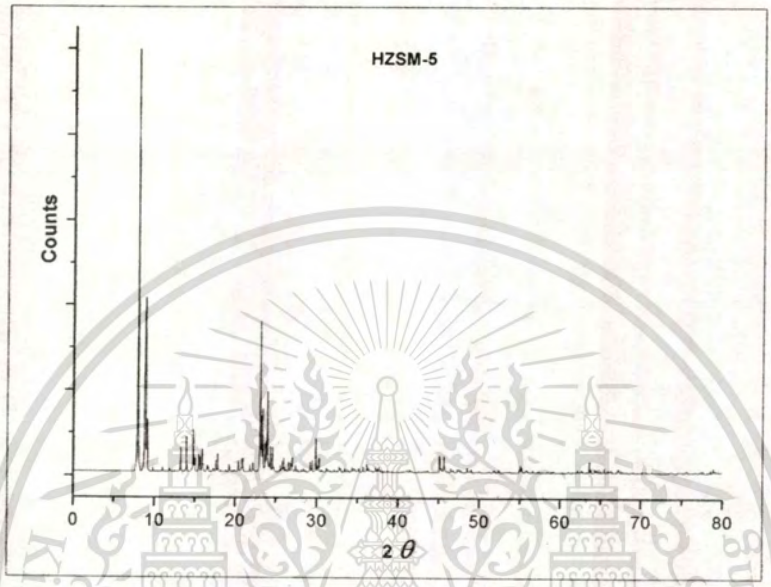

Figure A1 Reference X-ray diffraction pattern of HZSM-5

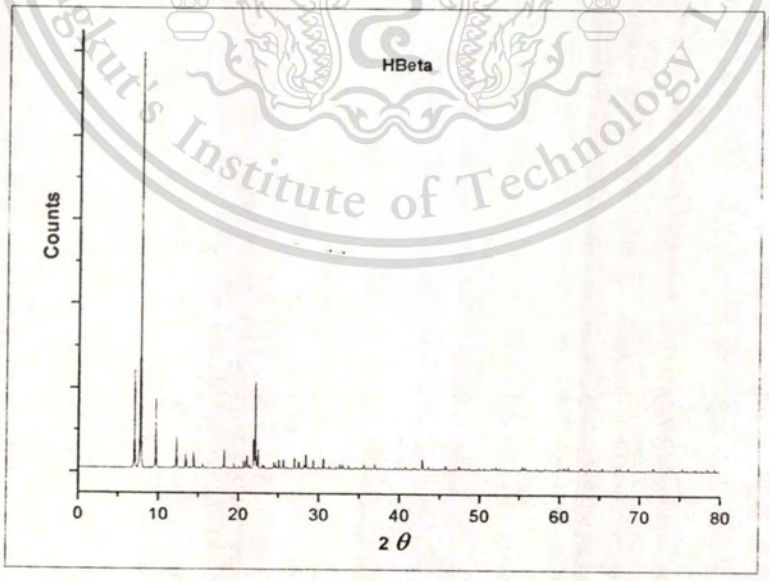

Figure A2 Reference X-ray diffraction pattern of HBeta

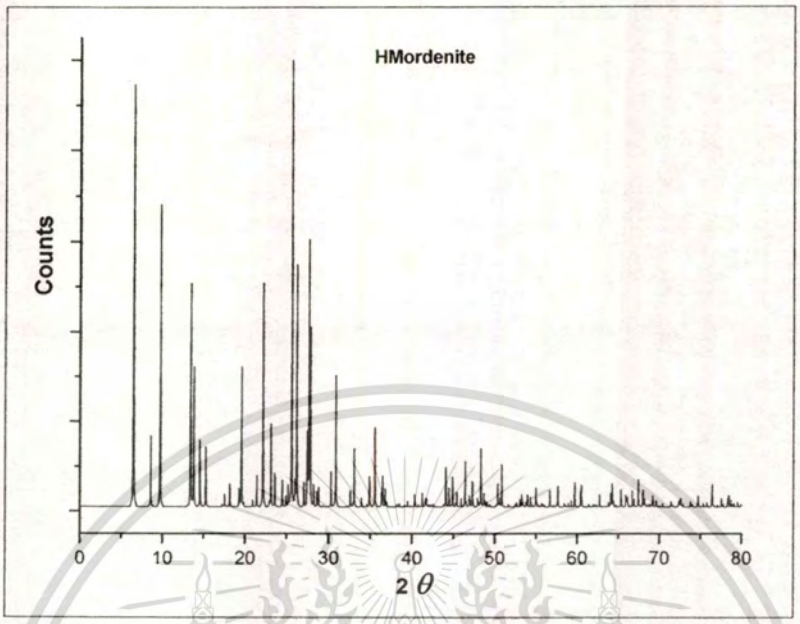

Figure A3 Reference X-ray diffraction pattern of HMordenite

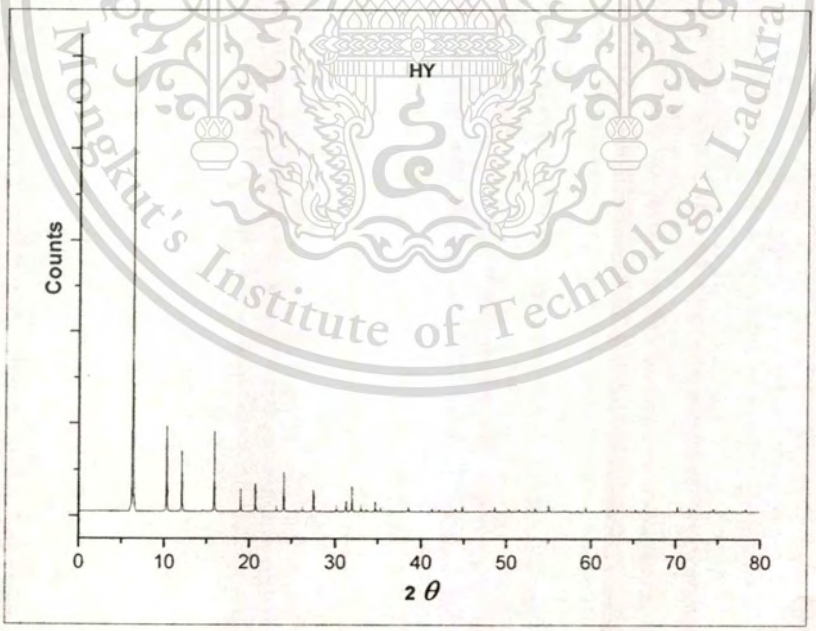

Figure A4 Reference X-ray diffraction pattern of HY

APPENDIX B

Thermogravimatic Analysis of Catalysts

** Test condition; in air from 50 to 900 °C (10 °C/min)*

B1 Used Zeolites

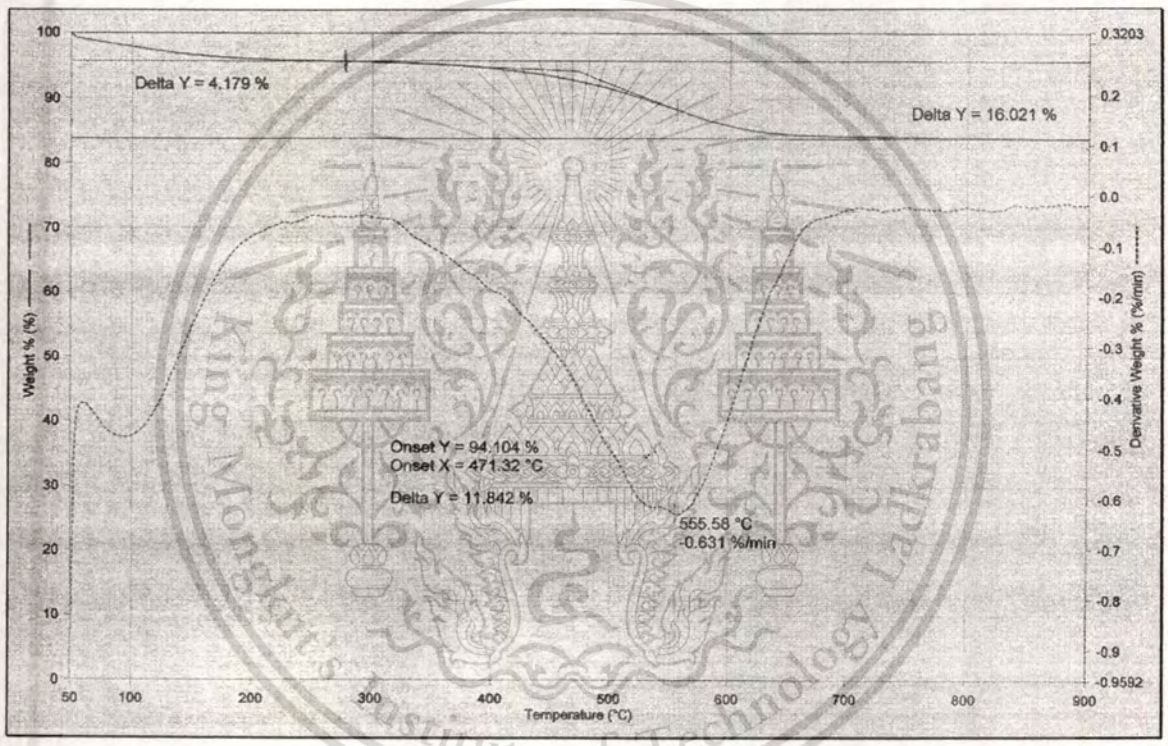

Figure B1 TGA of used HZSM-5 (13); *result shown in Table 4.5, 4.7*

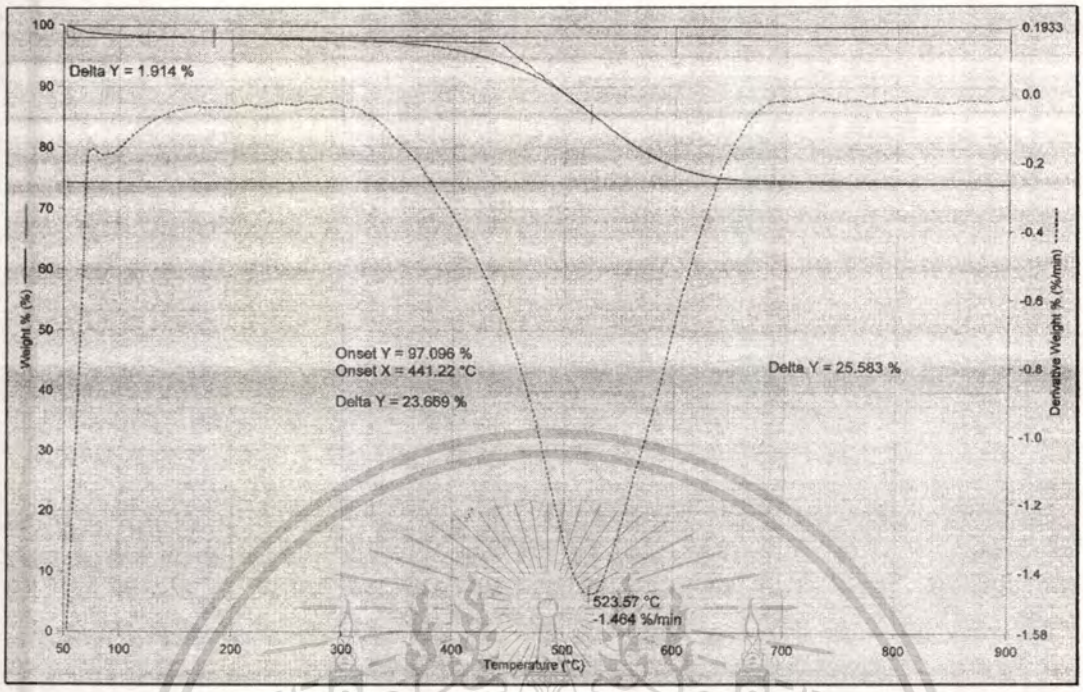

Figure B2 TGA of used HBeta (14); *result shown in Table 4.5*

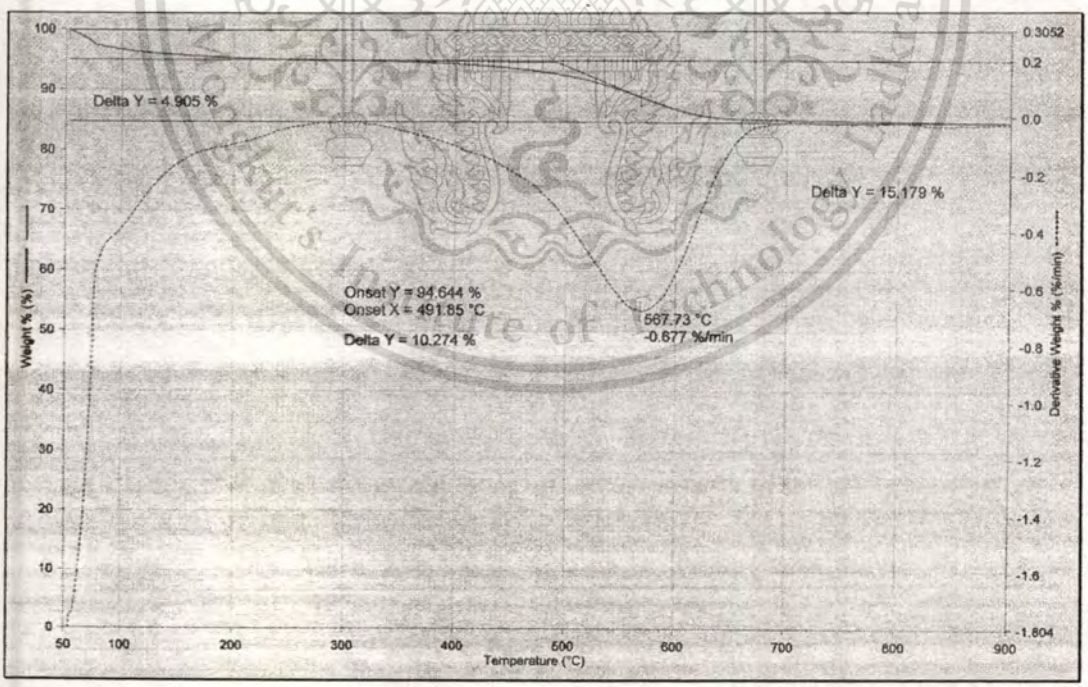

Figure B3 TGA of used HMordenite (15); *result shown in Table 4.5*

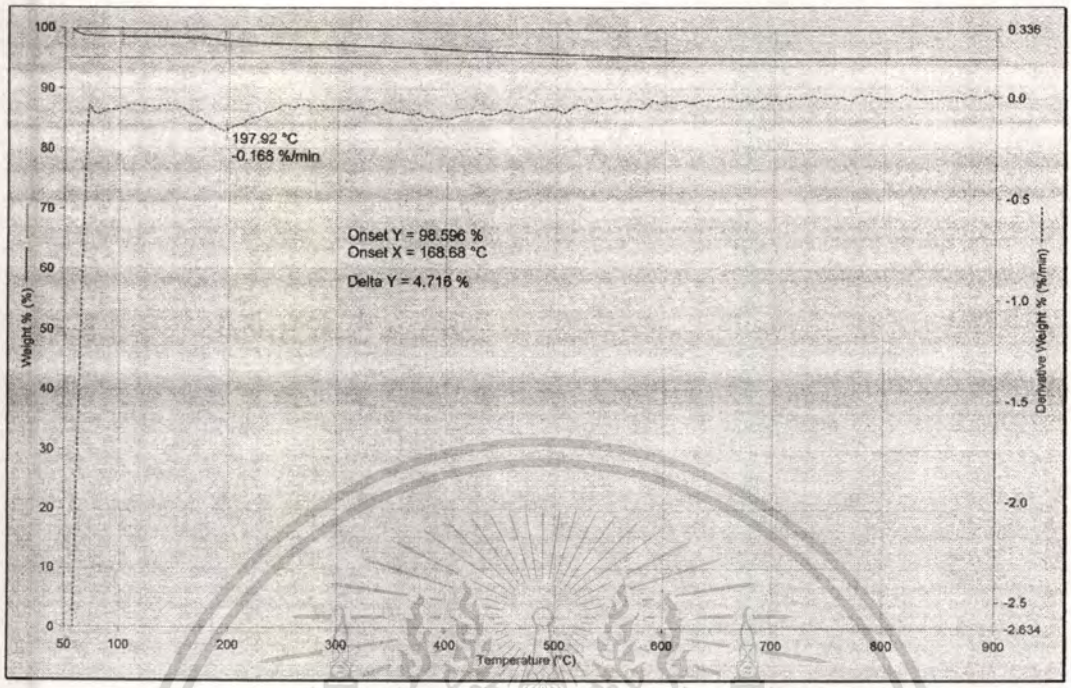

Figure B4 TGA of used HY (100)

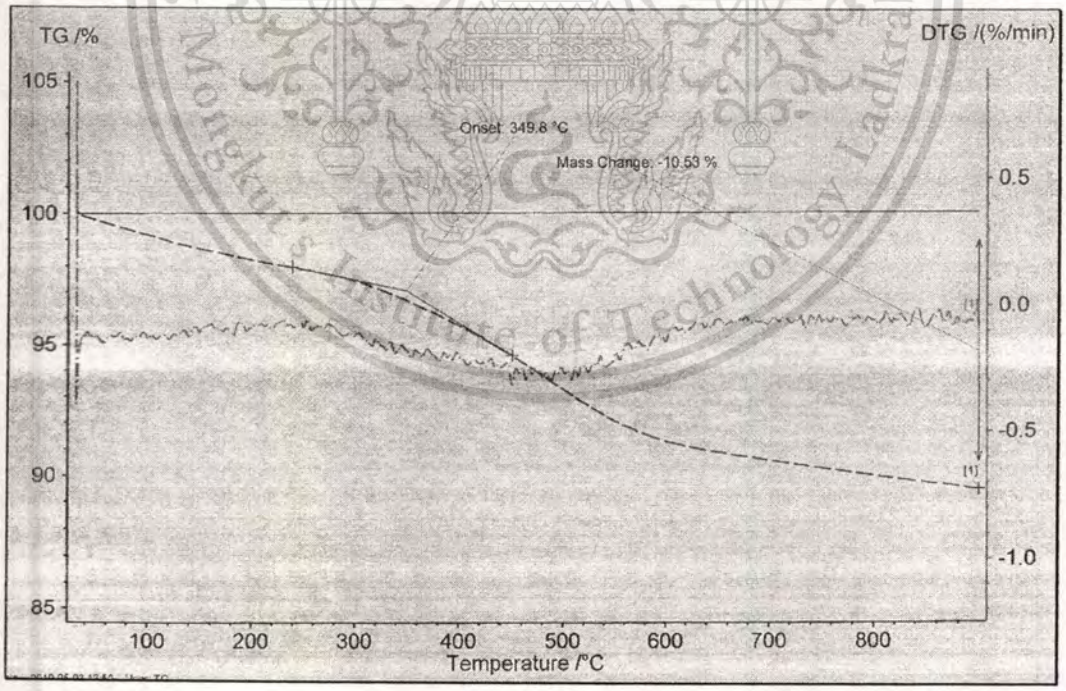

Figure B5 TGA of used HZSM-5 (180) at 300 °C; *result shown in Table 4.6*

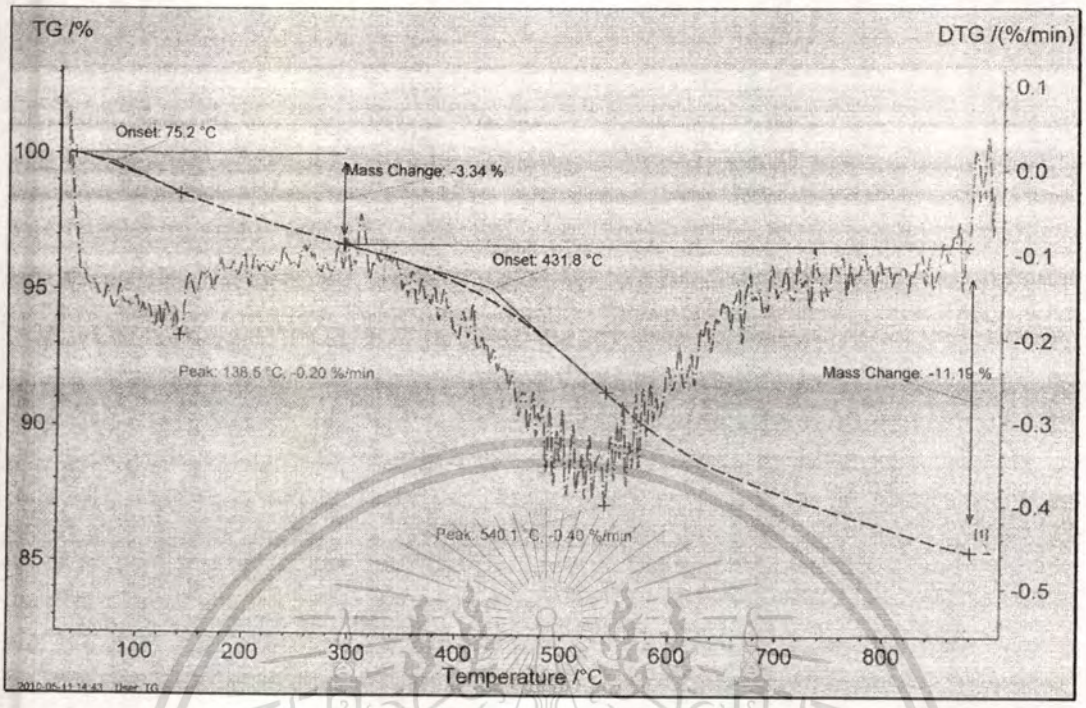

Figure B6 TGA of used HZSM-5 (180) at 325 °C; *result shown in Table 4.6*

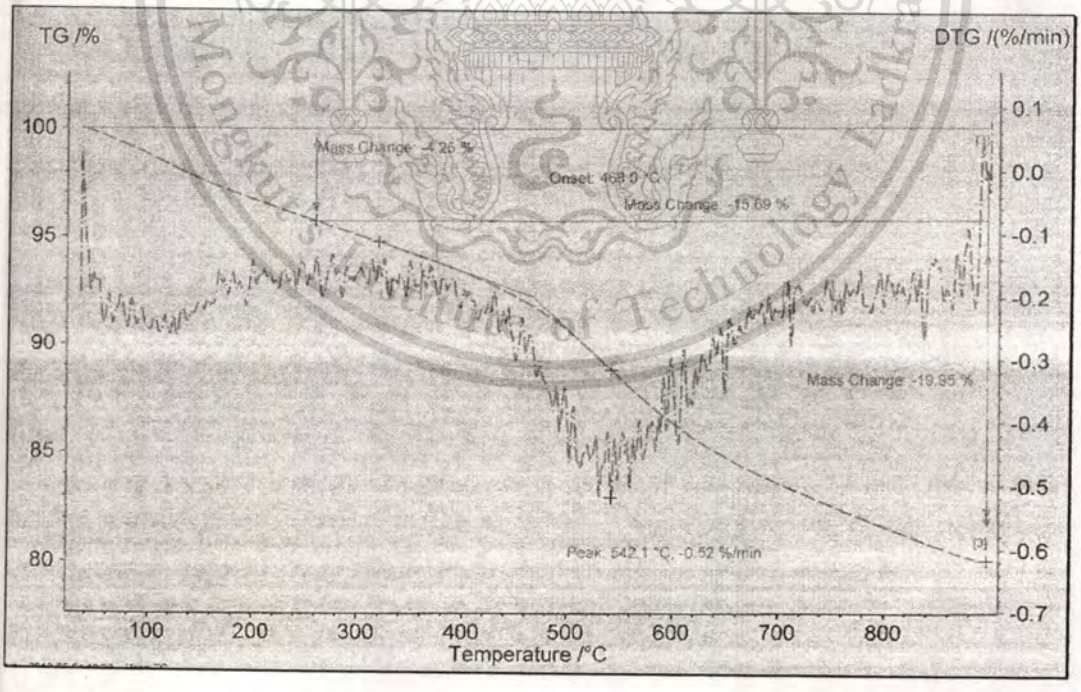

Figure B7 TGA of used HZSM-5 (180) at 400 °C; *result shown in Table 4.6*

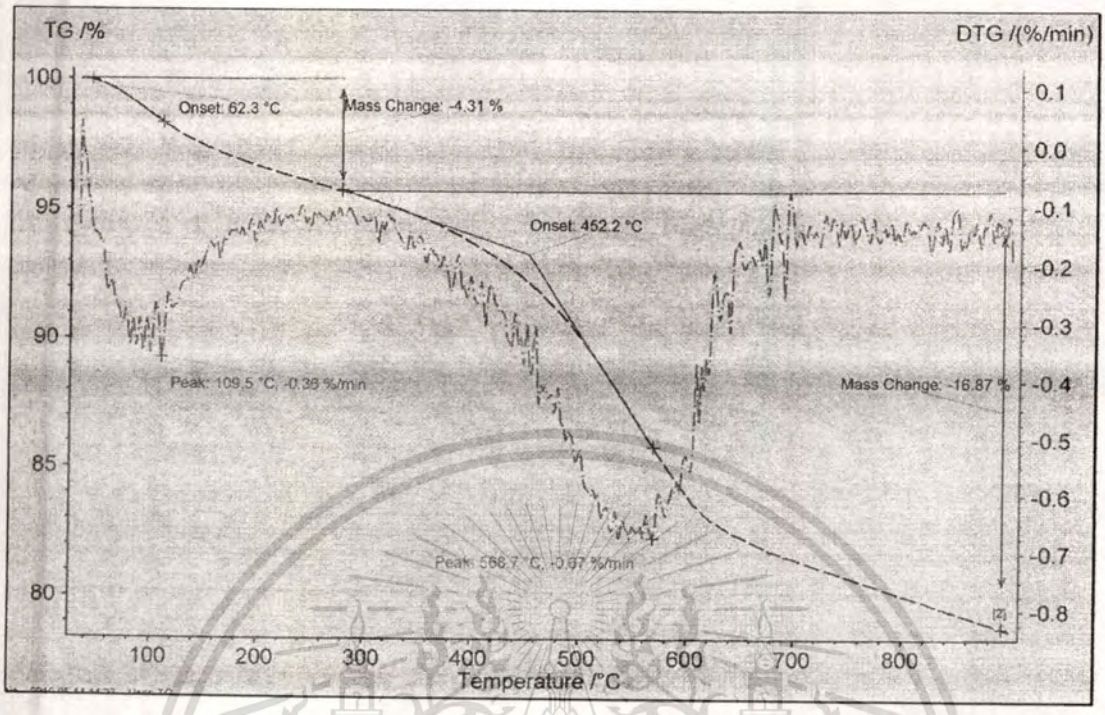

Figure B8 TGA of used HZSM-5 (28); *result shown in Table 4.7*

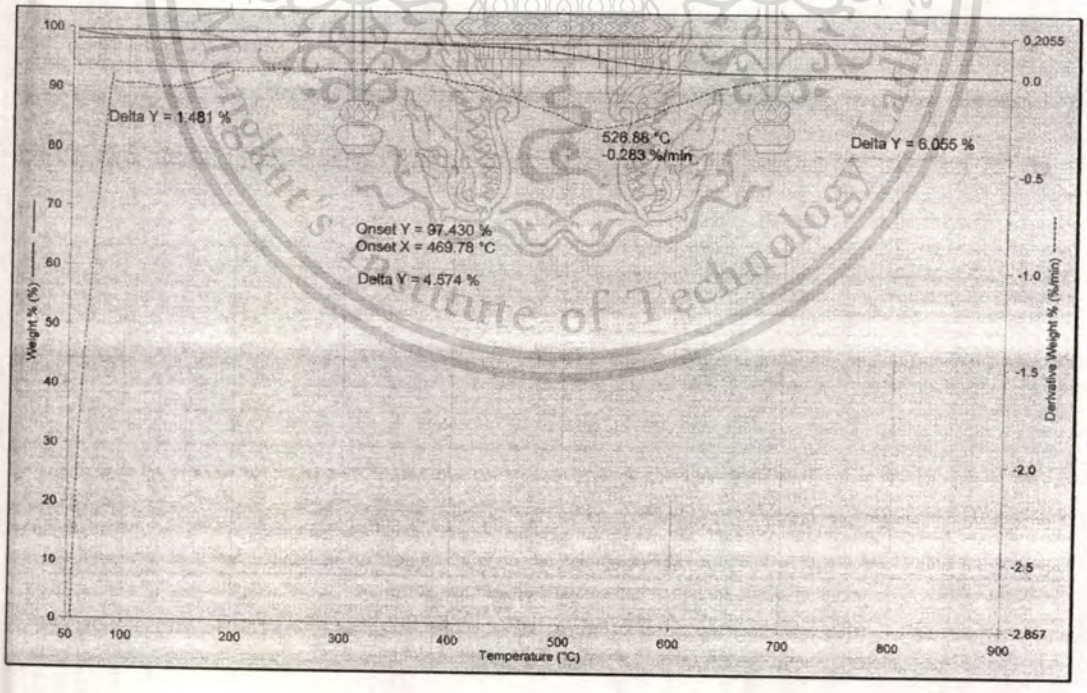

Figure B9 TGA of used HZSM-5 (180); *result shown in Table 4.7*

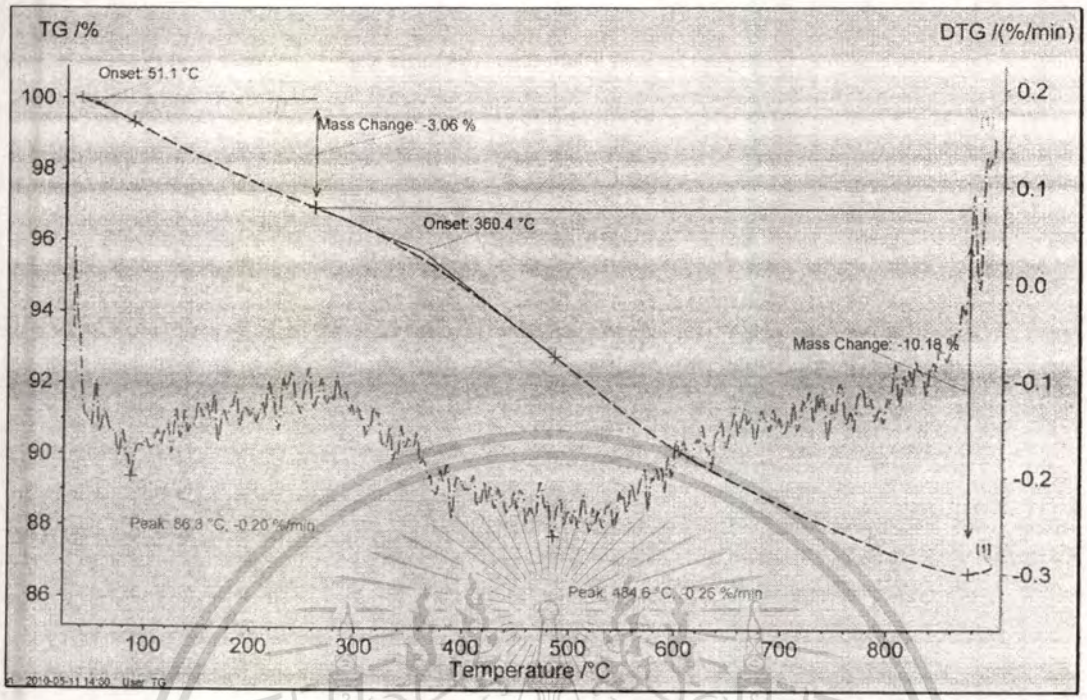

Figure B10 TGA of used HZSM-5 (500); *result shown in Table 4.7*

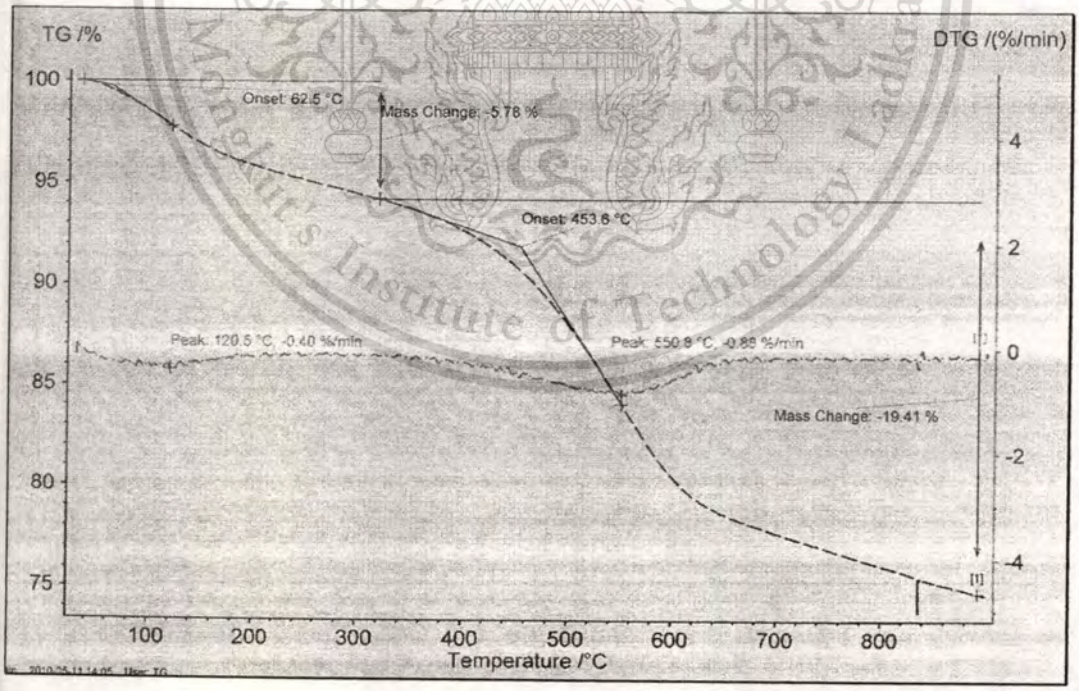

Figure B11 TGA of used HZSM-5 (13) with 10% glycerol feeding; *result shown in Table 4.8*

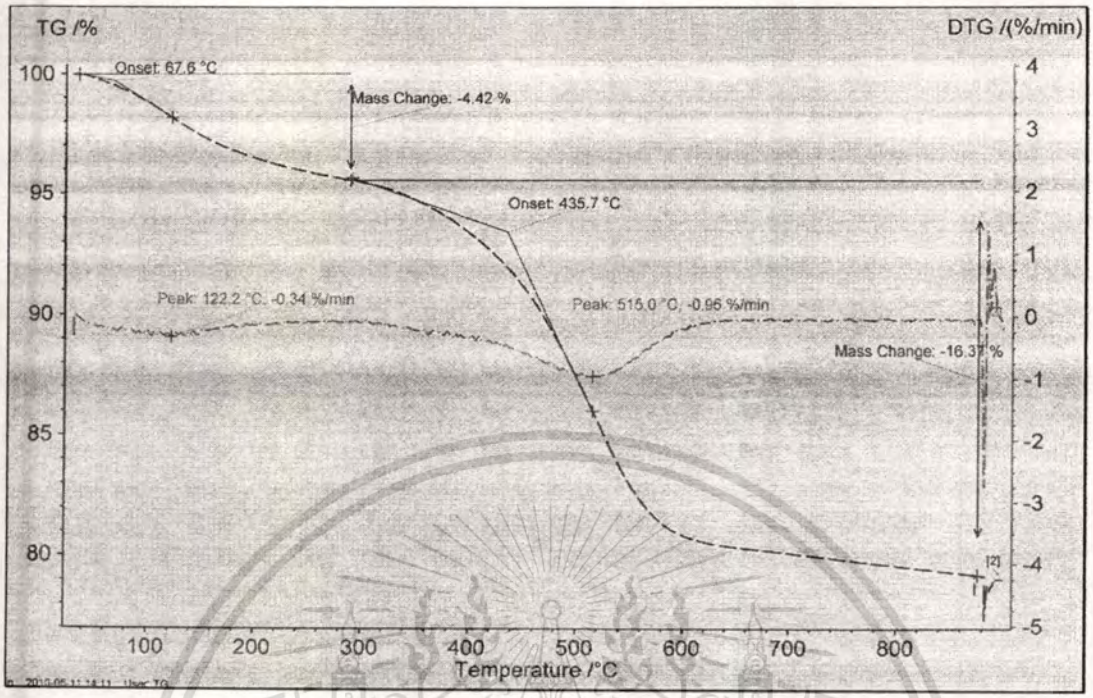

Figure B12 TGA of used HZSM-5 (13) with 30% glycerol feeding; *result shown in Table 4.8*

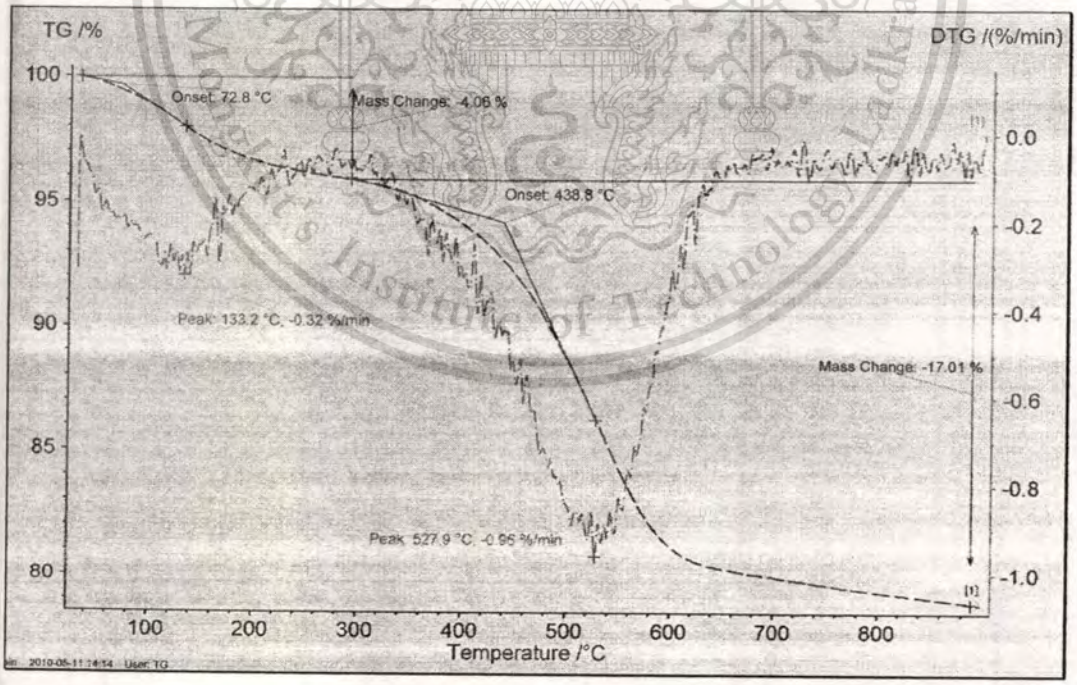

Figure B13 TGA of used HZSM-5 (13) with 50% glycerol feeding; *result shown in Table 4.8*

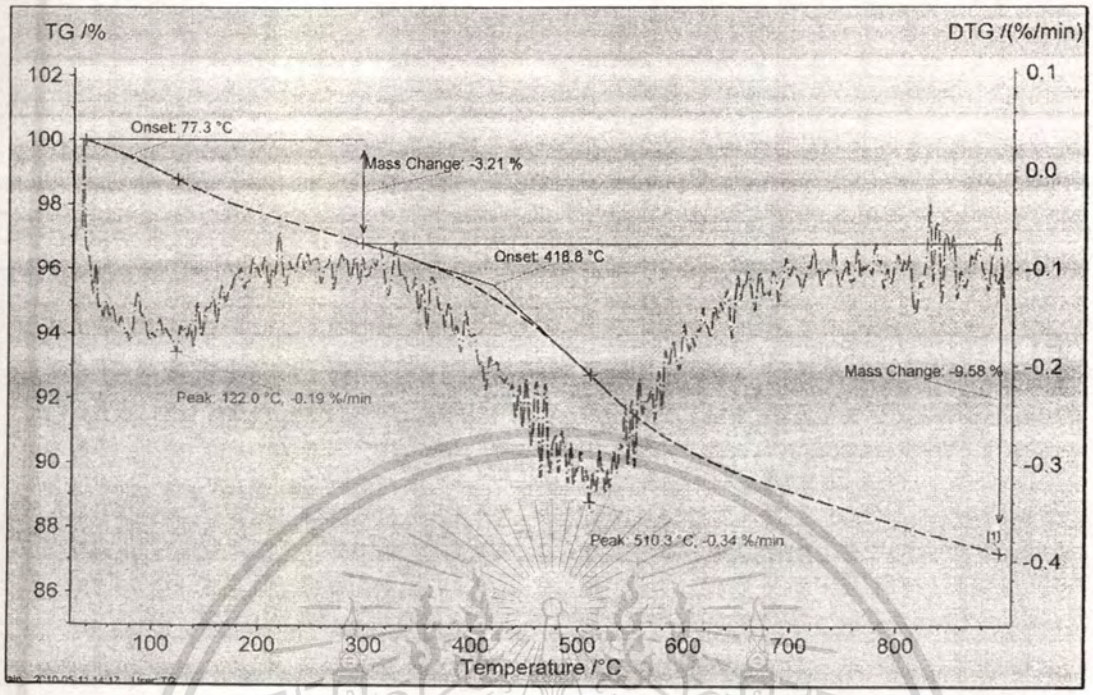

Figure B14 TGA of used HZSM-5 (180) with acetol feeding

B2 Vanadium-Molybdenum Oxides

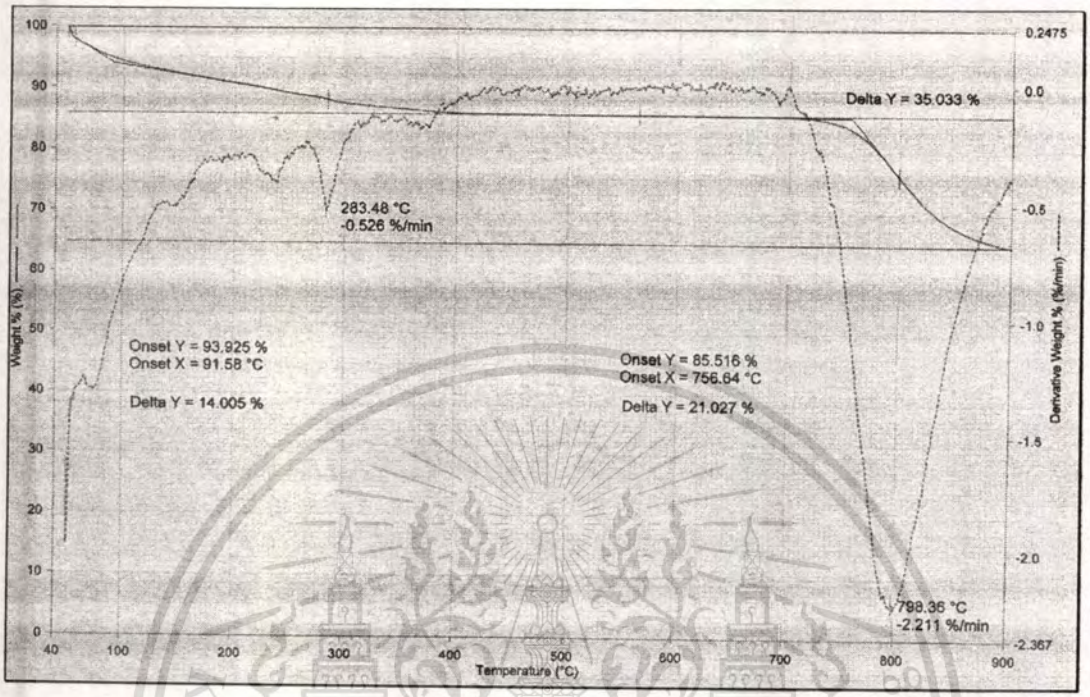

Figure B15 TGA of non-calcined 45VMo(0.3)

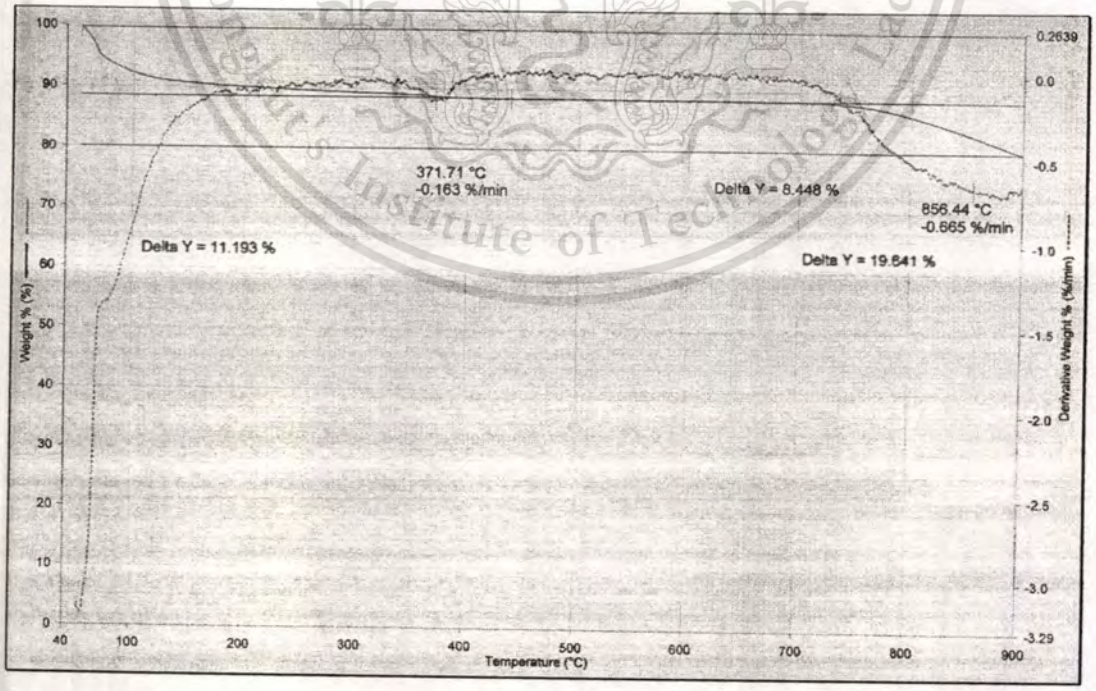

Figure B16 TGA of calcined 45VMo(0.3)

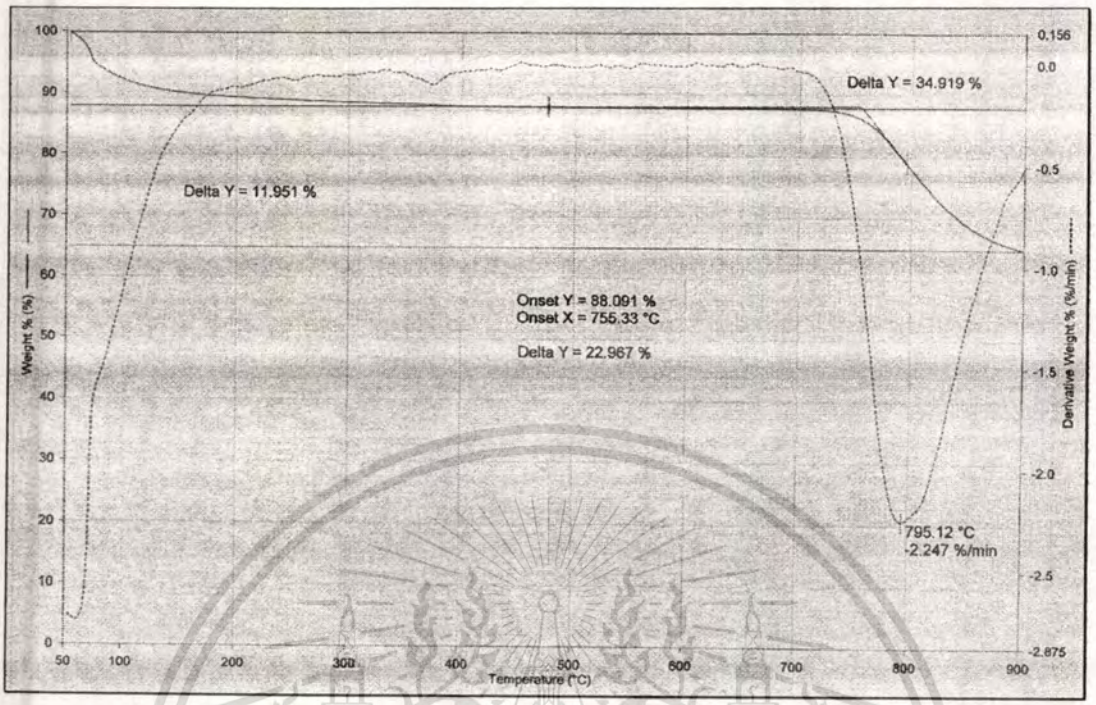

Figure B17 TGA of used 45VMo(0.3)

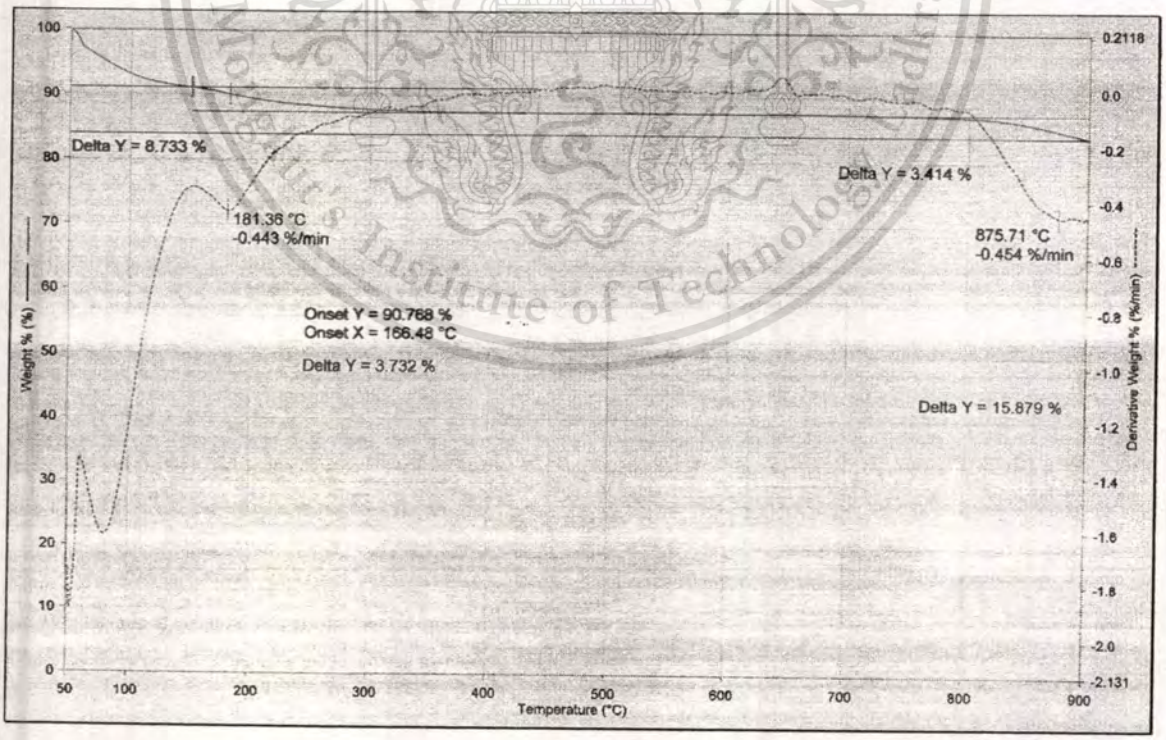

Figure B.18 TGA of used 45VMo(0.6)

APPENDIX C

Product Calculation

Prior analysis, the structure of products in sample is identified the by GC-MS (gas chromatography with mass spectrometer detector). Then, the quantitative analysis of products was carried out by GC-FID (gas chromatography with flame ionization detector) with the condition expressed in Table C1. An example of chromatogram from glycerol dehydration subsequent selective oxidation is present in Figure C1. The chromatogram were integrated to obtain the peak area as shown in Table C2.

Table C1 The GC condition for quantitative analysis

Column	EC™ – wax, 30 m X 0.32 mm X 0.25 µm
Temperature program	60 °C (2 min hold) to 200 °C (30.5 min hold) at 8 °C/min
Carrier gas	Helium at 2.00 ml/min
Injection	230 °C, 0.1 µl
Detector	FID at 230 °C

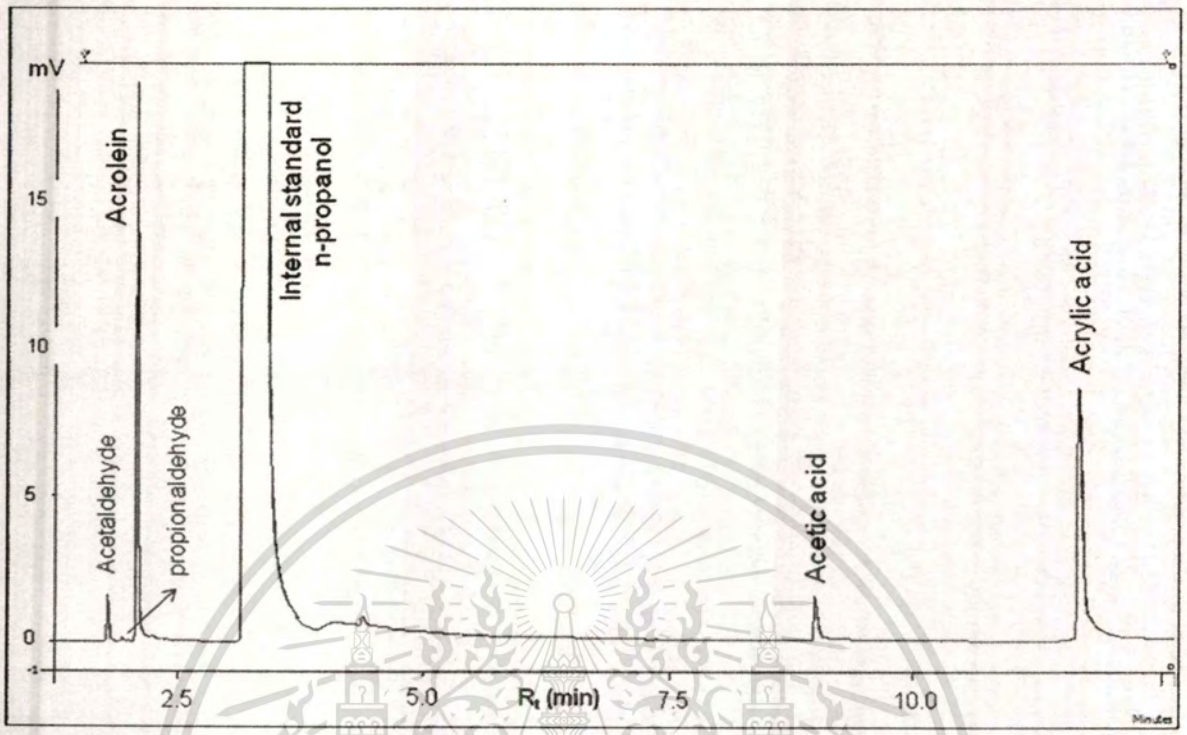

Figure C1 The GC chromatogram of the subsequent oxidation (over 45VMo(0.6)) of glycerol dehydrated products at fifth hour on stream

** The conditions are same as Figure 4.15*

Table C2 The peak area from chromatogram in Figure C1 and calculation for obtaining the products yield

Products	Peak area	Peak area of product / Peak area of internal standard ($x10^{-4}$)	wt% in sample	mol concentration (mmol product/100 g sample)	Production rate (mmol/h)	Yield (mol%)
Acetaldehyde	1863	5.70	0.247	5.62	0.080	4.69
Propionaldehyde	162	0.50	0.012	0.20	0.003	0.17
Acrolein	25325	77.5	1.81	32.3	0.457	26.9
Acetic acid	4985	15.3	0.532	8.87	0.126	7.40
Acrylic acid	37502	115	3.75	52.1	0.738	43.5 (72.4)*
n-Propanol (Int Std)	3268037	-	-	-	-	-
Carbon monoxide					0.30	17.33

*Selectivity to acrylic acid at 69 mol% acrolein conversion in second bed

In this study, the internal standard, n-propanol, is used for quantitative analysis. Firstly, the peak area of products must be corrected by the peak area of internal standard to eliminate the effect of volume injection.

$$\text{Corrected area of product} = \frac{\text{Peak area of product}}{\text{Peak area of internal standard}}$$

For example, in case of acrylic acid

Corrected area of acrylic acid = *37502 / 3268037*

= 115×10^{-4}

The quantity of products in collected sample is calculated from the corrected area and response factor (Table C3) as in the following formula

wt % of product in sample = Corrected area X Response factor

For example,

wt % of acrylic acid = $(115 \times 10^{-4})(327.05\ wt\%)$

= *3.75 wt%*

This result can be transformed into mole concentration consecutively.

$$\text{mol concentration} = \frac{\text{wt \% of product in sample}}{\text{molecular weight of product}}$$

For example,

mol of acrylic acid in sample = $3.75\ wt\% / 72\ g.mol^{-1}$

= *52.1 mmol / 100 g of sample*

Table C3 The retention time and response factor of products from the GC condition in Table C1

Products	**Retention time** (min)	**Response factor** (wt%/corrected area)
Acetaldehyde	1.81	434.05
Propionaldehyde	1.95	202.70
Acetone	2.01	126.98
Acrolein	2.10	202.70
Pyruvaldehyde	2.27	327.05
Dihydrofuran	3.30	120.47
n-Propanol (internal standard)	3.40	-
Acetol	6.81	208.89
Cyclopentenone	7.82	111.48
2-Methylcyclopentenone	7.97	124.32
Acetic acid	9.05	348.90
3-Methylcyclopentenone	10.15	124.32
Propanoic acid	10.36	327.05
Acrylic acid	11.76	327.05
Phenol	16.61	111.48
Glycerol	20.25	1136.0

Then, the weight of liquid sample collected in an hour is combined to calculate the production rate by the following formula

$$\text{Production rate} = \frac{\text{mol of concentration X weight collected in an hour}}{100}$$

For example, the liquid sample collected is 1.4157 g.h^{-1}

$$\textit{Production rate} = \textit{(52.1 mmol)(1.4157 g. h}^{-1}\textit{) / 100 g}$$

$$= \textit{0.738 mmol.h}^{-1}$$

Once the production rate of all products is known, the loss of feed to carbon monoxide can be calculated from difference between mole of glycerol introduced and total mole collected in liquid sample.

Carbon monoxide = mole of feed introduced – total products mole in liquid sample

For example, the glycerol fed is 1.70 mmol.h^{-1}, From Table C2, the total products mole is 1.40 mmol.h^{-1}

$$\textit{Carbon monoxide} = \textit{1.70 mmol.h}^{-1} - \textit{1.40 mmol.h}^{-1}$$

$$= \textit{0.30 mmol of glycerol.h}^{-1}$$

After that, the yield by mole of products can be calculate from the production rate and total feed rate as express below

$$\text{Yield} = \frac{\text{Production rate}}{\text{Glycerol feed rate}} \times 100$$

For example,

Yield of acrylic acid = *(0.738 mmol.h^{-1} / 1.70 mmol.h^{-1}) X 100*

= *43.5 mol%*

The remaining feed can be evaluated the conversion by the following formula

$$\% \text{ Conversion} = \frac{\text{(Feed introduced - Feed remaining)}}{\text{Feed introduced}} \times 100$$

For example, the conversion of acrolein in second bed, the acrolein introduced from first bed is 87.0 mol% (Table D20)

Glycerol conversion = *[(87.0 mol% – 26.9 mol%) / 87.0 mol%] X 100*

= *69.1 mol%*

Finally, the selectivity to the product can be derived from yield and conversion as seen below

$$\% \text{ Selectivity to product} = \frac{\text{Product yield}}{\text{Feed converted}} \times 100$$

For example, selectivity to acrylic acid by second bed

Selectivity to acrylic acid = *[43.5 mol% / (87.0 mol% – 26.9 mol%)] X 100*

= *72.4 mol%*

APPENDIX D

Reaction Data

D1 Glycerol Dehydration

D1.1 Effect of Contact Time

Table D1 The yield of glycerol dehydration at contact time = 29 g.h.mol^{-1}

Time on stream (h)	Yield (mol%)							Conversion (mol%)
	Acetaldehyde	Propionaldehyde	Acrolein	Pyruvaldehyde	Acetol	Glycerol	Others	
1	13.0	2.7	74.9	0.7	8.3	0.0	0.3	100.0
2	12.3	2.2	72.6	0.7	11.1	0.0	1.1	100.0
3	9.2	1.5	46.0	1.5	8.3	31.9	1.6	68.1
4	7.0	1.1	34.8	1.2	5.5	49.2	1.2	50.8
5	6.7	0.9	29.3	0.3	4.8	56.3	1.0	43.7
6	5.4	0.7	23.1	0.8	3.8	64.4	1.8	35.6
7	5.6	0.7	21.0	0.9	3.7	66.1	2.0	33.9

** Reaction conditions; Catalyst: HZSM-5 (180), Temperature: 350 °C, Feed: 1.7 mmol.h^{-1} of glycerol at 10 wt%, Carier gas: 30 ml.min^{-1} of helium*

Table D2 The yield of glycerol dehydration at contact time = 59 g.h.mol^{-1}

Time on stream (h)	Yield (mol%)						Conversion (mol%)
	Acetaldehyde	Propionaldehyde	Acrolein	Pyruvaldehyde	Acetol	Others	
1	22.8	2.9	68.4	0.9	4.1	0.9	100.0
2	18.4	2.0	66.8	0.8	9.2	1.6	100.0
3	20.1	2.1	63.4	2.1	10.5	1.3	100.0
4	19.9	2.0	64.5	2.0	11.3	0.3	100.0
5	20.1	1.9	62.7	2.2	12.2	0.2	100.0
6	20.7	1.9	60.2	2.3	12.6	1.7	100.0
7	21.3	2.1	63.5	2.2	10.4	0.6	100.0

** The conditions are same as Table D1*

Table D3 The yield of glycerol dehydration at contact time = 177 g.h.mol^{-1}

Time on stream (h)	Yield (mol%)						Conversion (mol%)
	Acetaldehyde	Propionaldehyde	Acrolein	Pyruvaldehyde	Acetol	Others	
1	30.2	4.6	50.5	2.3	0.6	2.8	100.0
2	21.7	3.0	65.5	0.9	4.4	2.0	100.0
3	17.8	2.6	67.1	0.9	8.3	1.2	100.0
4	16.0	2.4	69.8	0.8	8.0	1.5	100.0
5	15.7	2.3	68.3	0.8	10.5	0.7	100.0
6	15.7	2.3	70.2	0.8	9.5	0.3	100.0
7	16.9	2.3	69.2	0.6	10.9	0.1	100.0

** The conditions are same as Table D1*

Table D4 The yield of glycerol dehydration at contact time = 295 g.h.mol^{-1}

Time on stream (h)	Yield (mol%)						Conversion (mol%)
	Acetaldehyde	Propionaldehyde	Acrolein	Pyruvaldehyde	Acetol	Others	
1	28.7	4.5	44.6	3.5	0.0	2.7	100.0
2	20.6	3.8	64.8	0.0	2.8	3.6	100.0
3	18.2	3.1	65.6	2.4	5.0	2.6	100.0
4	17.7	2.9	67.5	2.5	5.8	2.7	100.0
5	18.0	2.8	65.9	2.6	7.6	2.0	100.0
6	17.4	2.7	66.7	2.8	7.3	2.4	100.0
7	17.5	2.6	64.8	2.0	9.0	2.5	100.0

** The conditions are same as Table D1*

D1.2 Acetol Conversion over HZSM-5

Table D5 The yield of acetol conversion over HZSM-5 (180)

Time on stream (h)	Yield (mol%)							Conversion (mol%)
	Acetaldehyde	Propionaldehyde	Acetone	Acetol	Acetic acid	Phenol	Others	
1	5.0	1.0	4.7	19.0	31.6	9.6	26.7	81.0
2	2.8	0.9	2.7	58.2	3.7	2.2	29.0	41.8
3	1.9	0.8	2.0	68.0	1.8	2.9	22.6	32.0
4	1.8	0.9	1.9	72.6	0.0	2.6	20.1	27.4
5	1.5	1.1	1.9	74.2	0.0	1.7	19.5	25.8
6	1.6	1.2	2.0	75.2	0.7	2.5	16.8	24.8
7	1.3	0.9	1.5	76.4	0.6	2.8	16.5	23.6

** Reaction conditions; Catalyst: HZSM-5 (180), Contact time: 142 g.h.mol^{-1}, Temperature: 350 ^{o}C, Feed: 2.1 mmol.h^{-1} of acetol at 10 wt%, Carier gas: 30 ml.min^{-1} of helium*

D1.3 Effect of Zeolite Frameworks

Table D6 The yield of glycerol dehydration over HZSM-5 (13)

Time on stream (h)	Yield (mol%)						Conversion (mol%)
	Acetaldehyde	Propionaldehyde	Acrolein	Pyruvaldehyde	Acetol	Others	
1	14.2	3.9	71.6	2.2	1.9	0.9	100.0
2	8.3	3.1	79.9	0.7	7.5	0.6	100.0
3	7.2	2.7	79.8	0.7	9.3	0.4	100.0
4	6.3	2.4	81.6	0.6	8.8	0.3	100.0
5	5.9	2.3	81.4	0.6	9.6	0.3	100.0
6	5.9	2.3	79.7	0.7	11.1	0.3	100.0
7	5.4	2.0	82.1	0.6	9.6	0.2	100.0

** Reaction conditions; Contact time: 177 g.h.mol^{-1}, Temperature: 300 ^{o}C, Feed: 1.7 mmol.h^{-1} of glycerol at 10 wt%, Carrier gas: 30 ml.min^{-1} of helium*

Table D7 The yield of glycerol dehydration over HBeta (14)

Time on stream (h)	Yield (mol%)								conversion
	Acetaldehyde	Propionaldehyde	Acrolein	Pyruvaldehyde	Acetol	Acetic acid	Glycerol	Others	
1	42.5	8.7	44.8	2.6	0.0	0.0	0.0	1.4	100.0
2	19.2	5.1	66.7	2.6	4.9	0.0	0.0	1.5	100.0
3	15.9	3.6	66.2	2.5	8.0	1.0	0.0	2.8	100.0
4	14.6	3.1	67.2	2.3	9.0	1.4	0.0	2.5	100.0
5	13.1	2.7	60.0	1.8	9.0	1.6	9.1	2.7	90.9
6	11.4	2.2	52.4	1.8	8.9	1.9	18.9	2.5	81.1
7	9.7	1.8	44.4	2.0	7.9	2.3	26.9	4.7	73.1

** The conditions are same as Table D6*

Table D8 The yield of glycerol dehydration over HMordenite (15)

Time on stream (h)	Yield (mol%)								conversion
	Acetaldehyde	Propionaldehyde	Acrolein	Pyruvaldehyde	Acetol	Acetic acid	Propanoic acid	Glycerol	Others	
1	7.4	2.1	84.1	0.9	3.8	1.4	0.0	0.0	0.4	100.0
2	3.8	0.9	46.1	1.4	5.2	1.8	0.0	39.9	0.8	60.1
3	1.8	0.3	19.2	0.7	2.5	0.7	0.4	74.0	0.3	26.0
4	0.9	0.2	9.3	0.4	1.2	0.2	0.2	86.8	0.6	13.2
5	0.7	0.2	6.6	0.3	1.0	0.3	0.3	90.2	0.5	9.8
6	0.7	0.1	6.1	0.3	0.9	0.2	0.2	91.3	0.2	8.7
7	0.6	0.1	5.0	0.3	0.8	0.2	0.3	92.3	0.5	7.7

** The conditions are same as Table D6*

Table D9 The yield of glycerol dehydration over HZSM-5 (250)

Time on stream (h)	Yield (mol%)						Conversion (mol%)
	Acetaldehyde	Propionaldehyde	Acrolein	Pyruvaldehyde	Acetol	Others	
1	9.6	3.6	78.8	2.4	4.9	0.8	100.0
2	6.1	2.9	82.8	0.0	7.8	0.4	100.0
3	5.1	2.4	76.8	2.8	9.0	1.9	100.0
4	4.9	2.4	76.2	2.3	9.7	3.0	100.0
5	2.6	1.2	42.2	0.5	5.0	1.9	54.4
6	0.0	0.0	39.0	0.0	3.9	0.0	43.0
7	2.1	0.9	36.4	1.3	3.5	1.8	47.3

** The conditions are same as Table D6*

Table D10 The yield of glycerol dehydration over HY (100)

Time on stream (h)	Yield (mol%)									conversion
	Acetaldehyde	Propionaldehyde	Acrolein	Pyruvaldehyde	Acetol	Acetic acid	Propanoic acid	Glycerol	Others	
1	19.5	2.2	30.6	1.7	5.4	1.6	0.0	29.6	9.3	70.4
2	3.0	0.3	4.4	0.4	0.9	0.3	0.1	87.9	2.7	12.1
3	2.1	0.2	3.2	0.3	0.6	0.2	0.1	91.7	1.6	8.3
4	1.7	0.2	2.6	0.3	0.6	0.2	0.1	93.2	1.2	6.8
5	1.7	0.2	2.6	0.3	0.5	0.0	0.0	93.8	1.0	6.2
6	1.1	0.1	1.8	0.2	0.3	0.2	0.0	95.6	0.6	4.4
7	1.0	0.1	1.7	0.2	0.3	0.0	0.1	95.8	0.6	4.2

** The conditions are same as Table D6*

D1.4 Effect of Dehydration Temperature

Table D11 The yield of glycerol dehydration at 275 °C

Time on stream (h)	Yield (mol%)							Conversion (mol%)
	Acetaldehyde	Propionaldehyde	Acrolein	Pyruvaldehyde	Acetol	Glycerol	Others	
1	9.0	3.7	78.8	0.6	3.7	0.0	2.8	100.0
2	4.6	3.2	79.6	0.7	7.7	0.0	3.4	100.0
3	3.7	3.0	78.8	0.8	9.0	0.0	3.1	100.0
4	3.2	2.7	81.7	0.0	8.8	0.0	2.4	100.0
5	2.4	2.1	62.0	0.8	7.3	21.6	1.9	78.4
6	1.9	1.7	45.9	0.5	5.6	38.2	3.4	61.8
7	1.3	1.3	32.7	0.5	5.0	55.2	2.2	44.8

** Reaction conditions; Catalyst: HZSM-5 (180), Contact time: 177 g.h.mol^{-1}, Feed: 1.7 mmol.h^{-1} of glycerol at 10 wt%, Carrier gas: 30 ml.min^{-1} of helium*

Table D12 The yield of glycerol dehydration at 300 °C

Time on stream (h)	Yield (mol%)						Conversion (mol%)
	Acetaldehyde	Propionaldehyde	Acrolein	Pyruvaldehyde	Acetol	Others	
1	11.4	3.8	75.1	0.8	2.6	2.2	100.0
2	7.8	3.4	77.9	0.7	7.3	1.1	100.0
3	6.7	3.1	77.4	0.7	8.6	1.6	100.0
4	6.2	3.0	76.8	0.7	9.5	1.8	100.0
5	6.1	3.0	77.1	0.0	9.0	3.2	100.0
6	6.3	3.1	75.8	0.7	11.0	0.9	100.0
7	5.9	2.8	76.8	0.8	10.8	0.8	100.0

** The conditions are same as Table D11*

Table D13 The yield of glycerol dehydration at 325 °C

Time on stream (h)	Yield (mol%)						Conversion (mol%)
	Acetaldehyde	Propionaldehyde	Acrolein	Pyruvaldehyde	Acetol	Others	
1	19.0	3.8	59.0	2.7	2.3	4.3	100.0
2	14.6	3.3	73.7	1.6	6.4	0.4	100.0
3	12.8	2.8	70.6	2.4	8.6	1.3	100.0
4	11.8	2.6	71.4	2.4	9.1	2.3	100.0
5	12.4	2.6	68.6	2.4	11.9	1.9	100.0
6	11.8	2.5	72.0	2.4	9.8	1.5	100.0
7	13.1	2.6	70.8	1.7	11.8	0.0	100.0

** The conditions are same as Table D11*

- The yield of glycerol dehydration at 350 °C; *see also Table D3*

Table D14 The yield of glycerol dehydration at 400 °C

Time on stream (h)	Yield (mol%)							Conversion (mol%)
	Acetaldehyde	Propionaldehyde	Acrolein	Pyruvaldehyde	Acetic acid	Propanoic acid	Others	
1	44.9	5.2	24.7	2.2	9.9	7.1	4.4	100.0
2	41.3	4.8	41.6	1.9	3.2	3.3	3.0	100.0
3	42.8	3.8	43.8	1.9	1.9	2.0	3.1	100.0
4	41.1	3.6	46.9	2.7	1.4	1.4	2.9	100.0
5	42.1	3.2	46.2	2.6	1.3	1.2	3.1	100.0
6	41.8	3.0	47.6	2.5	1.0	1.1	2.5	100.0
7	40.6	2.8	47.6	2.5	1.2	1.0	3.1	100.0

** The conditions are same as Table D11*

D1.5 Effect of Aluminium Content in Zeolite

- The yield of glycerol dehydration over HZSM-5 (13), Al content = 2.4 mol% ; *see also Table D6*

Table D15 The yield of glycerol dehydration over HZSM-5 (28), Al content = 1.2 mol%

Time on stream (h)	Yield (mol%)						Conversion (mol%)
	Acetaldehyde	Propionaldehyde	Acrolein	Pyruvaldehyde	Acetol	Others	
1	15.5	4.1	65.5	3.2	3.5	0.8	100.0
2	6.5	2.8	74.7	3.1	8.0	2.8	100.0
3	6.2	2.6	76.8	2.4	10.8	0.3	100.0
4	5.5	2.4	77.1	2.6	11.0	0.3	100.0
5	5.4	2.3	79.4	1.0	11.7	0.3	100.0
6	5.6	2.2	76.1	2.4	12.8	0.8	100.0
7	5.0	2.0	76.9	2.9	11.7	0.5	100.0

** Reaction condition; Catalyst: HZSM-5, Contact time: 177 g.h.mol^{-1}, Temperature 300 ^{o}C, Feed: 1.7 mmol.h^{-1} of glycerol at 10 wt%, Carrier gas: 30 ml.min^{-1} of helium*

Table D16 The yield of glycerol dehydration over HZSM-5 (180), Al content = 0.32 mol%

Time on stream (h)	Yield (mol%)						Conversion (mol%)
	Acetaldehyde	Propionaldehyde	Acrolein	Pyruvaldehyde	Acetol	Others	
1	11.4	3.8	75.1	0.8	2.6	2.2	100.0
2	7.8	3.4	77.9	0.7	7.3	1.1	100.0
3	6.7	3.1	77.4	0.7	8.6	1.6	100.0
4	6.2	3.0	76.8	0.7	9.5	1.8	100.0
5	6.1	3.0	77.1	0.0	9.0	3.2	100.0
6	6.3	3.1	75.8	0.7	11.0	0.9	100.0
7	5.9	2.8	76.8	0.8	10.8	0.8	100.0

** The conditions are same as Table D15*

- The yield of glycerol dehydration over HZSM-5 (250), Al content = 0.22 mol%; *see also Table D9*

Table D17 The yield of glycerol dehydration over HZSM-5 (500), Al content = 0.17 mol%

Time on stream (h)	Yield (mol%)							Conversion (mol%)
	Acetaldehyde	Propionaldehyde	Acrolein	Pyruvaldehyde	Acetol	Glycerol	Others	
1	7.6	2.8	79.1	3.0	3.6	0.0	1.7	100.0
2	1.9	0.8	24.5	0.9	2.1	66.3	2.1	33.7
3	0.9	0.4	11.3	0.5	1.2	83.5	1.1	16.5
4	0.7	0.3	9.1	0.4	0.9	87.2	0.7	12.8
5	0.6	0.2	7.2	0.3	0.7	89.9	0.6	10.1
6	0.6	0.2	6.7	0.4	0.7	90.4	0.5	9.6
7	0.4	0.2	5.8	0.3	0.6	91.4	0.8	8.6

** The conditions are same as Table D15*

D1.6 Effect of Glycarol Concentration

Table D18 The yield of glycerol dehydration at 10 wt% glycerol

Time on stream (h)	Yield (mol%)					Conversion (mol%)
	Acetaldehyde	Propionaldehyde	Acrolein	Acetol	Others	
1	19.2	2.7	68.6	3.5	3.2	100.0
2	13.7	2.0	75.5	7.0	1.7	100.0
3	13.1	1.7	75.2	8.7	1.2	100.0
4	12.5	1.7	75.1	9.2	1.6	100.0
5	12.3	1.5	75.1	9.8	1.2	100.0
6	12.5	1.4	75.3	9.5	1.3	100.0
7	12.0	1.5	74.9	10.4	1.2	100.0

** Reaction condition; Catalyst: HZSM-5 (13), Contact time: 59 g.h.mol^{-1}, Temperature: 300 ^{o}C, Carrier gas: 30 ml.min^{-1} of helium*

Table D19 The yield of glycerol dehydration at 30 wt% glycerol

Time on stream (h)	Yield (mol%)					Conversion (mol%)
	Acetaldehyde	Propionaldehyde	Acrolein	Acetol	Others	
1	12.1	3.0	77.7	3.8	0.5	100.0
2	10.0	2.4	80.7	6.8	0.2	100.0
3	9.3	2.1	80.5	8.0	0.1	100.0
4	8.7	1.8	80.5	8.5	0.5	100.0
5	8.3	1.7	79.6	9.0	1.0	100.0
6	8.2	1.6	79.5	9.2	1.0	100.0
7	7.8	1.5	79.5	8.9	1.7	100.0

* *The conditions are same as Table D18*

Table D20 The yield of glycerol dehydration at 50 wt% glycerol

Time on stream (h)	Yield (mol%)					Conversion (mol%)
	Acetaldehyde	Propionaldehyde	Acrolein	Acetol	Others	
1	16.2	3.4	66.7	5.6	1.3	100.0
2	14.7	2.8	64.5	15.3	2.0	100.0
3	14.1	2.4	62.1	18.3	3.2	100.0
4	13.5	2.2	60.3	20.3	3.7	100.0
5	12.7	2.0	61.7	18.3	5.4	100.0
6	12.8	1.9	58.0	22.9	4.4	100.0
7	12.3	1.7	56.3	23.2	6.5	100.0

* *The conditions are same as Table D18*

D2 Subsequent Oxidation of Glycerol Dehydrated Products

D2.1 Yield from First Bed

Table D21 The yield of glycerol dehydration for the study of subsequent oxidation when carried by 10 mol % O_2

Time on stream (h)	Yield (mol%)						Conversion (mol%)
	Acetaldehyde	Propionaldehyde	Acrolein	Acetol	Acetic acid	Others	
1	8.1	2.5	82.9	2.9	1.6	1.2	100.0
2	5.1	2.0	86.6	5.1	0.7	0.5	100.0
3	4.7	1.8	86.3	5.7	0.9	0.4	100.0
4	4.8	1.8	86.6	5.4	0.9	0.5	100.0
5	4.2	1.4	86.8	5.8	1.0	0.6	100.0
6	4.1	1.4	88.2	4.9	1.0	0.3	100.0
7	4.3	1.3	87.0	5.9	1.1	0.3	100.0

** Reaction conditions; Catalyst: HZSM-5 (13), Contact time: 88 g.h.mol^{-1}, Temperature: 300 ^{o}C, Feed: 1.7 mmol.h^{-1} of glycerol at 10 wt%, Carier gas: 30 ml.min^{-1} of 10 vol% O_2 in N_2*

Table D22 The yield of glycerol dehydration for the study of subsequent oxidation when carried by 20 mol % O_2

Time on stream (h)	Yield (mol%)						Conversion (mol%)
	Acetaldehyde	Propionaldehyde	Acrolein	Acetol	Acetic acid	Others	
1	6.5	2.6	85.3	3.2	1.1	0.6	100.0
2	4.5	2.1	87.3	5.4	0.4	0.3	100.0
3	4.1	1.9	87.8	5.4	0.5	0.3	100.0
4	3.9	1.8	87.2	6.0	0.8	0.3	100.0
5	4.2	1.7	82.1	10.5	1.2	0.3	100.0
6	3.4	1.6	87.6	7.0	0.0	0.3	100.0
7	3.5	1.4	86.4	7.2	1.1	0.2	100.0

** Reaction conditions; Catalyst: HZSM-5 (13), Contact time: 88 g.h.mol^{-1}, Temperature: 300 ^{o}C, Feed: 1.7 mmol.h^{-1} of glycerol at 10 wt%, Carier gas: 30 ml.min^{-1} of 20 vol% O_2 in N_2*

D2.2 Separate and Mix System

Table D23 The yield from subsequent oxidation of glycerol dehydrated products by separate system

Time on stream (h)	Yield (mol%)						2nd bed	
	Acetaldehyde	Propionaldehyde	Acrolein	Acetic acid	Acrylic acid	Others	Acrolein conversion	Acrylic acid selectivity
1	9.4	0.3	50.0	9.8	29.1	0.2	42.4	79.4
2	6.9	0.2	44.9	8.1	39.3	0.3	48.2	94.3
3	6.2	0.2	46.0	8.0	39.3	0.1	46.9	96.5
4	6.7	0.2	48.3	7.1	37.7	0.0	44.2	98.3
5	6.1	0.2	45.2	7.4	41.1	0.0	47.9	99.1
6	6.1	0.2	45.2	7.4	41.1	0.0	47.9	99.1
7	6.2	0.2	46.0	7.3	40.3	0.0	46.9	99.1

** Reaction condition; Temperature: 300 °C, Feed: 1.7 mmol.h^{-1} of glycerol at 10 wt%, Carrier gas: 30 ml.min^{-1} of 20 vol% O_2 in N_2, 1st bed: contact time: 88 g.h.mol^{-1}, catalyst: HZSM-5 (13), 2nd bed: contact time: 177 g.h.mol^{-1}, catalyst: 45 VMo(0.3)*

Table D24 The yield from subsequent oxidation of glycerol dehydrated products by mixed system

Time on stream (h)	Yield (mol%)					
	Acetaldehyde	Propionaldehyde	Acrolein	Acetic acid	Acrylic acid	Others
1	33.0	2.2	14.1	50.8	0.0	0.0
2	20.5	0.5	29.3	24.2	22.4	2.7
3	17.6	0.4	28.9	20.8	29.7	2.3
4	17.8	0.4	31.4	17.8	30.0	2.4
5	17.4	0.4	28.4	21.1	30.5	2.2
6	17.0	0.4	29.8	18.2	32.3	2.2
7	17.3	0.4	30.2	17.7	31.9	2.4

** Reaction condition; Temperature: 300 °C, Feed: 1.7 mmol.h^{-1} of glycerol at 10 wt%, Carrier gas: 30 ml.min^{-1} of 20 vol% O_2 in N_2, Contact time: 265 g.h.mol^{-1}, Catalyst 1:2 (by wt) of HZSM-5 (13): 45 VMo(0.3)*

D2.3 Effect of Contact Time

Table D25 The yield from subsequent oxidation of glycerol dehydrated products at contact time = 59 g.h.mol^{-1}

Time on stream (h)	Yield (mol%)						2nd bed	
	Acetaldehyde	Propionaldehyde	Acrolein	Acetic acid	Acrylic acid	Others	Acrolein conversion	Acrylic acid selectivity
1	13.3	1.8	73.6	5.9	3.5	0.5	15.1	26.7
2	8.6	1.3	82.0	3.4	4.1	0.4	5.4	88.6
3	8.0	1.2	81.8	4.2	4.3	0.3	5.6	88.0
4	8.4	1.1	81.1	4.6	4.1	0.3	6.4	74.5
5	8.2	1.0	81.8	4.5	3.9	0.3	5.7	80.6
6	8.1	1.0	82.2	4.5	4.0	0.2	5.2	89.2
7	8.1	0.8	76.1	7.3	7.2	0.3	12.2	67.8

** Reaction condition; Temperature: 300 °C, 1st bed: contact time: 88 g.h.mol^{-1}, catalyst: HZSM-5 (13), 2nd bed: catalyst: 45VMo(0.3), Feed: 1.7 mmol.h^{-1} of glycerol at 10 wt%, Carrier gas: 30 ml.min^{-1} of 10 vol% O_2 in N_2*

Table D26 The yield from subsequent oxidation of glycerol dehydrated products at contact time = 118 g.h.mol^{-1}

Time on stream (h)	Yield (mol%)						2nd bed	
	Acetaldehyde	Propionaldehyde	Acrolein	Acetic acid	Acrylic acid	Others	Acrolein conversion	Acrylic acid selectivity
1	11.4	1.0	71.6	6.0	8.6	0.2	13.6	76.5
2	9.6	0.7	73.5	5.5	10.6	0.1	15.5	78.5
3	9.4	0.6	71.6	6.1	12.3	0.1	17.7	90.0
4	9.1	0.5	69.7	6.6	14.0	0.0	19.8	90.8
5	9.3	0.5	69.5	6.6	14.1	0.0	20.1	90.6
6	9.2	0.5	68.1	7.0	15.2	0.0	21.7	90.5
7	8.4	0.5	64.9	8.1	18.2	0.0	25.4	92.2

** The conditions are same as Table D25*

Table D27 The yield from subsequent oxidation of glycerol dehydrated products at contact time = 177 g.h.mol^{-1}

Time on stream (h)	Yield (mol%)						2nd bed	
	Acetaldehyde	Propionaldehyde	Acrolein	Acetic acid	Acrylic acid	Others	Acrolein conversion	Acrylic acid selectivity
1	19.5	1.1	45.1	13.4	16.3	2.4	45.6	43.2
2	9.6	0.4	64.3	6.5	18.7	0.2	26.1	82.4
3	8.1	0.3	61.8	7.8	21.7	0.1	29.0	86.2
4	8.1	0.3	64.1	7.0	20.4	0.1	26.3	89.1
5	8.3	0.3	62.5	7.2	21.7	0.0	28.1	88.6
6	8.3	0.3	60.1	7.4	23.9	0.0	30.9	89.1
7	7.8	0.3	59.1	7.8	25.0	0.0	32.0	89.9

* *The conditions are same as Table D25*

Table D28 The yield from subsequent oxidation of glycerol dehydrated products at contact time = 295 g.h.mol^{-1}

Time on stream (h)	Yield (mol%)						2nd bed	
	Acetaldehyde	Propionaldehyde	Acrolein	Acetic acid	Acrylic acid	Others	Acrolein conversion	Acrylic acid selectivity
1	18.9	6.8	22.8	38.2	13.2	0.0	72.5	22.1
2	9.1	0.2	49.8	7.5	32.6	0.2	42.7	87.6
3	7.2	0.4	40.5	8.7	41.8	1.3	53.5	89.9
4	7.0	0.2	39.3	9.1	42.7	1.7	54.8	89.5
5	6.6	0.2	38.4	8.6	44.4	1.5	55.9	91.4
6	6.5	0.2	40.1	9.8	43.0	0.1	53.9	91.8
7	6.2	0.0	36.0	9.4	48.4	0.0	58.6	91.9

* *The conditions are same as Table D25*

D2.4 Effect of Vanadium-Molybdenum Oxides Loading on Silicic Acid

Table D29 The yield from subsequent oxidation of glycerol dehydrated products with 20VMo(0.3)

Time on stream (h)	Yield (mol%)						2nd bed	
	Acetaldehyde	Propionaldehyde	Acrolein	Acetic acid	Acrylic acid	Others	Acrolein conversion	Acrylic acid selectivity
1	22.2	0.8	57.3	11.2	4.1	3.0	30.9	15.9
2	13.5	0.3	78.8	3.8	3.5	0.1	9.4	43.2
3	12.0	0.2	75.1	5.1	7.4	0.1	13.6	62.3
4	11.7	0.2	73.2	5.4	9.4	0.1	15.8	68.3
5	11.8	0.3	73.2	5.5	9.2	0.0	15.9	67.0
6	11.5	0.2	73.6	5.2	9.2	0.1	15.4	69.0
7	11.4	0.2	71.6	6.7	10.0	0.1	17.7	64.6

** Reaction condition; Temperature: 300 °C, 1st bed: contact time: 88 g.h.mol^{-1}, catalyst: HZSM-5 (13), 2nd bed: contact time: 295 g.h.mol^{-1}, catalyst: xVMo(0.3), Feed: 1.7 mmol.h^{-1} of glycerol at 10 wt%, Carrier gas: 30 ml.min^{-1} of 10 vol% O_2 in N_2*

Table D30 The yield from subsequent oxidation of glycerol dehydrated products with 30VMo(0.3)

Time on stream (h)	Yield (mol%)						2nd bed	
	Acetaldehyde	Propionaldehyde	Acrolein	Acetic acid	Acrylic acid	Others	Acrolein conversion	Acrylic acid selectivity
1	14.4	0.4	71.7	5.7	6.3	0.2	13.4	57.0
2	11.2	0.2	72.0	6.4	9.7	0.1	17.2	64.7
3	10.6	0.2	71.9	6.3	10.4	0.1	17.3	69.2
4	10.8	0.2	70.9	6.6	11.0	0.1	18.5	68.4
5	11.0	0.2	70.9	6.9	10.8	0.0	18.5	66.9
6	10.5	0.3	70.9	7.1	11.3	0.0	18.5	70.0
7	10.4	0.2	72.2	7.1	10.0	0.0	17.0	67.7

** The conditions are same as Table D29*

Table D31 The yield from subsequent oxidation of glycerol dehydrated products with 40VMo(0.3)

Time on stream (h)	Yield (mol%)						2nd bed	
	Acetaldehyde	Propionaldehyde	Acrolein	Acetic acid	Acrylic acid	Others	Acrolein conversion	Acrylic acid selectivity
1	10.9	0.4	49.5	9.0	28.5	0.4	40.2	85.4
2	8.9	0.2	52.6	6.9	31.3	0.0	39.6	91.0
3	8.7	0.2	53.6	6.5	31.0	0.0	38.4	92.9
4	7.9	0.2	52.0	7.4	32.3	0.0	40.2	92.4
5	7.7	0.2	51.7	7.3	32.8	0.0	40.6	93.1
6	7.8	0.2	51.3	7.3	33.4	0.0	41.1	93.6
7	5.1	0.3	33.9	10.5	50.2	0.0	61.0	94.6

** The conditions are same as Table D29*

- The yield from subsequent oxidation of glycerol dehydrated products with 45VMo(0.3); *see also Table D27*

Table D32 The yield from subsequent oxidation of glycerol dehydrated products with 50VMo(0.3)

Time on stream (h)	Yield (mol%)						2nd bed	
	Acetaldehyde	Propionaldehyde	Acrolein	Acetic acid	Acrylic acid	Others	Acrolein conversion	Acrylic acid selectivity
1	8.5	0.3	39.6	10.2	40.4	0.2	52.2	93.4
2	6.8	0.2	39.1	8.1	45.3	0.3	55.0	94.7
3	6.6	0.2	33.6	9.2	50.2	0.2	61.4	94.0
4	5.9	0.2	34.6	8.5	50.5	0.2	60.2	96.4
5	6.1	0.2	36.2	9.1	48.4	0.0	58.4	95.3
6	6.2	0.2	37.0	8.2	48.2	0.1	57.5	96.4
7	5.9	0.2	35.1	8.5	50.0	0.1	59.7	96.3

* *The conditions are same as Table D29*

Table D33 The yield from subsequent oxidation of glycerol dehydrated products with 75VMo(0.3)

Time on stream (h)	Yield (mol%)						2nd bed	
	Acetaldehyde	Propionaldehyde	Acrolein	Acetic acid	Acrylic acid	Others	Acrolein conversion	Acrylic acid selectivity
1	9.1	0.5	38.9	13.1	35.4	1.7	53.0	80.6
2	7.3	0.2	48.6	7.0	36.6	0.1	44.1	95.4
3	6.5	0.2	44.1	8.1	41.0	0.0	49.3	95.5
4	6.2	0.2	42.7	7.7	43.1	0.2	50.9	97.2
5	6.2	0.2	42.6	8.1	42.7	0.1	51.0	96.3
6	5.6	0.2	41.0	8.0	45.1	0.2	52.9	98.0
7	5.6	0.2	41.0	8.4	44.6	0.2	52.9	97.0

* *The conditions are same as Table D29*

Table D34 The yield from subsequent oxidation of glycerol dehydrated products with 100VMo(0.3)

Time on stream (h)	Yield (mol%)						2nd bed	
	Acetaldehyde	Propionaldehyde	Acrolein	Acetic acid	Acrylic acid	Others	Acrolein conversion	Acrylic acid selectivity
1	6.7	0.8	47.6	10.8	32.8	0.3	42.5	93.0
2	5.7	0.5	44.0	8.5	41.0	0.1	49.4	95.4
3	5.3	0.4	43.9	8.0	42.4	0.1	49.6	98.3
4	6.0	0.6	47.9	8.4	36.9	0.1	44.9	94.5
5	5.9	0.5	47.0	8.5	38.0	0.1	46.0	95.1
6	5.2	0.4	45.6	7.7	41.0	0.1	47.6	98.8
7	5.4	0.4	42.7	9.2	42.2	0.1	50.9	95.5

** The conditions are same as Table D29*

D2.5 Effect of Mixed Oxides Composition

Table D35 The yield from subsequent oxidation of glycerol dehydrated products with 45VMo(0.2)

Time on stream (h)	Yield (mol%)						2nd bed	
	Acetaldehyde	Propionaldehyde	Acrolein	Acetic acid	Acrylic acid	Others	Acrolein conversion	Acrylic acid selectivity
1	4.4	0.1	23.1	2.3	3.5	0.1	72.1	5.8
2	10.5	0.3	70.1	6.5	13.6	0.0	19.4	80.6
3	9.6	0.3	67.9	6.9	14.8	0.1	21.9	77.5
4	9.2	0.2	66.7	7.0	15.8	0.0	23.3	77.8
5	8.9	0.2	66.5	7.3	16.2	0.0	23.5	79.3
6	8.1	0.2	64.6	7.9	18.8	0.2	25.8	83.7
7	8.4	0.2	61.1	9.8	20.8	0.2	29.8	80.3

** Reaction condition; Temperature: 300 °C, 1st bed: contact time: 88 g.h.mol^{-1}, catalyst: HZSM-5 (13), 2nd bed: contact time: 177 g.h.mol^{-1}, catalyst: 45VMo(y), Feed: 1.7 mmol.h^{-1} of glycerol at 10 wt%, Carrier gas: 30 ml.min^{-1} of 10 vol% O_2 in N_2*

- The yield from subsequent oxidation of glycerol dehydrated products with 45VMo(0.3); *see also Table D27*

Table D36 The yield from subsequent oxidation of glycerol dehydrated products with 45VMo(0.6)

Time on stream (h)	Yield (mol%)							2nd bed	
	Acetal dehyde	Propional dehyde	Acrolein	Acetic acid	Acrylic acid	Gas	Others	Acrolein conversion	Acrylic acid selectivity
1	2.8	0.1	13.0	4.6	15.9	63.1	0.0	84.4	22.8
2	5.4	0.2	30.8	7.4	36.4	19.4	0.2	64.6	64.8
3	5.4	0.2	29.9	7.7	44.3	12.2	0.2	65.7	77.6
4	5.0	0.2	29.2	8.2	39.6	17.6	0.2	66.4	85.9
5	4.7	0.2	26.9	7.4	43.5	17.3	0.0	69.0	72.4
6	5.0	0.2	28.3	9.0	44.3	12.9	0.2	67.4	75.5
7	3.9	0.2	22.9	6.9	48.5	17.4	0.2	73.6	75.7

** The conditions are same as Table D35*

Table D37 The yield from subsequent oxidation of glycerol dehydrated products with 45VMo(2)

Time on stream (h)	Yield (mol%)							2nd bed	
	Acetal dehyde	Propional dehyde	Acrolein	Acetic acid	Acrylic acid	Gas	Others	Acrolein conversion	Acrylic acid selectivity
1	3.9	0.1	14.8	5.0	7.2	68.6	0.1	83.0	10.0
2	6.2	0.2	26.6	8.1	16.3	42.3	0.2	69.3	27.2
3	6.4	0.2	29.3	9.3	18.0	36.7	0.2	66.2	31.4
4	6.4	0.2	28.7	8.1	17.2	39.3	0.2	66.9	29.7
5	5.8	0.1	25.2	8.7	16.4	43.7	0.0	71.0	26.7
6	6.7	0.2	34.2	8.2	12.5	38.1	0.2	60.5	23.8
7	7.0	0.2	28.3	9.7	19.4	35.2	0.2	67.4	33.3

** The conditions are same as Table D35*

D2.6 Effect of Oxygen Concentration

Table D38 The yield from subsequent oxidation of glycerol dehydrated products in 5 % O_2

Time on stream (h)	Yield (mol%)						2nd bed	
	Acetaldehyde	Propionaldehyde	Acrolein	Acetic acid	Acrylic acid	Others	Acrolein conversion	Acrylic acid selectivity
1	13.8	0.8	70.4	6.1	7.7	0.2	15.0	62.0
2	9.8	0.5	67.7	5.1	16.4	0.2	22.2	84.9
3	9.1	0.5	72.6	4.3	13.4	0.2	16.5	92.9
4	9.7	0.6	74.2	5.0	10.3	0.1	14.7	80.5
5	9.1	0.5	72.0	5.5	12.9	0.1	17.3	85.9
6	8.8	0.4	65.9	7.4	17.3	0.2	24.3	82.1
7	8.4	0.4	67.9	6.7	16.4	0.0	21.9	86.4

** Reaction condition; Temperature: 300 °C, 1st bed: contact time: 88 g.h.mol^{-1}, catalyst: HZSM-5 (13), 2nd bed: contact time: 177 g.h.mol^{-1}, catalyst: 45VMo(0.3), Feed: 1.7 mmol.h^{-1} of glycerol at 10 wt%, Carrier gas: 30 ml.min^{-1} of 5-20 vol% O_2 in N_2*

- The yield from subsequent oxidation of glycerol dehydrated products in 10 % O_2; *see also Table D27*

Table D39 The yield from subsequent oxidation of glycerol dehydrated products in 15 % O_2

Time on stream (h)	Yield (mol%)						2nd bed	
	Acetaldehyde	Propionaldehyde	Acrolein	Acetic acid	Acrylic acid	Others	Acrolein conversion	Acrylic acid selectivity
1	11.6	0.4	55.8	9.2	21.9	0.0	32.7	80.8
2	8.6	0.2	58.3	6.8	25.9	0.0	33.0	90.2
3	7.6	0.2	57.0	7.2	28.0	0.0	34.5	93.3
4	6.8	0.2	54.1	8.3	30.7	0.0	37.8	93.1
5	7.5	0.2	57.3	6.8	28.2	0.0	34.2	94.9
6	7.3	0.2	54.9	7.4	30.1	0.0	36.9	93.9
7	7.1	0.2	54.2	7.5	31.0	0.0	37.6	94.5

** The conditions are same as Table D38*

- The yield from subsequent oxidation of glycerol dehydrated products in 20 % O_2; *see also Table D23*

AUTHOR BIOGRAPHY

Mr. Ayut Witsuthammakul was born on 16 November 1983 in Bangkok. He graduated a Bachelor Degree in Industrial Chemistry from the Department of Chemistry, Faculty of Science, King Mongkut's Institute of Technology Ladkrabang in 2006. In the same year, he also completed a Bachelor Degree in General Management from the Faculty of Business Administration, Ramkhamhaeng University. He has been a master degree student in Petrochemicals and Hydrocarbon Chemistry program of Faculty of Science, King Mongkut's Institute of Technology Ladkrabang since 2007.